

MASTER

**TRIANGLE UNIVERSITIES NUCLEAR LABORATORY
ANNUAL REPORT - TUNL, XV**

1 JANUARY, 1976 - 31 DECEMBER, 1976



**Duke University
University of North Carolina at Chapel Hill
North Carolina State University at Raleigh**

CONTENTS

Major portions of earlier TUNL reports (TUNL I - TUNL XIII) are contained in the reports of USNDC or its predecessor, the AEC Nuclear Cross Sections Advisory Committee.

A.	NEUTRON AND FISSION PHYSICS	1
	1. Fast Neutron Differential Cross Sections	1
	a. Experimental	1
	b. CTR Related Measurements	2
	c. Search for States of High Excitation (713 MeV) in ${}^7\text{Li}$	7
	d. Theoretical Analysis of Neutron Data	7
	2. Resolved Neutron Total Cross Sections and Intermediate Structure	8
	3. Theoretical Investigation of Neutron Cross Section Measurements	8
	4. A Selectively Excited and Distorted [Liquid] Drop (SEXDD) Fission Model	9
	5. Charged Particle Fission	12
B.	NEUTRON POLARIZATION STUDIES	13
	1. Analyzing Power Measurements for n-p Scattering from 10 to 18 MeV	13
	a. Measurements	13
	b. Corrections to The A_y Data	15
	2. Analyzing Power Measurements for n-d Scattering at 12 MeV	15
	3. Analyzing Power for ${}^{12}\text{C}(n,n){}^{12}\text{C}$ Scattering	15
	4. Neutron Polarization and Analyzing Power in the $\text{H}(\vec{f}, \vec{n}){}^3\text{He}$ Reaction Using a Polarized Triton Beam	16
	5. Similarities between $A_y(\theta)$ and $P_Y(\theta)$ for the ${}^3\text{H}(p,n){}^3\text{He}$ Reaction	16
	6. Remeasurement of P_Y for the ${}^2\text{H}(d, \vec{n}){}^3\text{He}$ Reaction and Its Implication to the f-wave Admixture of the 2^- State at 22 MeV in ${}^4\text{He}$	19
	7. Neutron Polarization Produced by the Breakup of Vector Polarized Deuterons on ${}^2\text{H}$ and ${}^4\text{He}$	19
	8. Polarization Transfer in the ${}^2\text{H}(\vec{f}, \vec{n}){}^4\text{He}$ Reaction	19
	9. A Calibrated Source of High Energy Polarized Neutrons Obtained from $A_{zz}(0^\circ)$ Measurements for the ${}^3\text{H}(d,n){}^4\text{He}$ Reaction	19
	10. Elastic Scattering of Polarized Neutrons from ${}^3\text{He}$	20
	11. Elastic Scattering of Nucleons from ${}^4\text{He}$	20
	a. Cross-Section Measurements for ${}^4\text{He}(n,n){}^4\text{He}$	20
	b. ${}^4\text{He}(\vec{n}, n){}^4\text{He}$ Analyzing Power Measurements at 14 and 17 MeV	20
	c. ${}^4\text{He}(\vec{n}, n){}^4\text{He}$ Analyzing Power Measurements from 20 to 29 MeV with a Calibrated Source of Polarized Neutrons	21
	d. ${}^4\text{He}(\vec{p}, p){}^4\text{He}$ Analyzing Power Measurements	21
	e. Phase Shift Analysis of the ${}^4\text{He}(n,n){}^4\text{He}$ and ${}^4\text{He}(p,p){}^4\text{He}$ Scattering Processes	21
	12. Polarization Transfer Studies in (\vec{p}, \vec{n}) Reactions	22
	a. Polarization Transfer in the $\text{D}(\vec{p}, \vec{n})2p$ Reaction from 10 to 15 MeV	22
	b. Polarization Transfer Effects in (\vec{p}, \vec{n}) Reactions on Light Nuclei at $\theta = 0^\circ$	22

NOTICE
 This report was prepared as an account of work sponsored by the United States Government. Neither the United States nor the United States Energy Research and Development Administration, nor any of its employees, nor any of their contractors, subcontractors, or their employees, makes any warranty, express or implied, or assumes any legal liability or responsibility for the accuracy, completeness, or usefulness of any information, apparatus, product or process disclosed, or represents that its use would not infringe privately owned rights.

B.	13.	Comparison of the Polarization and Analyzing Power in (p,n) Mirror Reactions on ^{15}N and ^9Be	22
	14.	Cross Sections and Polarizations in ($^3\text{He},n$) Reactions from ^{12}C and ^{13}C from 8 to 22 MeV	24
	15.	Polarization Transfer Studies of $^{12}\text{C}(\vec{d},\vec{n})^{13}\text{N}$, $^{14}\text{N}(\vec{d},\vec{n})^{15}\text{O}$, $^{16}\text{O}(\vec{d},\vec{n})^{17}\text{F}$ and $^{28}\text{Si}(\vec{d},\vec{n})^{29}\text{P}$ at $\theta = 0^\circ$	24
	16.	Depolarization Effects in Stripping a Polarized Negative Ion Beam in The Terminal of a Tandem Van de Graff	25
	17.	Pulsed Polarized Beam Studies	25
	18.	Sources of Polarized Fast-Neutron Beams--A Status Report	25
C.	HIGH RESOLUTION STUDIES		27
	1.	High Resolution Elastic Scattering	27
	a.	Review Article	27
	b.	^{26}Mg	28
	c.	^{30}Si	28
	d.	^{34}S	28
	e.	^{42}Ca	28
	f.	^{54}Fe , ^{58}Ni , ^{60}Ni	29
	g.	^{90}Zr	30
	2.	High Resolution Proton Capture	30
	3.	High Resolution Inelastic Scattering	30
	a.	Method	30
	b.	^{50}Cr	30
	c.	^{56}Fe	31
	d.	^{44}Ca	32
	4.	Isospin-Forbidden T = 3/2 Resonances	32
D.	GAMMA RAY SPECTROSCOPY		34
	1.	Mean Lifetimes of Excited States in ^{38}Ca	34
	2.	Mean Lifetimes of Levels in ^{55}Co	34
	3.	Measurement of Gamma-Ray Angular Distributions and Linear Polarizations for ^{48}V	34
	4.	Studies of The Gamma-Ray Decay of Excited Levels in ^{117}Sb	35
	5.	A Study of The Low Lying Levels of ^{77}Kr	35
	6.	Spin and Parity of The 11.86 MeV Level in ^{24}Mg	35
	7.	Magnetic Moment of 738 keV Level in ^{43}K	36
E.	CHARGED PARTICLE REACTIONS WITH POLARIZED BEAMS		
	1.	The Hamburger Effect in $^{207}\text{Pb}(\vec{d},p)^{208}\text{Pb}$ and $^{207}\text{Pb}(\vec{d},d)^{207}\text{Pb}$	39
	2.	The Study of The $^{207}\text{Pb}(\vec{d},t)^{206}\text{Pb}$ Reaction	39
	3.	The (\vec{d},α) Reaction on ^{28}Si , ^{37}S and ^{40}Ca	39
	4.	The Mechanism of ($\vec{d},^6\text{Li}$) Reactions on Light Nuclei	40

F.	RADIATIVE CAPTURE REACTIONS	41
1.	General Discussion of The Program	41
2.	Giant Resonance Region of ^{15}N Studied by Polarized and Unpolarized Proton Capture Measurements	41
3.	Giant Dipole Resonance in ^{56}Fe Observed via (p,γ) and (α,γ) Reactions	42
4.	Giant Dipole Resonances in $^{55,57,59}\text{Co}$ Using Polarized Proton Capture	42
5.	Study of The Giant Dipole Resonance Region of ^{31}P	43
6.	Study of The Radiation in The Giant E1 Resonance Region of ^{89}Y with The Reaction $^{88}\text{Sr}(\vec{p},\gamma)^{89}\text{Y}$	45
7.	A Study of The $\text{D}(p,\gamma)^3\text{He}$ Reaction	49
8.	Fast Neutron Capture Progress Report	49
9.	Study of The Giant Dipole Resonance Regions of ^{60}Ni	52
10.	A Study of The $^3\text{H}(p,\gamma)^4\text{He}$ Reaction from $17 < E_p < 30$ MeV	52
11.	Measurement of E2 Strength for The Capture Radiation from ^{56}Fe via The (α,γ) Reaction	54
12.	A Search for the Isovector E2 Resonances in ^{31}P , ^{89}Y and ^{60}Ni	54
G.	ATOMIC COLLISION PHYSICS	
1.	Two Electron-One Photon X-ray Transitions ($2e-1\gamma$)	58
2.	K X rays Arising from 20-80 MeV Ion Bombardment of Ti, Mn, Cu and KBr	60
3.	Radiative Electron Capture Resulting from 20-70 MeV Chlorine Ion Bombardment of C, Ti, Mn and Cu	60
H.	HEAVY ION REACTIONS	61
1.	Recoil Ranges and Range Straggling of Nuclei Resulting from $^{59}\text{Co}(^{16}\text{O},\text{X})\text{Y}$ Reactions	61
I.	APPLICATIONS	
1.	Neutron Spectra from Deuteron and Proton Bombardment of Thick Lithium Targets	65
2.	Development of a Facility for Production of ^{15}O	68
3.	Continuation of PIXE Development for Multielemental Analysis with 3 MeV Protons	68
J.	ION SOURCE DEVELOPMENT	70
1.	New Ion Sources for The Tandem Accelerator	70
2.	Intense Metastable Hydrogen Beams	70
3.	A New Polarized Ion Source for SATURNE II	70
4.	Comparison of a Duoplasmatron and a Duopigatron Ion Source	70

K.	ACCELERATOR DEVELOPMENT AND INSTRUMENTATION	71
1.	Injector Cyclotron	71
2.	High Resolution Development on The Tandem Accelerator	71
a.	Terminal Stabilizer	71
b.	90-90 Analyzing Magnets	74
3.	Polarization Monitoring and Beam Control	74
4.	Pulse Beam Time Pick-Off	74
5.	Improvements in Instrumentation in the 3 MeV Laboratory	75
L.	COMPUTER RELATED DEVELOPMENTS	77
1.	The Prime Computer	77
2.	Computer Program Development for Neutron Data Correction	77
3.	Beam Optics Computer Code	78
M.	NUCLEAR THEORY AND PHENOMENOLOGY	79
1.	Studies of Deuteron Scattering Potentials	79
2.	Wave Functions and Wave Packets	79
3.	Polarization Phenomena in Nuclear Reactions	79
4.	Isospin-Consistent DWBA Analysis of (d,t) and (d, ³ He) Reactions	79
5.	A DWBA Transfer-Reaction Code for Small Computers	79
6.	Dissipative Forces in Quantum Mechanics	79
7.	Survey of Nucleon-Nucleus Scattering Potentials	80
8.	Compound-Nucleus Effects and the Nucleon-Nucleus Spin-Spin Interaction	80
9.	Atomic Effects in Nuclear Resonances	80
10.	Projectile-Size Effects in Deformation Measurements	81
11.	Spin-Orbit Coupling in Heavy-Ion Scattering	81
12.	Compound-Nucleus Fluctuation Theory for Polarized Beams	81
13.	The Energy Splitting of the Lowest 6 ⁻ , T = 0 and T = 1 States in the (sd)-Shell	81
14.	Spectroscopic Factors for the ²⁸ Si(p,d) ²⁷ Si Reaction	82
15.	1975 Mass Predictions	82
16.	Computer Codes for High Accuracy Single Particle States	82
17.	Realistic Single Particle Hamiltonian for Fission and Heavy Ion Calculations	82
18.	Realistic α -Particle Potentials	83
19.	Applications of Group Theory to Rotational Vibrational Bands on Nuclei	83
20.	Exotic Configurations of Super Heavy Nuclei, Bubbles, Torus, etc.	84
21.	Level Density Studies for α Reactions with Targets of A \leq 40	84
22.	Dynamics of Heavy Ion Reactions in a Realistic Time-Dependent Hartree-Fock Model	84
23.	Deep Inelastic Heavy Ion Cross Sections in a T.D.H.F. Model	85
24.	Single Nucleon Induced Fission	85

M.	25.	Low Energy Behavior of Fusion Barriers in Heavy Ion Reactions	86
	26.	The Griffin Model, Complex Particles and Direct Nuclear Reactions	86

APPENDICES

I	TUNL JOURNAL ARTICLES AND ARTICLES BY TUNL PERSONNEL	88
	JOURNAL ARTICLES ACCEPTED FOR PUBLICATION	91
	JOURNAL ARTICLES SUBMITTED FOR PUBLICATION	92
II	TUNL CONFERENCE REPORTS AND REPORTS BY TUNL PERSONNEL January 1976-January 1977	93
III	ABSTRACTS OF TALKS AT AMERICAN PHYSICAL SOCIETY MEETINGS January 1976-January 1977	97
IV	MISCELLANEOUS PUBLICATIONS January 1976-January 1977	99
V	Articles Published, January 1976-January 1977, in Journal edited at TUNL by K. Way	100
VI	TUNL PERSONNEL	103

TRIANGLE UNIVERSITIES NUCLEAR LABORATORYA. NEUTRON AND FISSION PHYSICS

1. Fast Neutron Differential Cross Sections (F. O. Purser, C. R. Gould, P. W. Lisowski, L. W. Seagondollar, C. E. Nelson, P. Von Behren, W. Tornow, H. H. Hogue, S. G. Glendinning, Sadig El Kadi, E. G. Bilpuch, H. W. Newson)

- a. Experimental

- (1) New Neutron Detector

During this report period design work was completed and construction has begun on an additional neutron detector and shield for use in the neutron time-of-flight program. The massive new shield will contain 2700 kg of a 50/50 lithium carbonate and paraffin mixture, 600 kg. of copper, and approximately 900 kg of lead. The collimator is of the Langsdorf double truncated cone design adapted for a 12.7 cm. diameter NE-213 detector.

The angular carriage for the new detector is under construction by a local contractor. The carriage is designed to allow neutron flight paths ranging from 2.0 to 6.0 meters with an angular range from 0° to 165°. The carriage will traverse an elevated iron track similar in design to that in use with our 4 meter detector. The 4 meter track is being extended to cover a full 360° to allow operation with this detector on either side of the target beam line. Delivery of the new angular carriage is anticipated in January of 1977, with final installation of the new detector scheduled for mid to late Spring.

- (2) Tritium Gas Target Capability

Experimental requirements for some of the CTR related measurements planned dictate use of the $T(p,n)^3\text{He}$ reaction as the mono-energetic neutron source. A tritium gas handling system and a system of safeguards to allow use of tritium targets in a university environment has been designed. The system incorporates fast acting valves to isolate tritium spills to the beam line, LN_2 -activated charcoal trapping of pumping stations with vacuum pumps exhausted to an external exhaust stack, and additional air handling equipment in target rooms to allow emergency evacuation in the event of a room spill. Vented storage capacity for tritium contaminated parts and a vented glove box for repair of essential tritium contaminated beam line components are provided. Tritium monitors in the exhaust stack and target room will be installed with remote readouts and permanent tritium level recording in the control room.

b. CTR Related Measurements

(1) Natural Carbon

These data have been published in Nuclear Science and Engineering, vol. 61, page 521, December 1976.

(2) Beryllium 9

The elastic and inelastic data are being prepared for publication and will be submitted to Nuclear Science and Engineering.

Additional measurements on Beryllium were undertaken during this report period to measure the continuum neutron production cross sections at incident neutron energies of 7.0 and 7.5 MeV. For these measurements the bias level of the detector was set at 1/10 the pulse height of the ^{137}Cs gamma or approximately 450 keV neutron energy. Analysis of these data and application of various self consisting checks is in progress.

(3) Lithium 6

Seven elastic and inelastic ($Q = -2.18$) cross section angular distributions have been measured for incident neutron energies of 7.5, 9.0, 10.0, 11.0, 12.0, 13.0 and 14.0 MeV. Preliminary data are shown in Fig. A1-1. Final data analysis required modification of our Monte Carlo multiple scattering code and will be complete in January 1977.

(4) Lithium 7

Eight elastic plus first inelastic ($Q = -0.478$) and second inelastic ($Q = -4.63$) cross section angular distributions have been measured. The preliminary data are shown in Figs. A1-2 and A1-3. Again final data results require the modified Monte Carlo multiple scattering code and will be available in January 1977.

(5) Oxygen 16

Ten elastic scattering angular distributions for ^{16}O have been measured for incident neutron energies from 9.25 MeV to 15.0 MeV. Approximately four more distributions are required to survey the resonance structure in this energy region. The scattering sample used is a 3/4" diameter by 1" high cylinder of BeO. Backgrounds were measured and the effect of the Beryllium removed from the spectra by using a cylinder of pure Beryllium as the "out" count scatterer. Preliminary data at a few energies, uncorrected for geometric and multiple scattering effects are shown in Fig. A1-4.

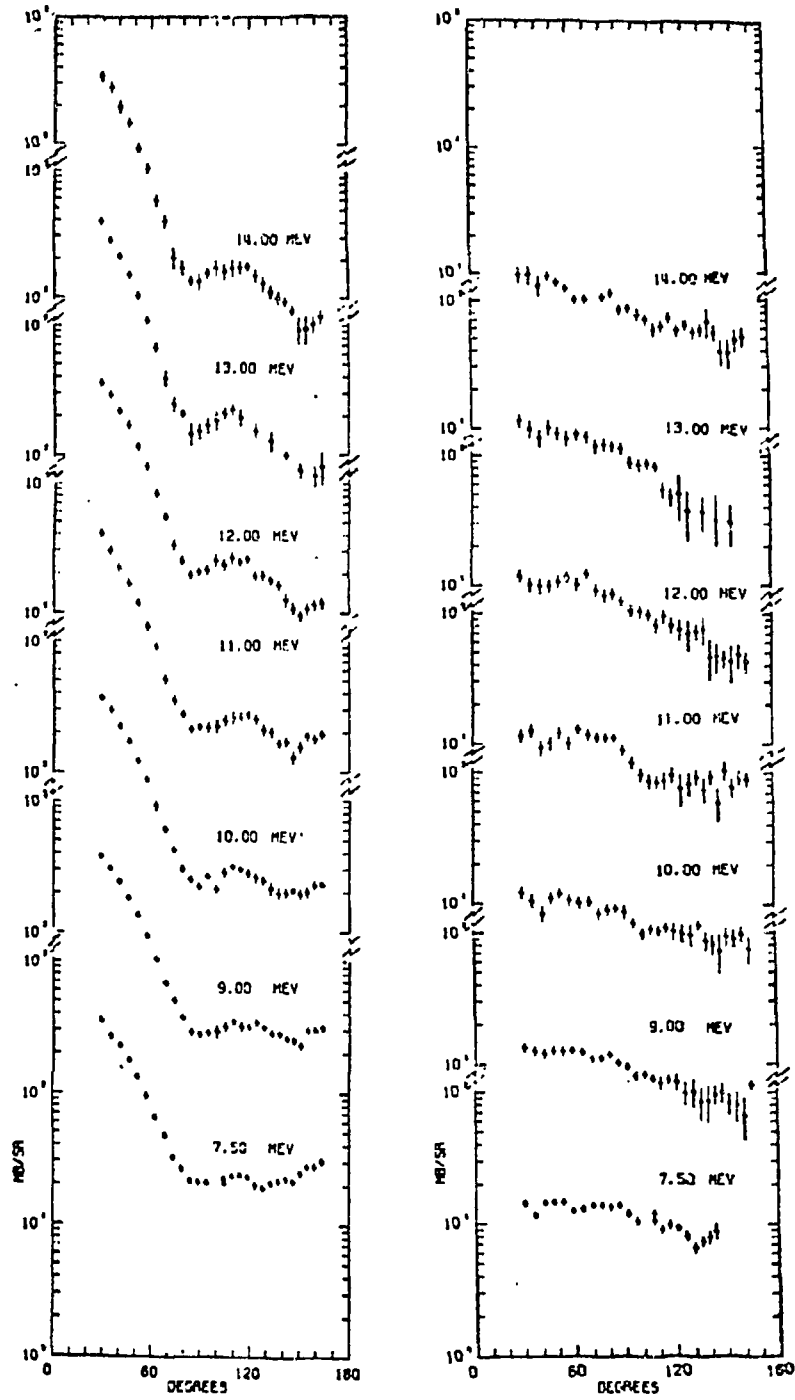


Fig. A1-1. Elastic and inelastic ($Q = -2.184$ MeV) neutron scattering angular distributions for ${}^6\text{Li}$. The large error bars assigned to the inelastic data at back angles are due to large background subtraction uncertainties.

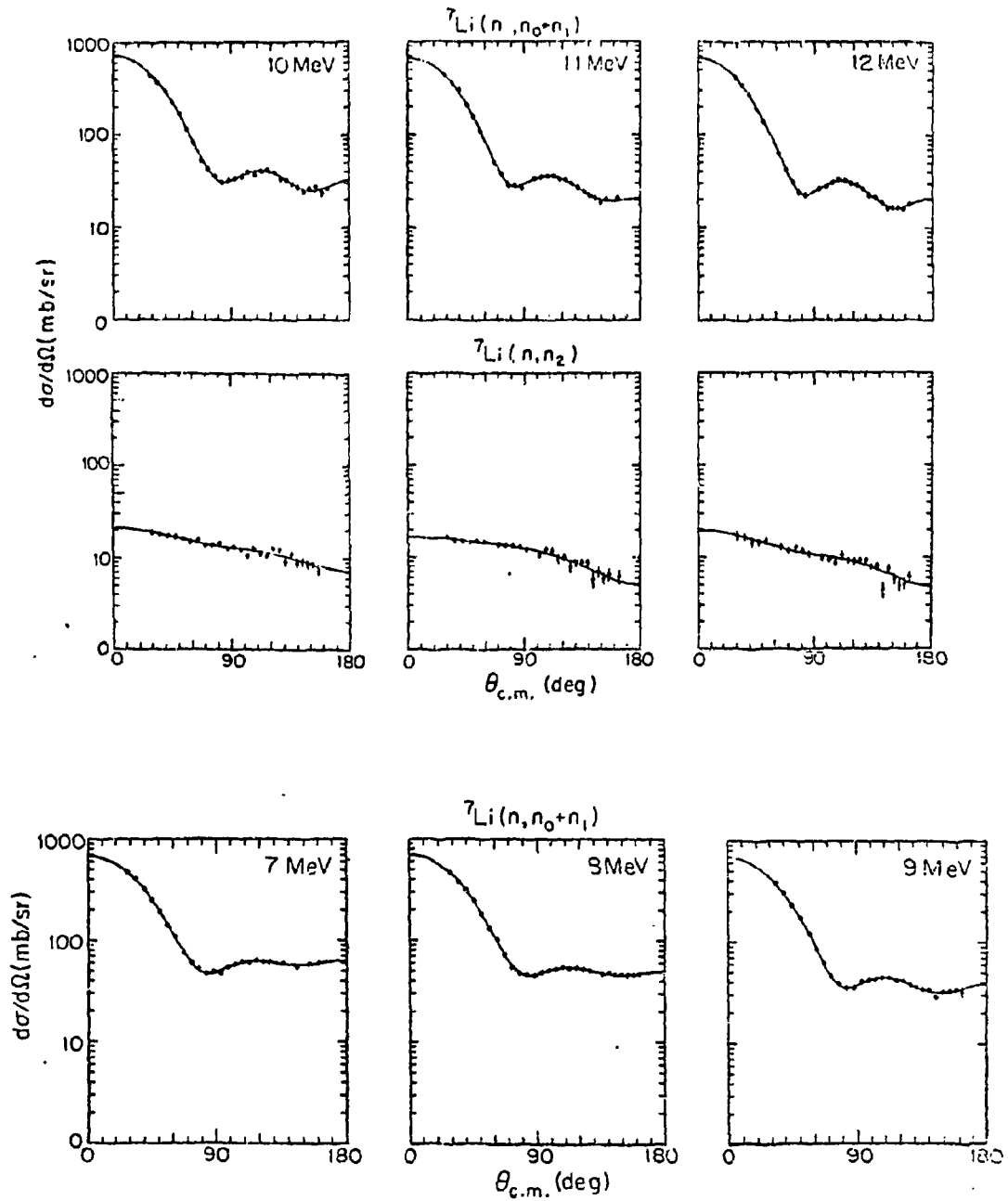


Fig. A1-2. Neutron elastic and inelastic ($Q = -4.63$ MeV scattering angular distributions from ${}^7\text{Li}$. Contributions from the 0.478 MeV state were non-separable from elastic scattering and are included in the elastic data.

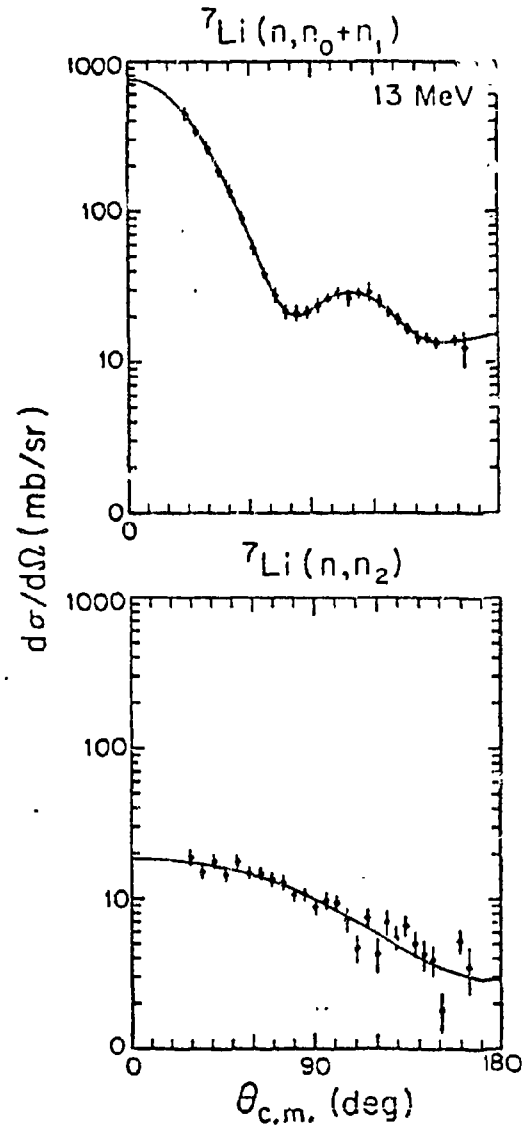


Fig. A1-3. Neutron elastic and inelastic ($Q = -4.63$ MeV scattering angular distributions from ${}^7\text{Li}$. Contributions from the 0.478 MeV state were non-separable from elastic scattering and are included in the elastic data.

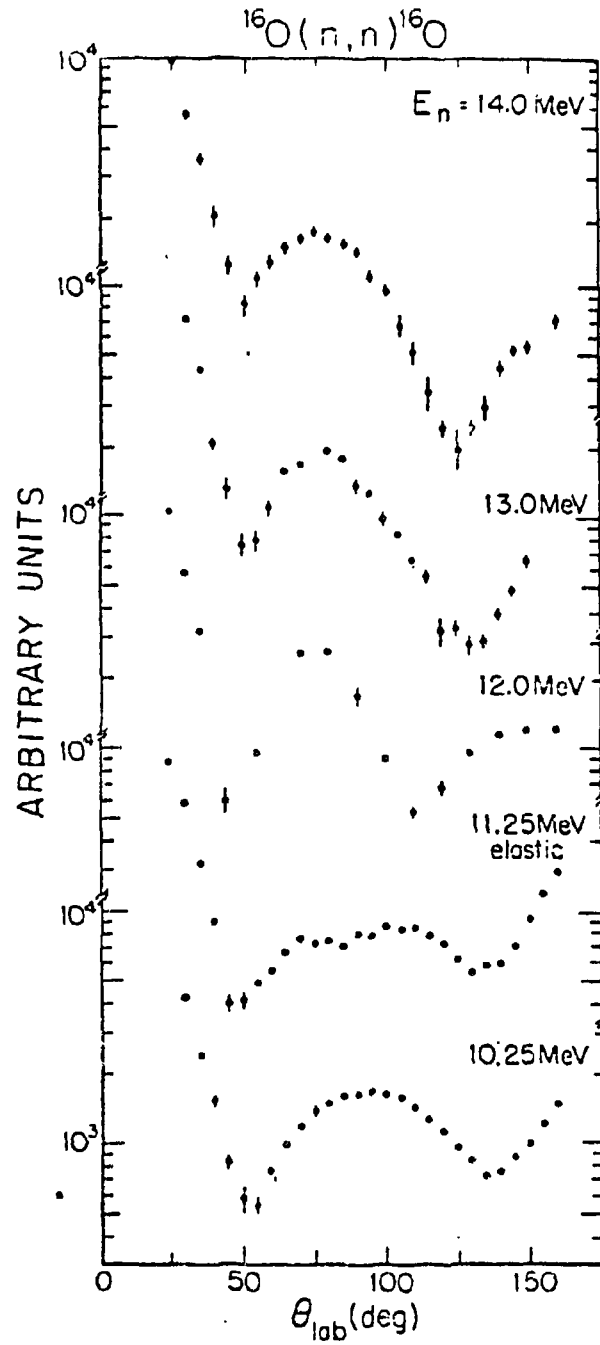


Fig. A1-4. Partial and preliminary results for neutron elastic scattering from ^{16}O . These data have not been corrected for finite geometry or multiple scattering effects and have not been converted to absolute cross sections.

(6) Boron 10 and Boron 11

Scattering samples for these isotopes have been ordered and are due to arrive in January.

(7) Small Angle Measurements

This program has been inactive for the present report period. However, the data acquisition electronics set up has been modified to be more compatible with the high levels of raw counting rates associated with this type of measurement. A scattering sample of ^{93}Nb has been provided by A. B. Smith at ANL and small angle measurements ($3^\circ \leq \theta_L \leq 15^\circ$) of this isotope are scheduled for Spring 1977.

c. Search for States of High Excitation (713 MeV) in ^7Li (P. Von Behren and C. E. Nelson)

Neutron elastic and inelastic differential cross sections to the first excited state in ^6Li are being measured to determine the existence of a possible broad (>4 MeV) state in ^7Li at 16.8 MeV excitation energy. Excitation functions at two angles, 89° and 108° in the laboratory, have been measured in 250 keV steps from $E_n = 10.5$ to 13.0 MeV. The elastic data showed no structure at the backward angle and at 89° was indeterminate due to background problems. The inelastic data at both angles show a peak at approximately 11.2 MeV incident neutron energy which corresponds to an excitation energy of 16.9 MeV in the ^7Li system. The indicated resonance width is uncertain but is greater than 1.0 MeV. The excitation energy of 16.9 MeV agrees well with the value of 16.9 MeV observed in (γ, n) data.

There are predictions of possible levels at these higher excitation energies in ^7Li . R-matrix calculations¹⁾ suggest $1/2^+$, $3/2^+$ and $5/2^+$ states in the region of interest while resonating group theory calculations²⁾ predict a $1/2^+$ resonance in neutron elastic scattering from ^6Li at 11.7 MeV incident neutron energy. It is important to the understanding of the structure of ^7Li to determine if such levels do exist. We plan to improve the neutron energy resolution of measurements and extend our data to both higher and lower excitation energies in ^7Li .

d. Theoretical Analysis of Neutron Data

This program has been inactive for the current report period.

1) G. M. Hale, private communication

2) W. Laskar and B. Remaud, *Le Journal de Physique*, vol. 34, p. 783 (1973)

2. Resolved Neutron Total Cross Sections and Intermediate Structure
(J. Clement, * B.-H. Choi, ** W. F. E. Pineo, + M. Divadeenam, ++
H. W. Newson)

The paper entitled "Intermediate Structure in the $^{28}\text{Si} + n$ Reaction: R-Matrix Interpretation of Experimental Data" will appear in Vol. 102, No. 2 (1977) of Annals of Physics as Part Xf(i) of our series "s- and p-wave Neutron Spectroscopy". The revised abstract follows:

"A multi-level R-matrix analysis of Si neutron cross section data measured at NBS has been performed up to about 4.5 MeV neutron energy. Only a small fraction of the p- and s-wave s.p. strength is observed, but both exhibit local concentrations of strength indicative of doorway structure around 1 MeV and 0.2 MeV respectively. Besides the well known 180 keV, strong, $1/2^+$ resonance, the s-wave resonance structure is of moderate strength and widely distributed. The f- and d-wave assignments are not unambiguous, but $J > 3/2$ resonances show strong signs of intermediate structure at least for d-waves. A possible correlation between neutron and gamma decay channels and the connection between the states observed in (n,n) , (d,p) , (n,γ) and (γ,n) channels is discussed. A core-particle doorway interpretation for s- and p-waves is presented in the same issue of the Annals of Physics."

3. Theoretical Investigation of Neutron Cross Section Measurements
(M. Divadeenam, ++ S. Ramavataram, ++ B. Castel, ++ D. Halderson, ++
H. W. Newson)

S- and P-wave Neutron Spectroscopy: Part Xf(ii) Intermediate Structure in the $^{28}\text{Si} + n$ Reaction: Doorway State Calculation. The abstract follows.

"A core-particle calculation developed to describe the low-lying structure of ^{29}Si is extended above neutron threshold energy to yield information on the structure of doorway states indicated by the $^{29}\text{Si} + n$ reaction. The recent experimental evidence for a $J = 3/2^-$ doorway state common to the $^{28}\text{Si} + n$ and the $^{29}\text{Si} + \gamma$ channels is supported by the calculation which also reproduces correctly the magnitudes of the neutron escape widths and the E1 radiative strengths of the $1/2^-$ and $3/2^-$ doorway states."

* Rice University, Houston, Texas

** Pacific Lutheran University, Tacoma, Washington

+ Meadville, Pa.

++ Brookhaven National Laboratory, Upton, New York

+++ Universite de Laval, Quebec, Canada

4. A Selectively Excited and Distorted [Liquid] Drop (SEXDD) Fission Model
(H. W. Newson)

These Selection Rules have been simplified as follows:

- I. THE EXCITED NUCLEONS AT SCISSION ARE DISTRIBUTED IN THE ORBITS STATISTICALLY FAVORED FOR DEFORMABLE FRAGMENTS, IF (AT LEAST FOR SPONTANEOUS FISSION)
- II. THE FINAL BARRIER SELECTS IN THE TWO INCIPIENT FRAGMENTS THE MAXIMUM COMBINED NUMBER:
 - a) OF FILLED MAJOR SHELLS WHICH ARE CONSERVED SELECTIVELY BY KINEMATIC EFFECTS AND
 - b) OF PAIRS OF NUCLEONS MOST OF WHICH ARE EFFECTIVELY CONSERVED IF
- III. THE LIQUID DROP MODEL (LDM) DESCRIBES THE COLLECTIVE ASPECTS OF THE FISSION PROCESS ADEQUATELY, AT LEAST AFTER THE FINAL BARRIER.

Rule III should certainly be acceptable to the conventional wisdom, and it includes, of course, the statistics of the collective states. Since individual nucleons in excited orbits can not be ruled out, consideration of their statistics as in Rule I is necessary. Note that, unlike references 1 and 2, Rule I does not assume a priori that the spherical shell model is applicable at scission. Rule IIb is reasonable to the extent that pairing of all nucleons should help to penetrate the fission barrier and a complex potential implies a slow breakup of pairs relative to the fast transition between barrier and scission predicted by the LDM.

However, Rule IIa is radical in that it implies a spherical shell effect at a saddlepoint which we visualize as highly distorted and conservation even of the pairs (e.g., $s^{1/2}$, $p^{1/2}$, $d^{3/2}$) with lower pairing energies than some of the valence nucleons. Since we define Rule II for very improbable barrier penetrations we have assumed only a residual shell effect, and some of the closed subshells (e.g., $g^{9/2}$, $h^{11/2}$, etc.) should be very strongly conserved, but if Rule IIa is to be useful, it should be a valid approximation for thermal neutron, as well as, spontaneous fission.

We have therefore devised a simple test: If Rule IIa is valid at all excitation energies, the average, median, and/or maximum fission yield should never be less than $50 + 82 = 132$ in the heavy fragment since Rule IIa requires that the 82N and 50Z shells be filled in the majority of heavy fragments. Also if Rule IIb is valid, there should be sufficient events in which all nucleons are paired in one slightly excited fragment to observe fine structure since the even-even fragments which most nearly satisfy the equation $A_L/Z_L = A_H/Z_H$ are energetically favored and are known to be the most prolific primary fragment in each even mass chain. One primary fragment in all odd mass chains satisfies $\langle \text{UCD} \rangle$ so well that little fine structure is expected in them.

Data³⁾ taken by the ORNL group have been reanalyzed to form a family of adiabatic curves which give the yield as a function of mass at various total excitation energies (both fragments) varying between about ~ 2 MeV and ~ 50 MeV. These were formed from the published contour diagrams by plotting the empirical $Q(A)$ on the

same scale, displacing it downward by various amounts between 3 and 50 MeV, and plotting the intersection of the displaced Q values with the contour lines. Since the excitation energy, $E_x(A) = Q(A^-) - E_k(A)$ (the total kinetic energy of both fragments) all points on any resulting yield curves are at the same E_x . The adiabat of the lowest excitation energy is very narrow with a median corresponding to the product ${}^{132}_{50}\text{Sn}_{82}$ with no detectable heavy fragments lighter than ${}^{128}_{50}\text{Sn}$. As excitation energy increases the median and maximum values move toward larger A_H and at $E_x = 25$ MeV the curve is very similar to the total fission yield curve. At higher excitation energies inferred from the more accurate empirical Q , the effect reverses, the median value goes to smaller A_H as excitation energy increases, but the median value does not sink below $A_H \approx 132$ as predicted by Rule IIa. This treatment of thermal fission of U^{233} , U^{235} , Pu^{239} , Pu^{241} , and $\text{Cf}^{252}(\text{sf})$ all showed the same effect.

The above treatment averaged out all signs of fine structure in the yields. In order to eliminate the pointscatter in the empirical Q value, Seeger's mass formula was used in a more detailed treatment. This analysis gave adiabats in E_x steps of 6 MeV and showed the expected (Fig. A4-1d) fine structured peaks at $A_H = 134, 138$ and 144 but none for odd fragments (Fig. A4-1a). This effect has already been reported using the⁴⁾ fairly good approximation $Q(A) \approx Q(134)$. As excitation energy increases (Fig. A4-1a) this fine structure nearly dies out before $E_x = \langle E_x \rangle \approx 20$ MeV. At higher excitation energy the smooth behavior persists (Fig. A4-1b) up to $E_x = 30$ MeV (which includes nearly all of the fission yield) while the median A_H decreases. However, strong fine structure also reappears over a wider range (Fig. A4-1d) and the adiabat at greatest observable excitation energies ($E_x > 45$ MeV) is very similar to that at $E_x < 5$ MeV. Since fine structure should be most easily observable when all nucleons in one fragment are paired, (a condition which is probable only at low excitation energies), this behavior shows that not only are the major shells at 28, 50, and 82, but also pairs are effectively conserved as predicted by Rule II when one of the fragments is slightly excited. The statistics of Rules I and III modified by Rule II predict little fine structure when $(E_x)_L \approx (E_x)_H \approx E_x/2$ but at sufficiently high $E_x (\equiv (E_x)_L + (E_x)_H)$ one fragment should be much more excited than the other which should then be capable of exhibiting obvious fine structure. These statistical arguments are similar to those used in Ref. 1.

Caption Fig. A4-1a: Adiabats (a family of curves of yield as functions of A) for various excitation energies $\langle E_x \rangle \approx E_x [\equiv (E_x)_L + (E_x)_H]$. Since marked fine structure is expected only for even fragments the curves for lower E_x were interpreted by connecting every other point with a solid line and the remaining points with dashed lines which generate rather smooth curves. We interpret the latter as the odd mass chains. The points connected by solid lines show sharp peaks where fine structure peaks are expected in Fig. A4-1c which is a plot of empirical charge distribution expression: $1/[\text{Exp}2(Z_p - Z^{\text{even}})^2]$ where $Z_p = [(236/92)/A^{\text{even}}]^{-1} = A^{\text{even}}/2.65$ and Z^{even} is the nearest even Z to Z_p for a given A . Since relatively few primary fission fragments have no unpaired nucleons, the curve in (c) approximates only the most favorable case where E_x approaches zero and even then it should be compared to the difference between the solid and the dashed curves. (b) and (d) show the same interpretation of the data when $\langle E_x \rangle \ll E_x$. Note that in the upper curves of both (a) and (b) there is also evidence for fine structure, but not much.

- 1) H.W. Newson, Phys. Rev. 122 (1961) 1224
- 2) P. Fong, Phys. Rev. 102 (1956) 439
- 3) F. Pleasonton, Phys. Rev. 174 (1968) 1500 and previous ORNL data
- 4) J. Punik, et al., Physics and Chemistry of Fission (1973) Vol. II, p. 19

$^{235}\text{U}(n_{th}, f)$

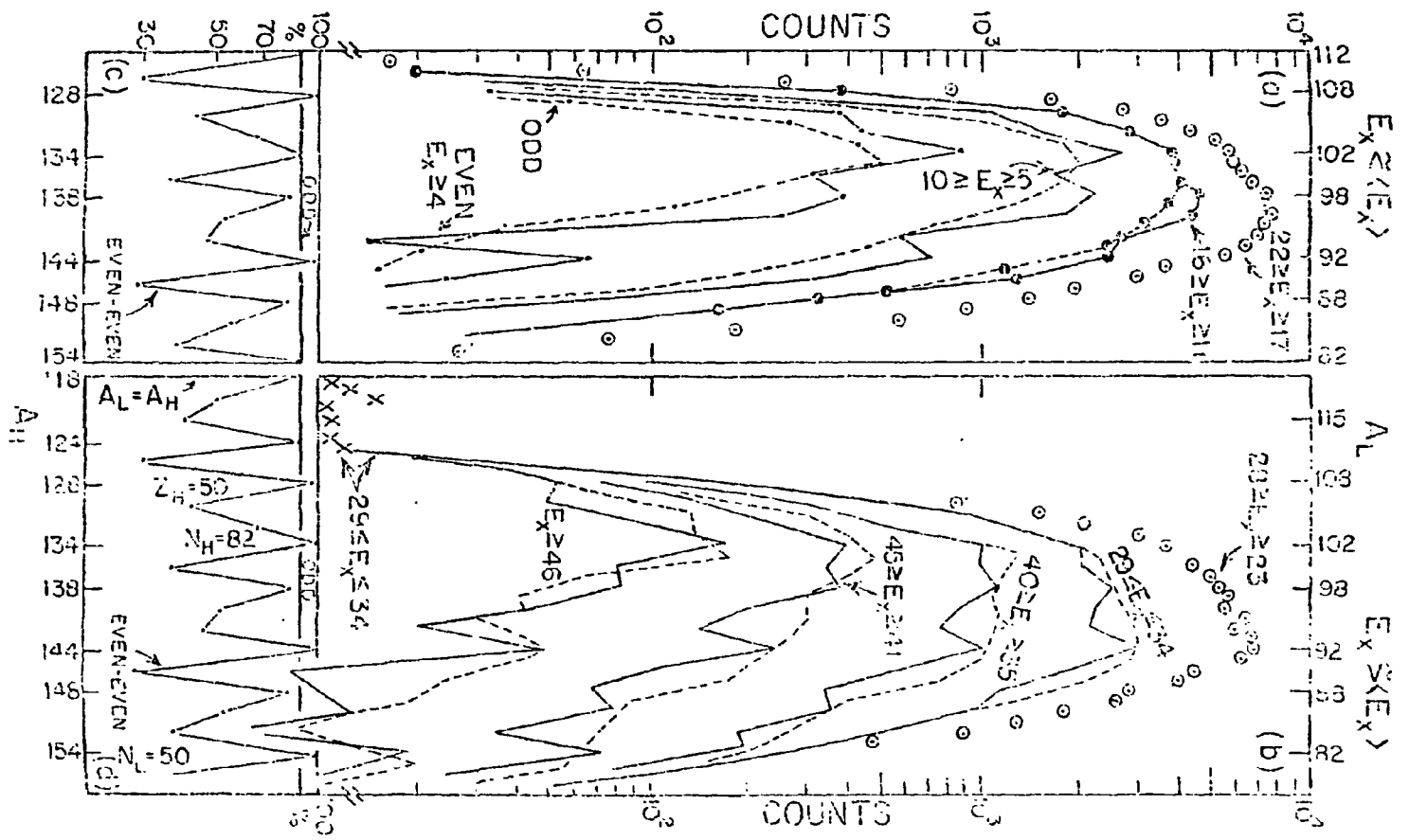


Fig. A4-1a

BLANK PAGE

5. Charged Particle Fission (F. O. Purser, D. H. Epperson, H. W. Schmitt, E. G. Bilpuch, H. W. Newson)

In order to unfold contributions of sequential fission channels in the fragment mass and kinetic energy distributions of ^{236}Np for excitation energies ranging from subthreshold to 27 MeV it is necessary to have an accurate estimate of the total fission probability as well as the fission probabilities for first, second and third chance fission as functions of excitation energy. The total fission probability was obtained by dividing the experimental fission cross sections of Boyce¹⁾ et al. by the proton total reaction cross sections as calculated by an optical model. Due to the lack of optical model parameters for heavy nuclei at low proton energies it was not surprising that the resulting probabilities in the low energy region did not compare favorably with the direct measurements in the first chance region by Gavron²⁾ et al. In order to get reasonable agreement in this excitation energy region it was necessary to assume that uranium has an effective charge of 94.92 in the spherical optical model formulation utilized to calculate the reaction cross sections.

The neutron partial decay width Γ_n calculated by Weisskopf³⁾ uses neutron reaction cross sections. In Boyce's work, these cross sections were calculated with the optical model and were assumed identical for all isotopes of Np. It was observed that the experimental cross sections of the uranium isotopes, demonstrated a strong $E_f - B_n$ dependence. A table of neutron cross sections dependent on $E_f - B_n$ was generated for the Np isotopes as follows: A search of the ENDL⁴⁾ library of neutron cross sections for the actinides yielded cross sections for nuclei close to Np on the chart of nuclides with similar neutron binding energies and fission barrier heights. From these nuclei a set of neutron cross sections displaying the same $E_f - B_n$ dependence as does the uranium set was obtained and incorporated into the statistical decay model calculation of the first, second and third chance fission probabilities and produced improved agreement with the data.

A comparison of the statistical decay model calculation of the fission probabilities with the Gavron data revealed that at low excitation energies (3-9 MeV) the model was not giving a good approximation. The agreement is good from 9 MeV to 12 MeV where the Gavron data stops. The poor agreement is probably due to the inadequacy of the Gilbert and Cameron⁵⁾ form of the level density at the saddle point of the fissioning nucleus. The calculation was revised to use the experimental fission probabilities of Gavron et al. in the excitation energy range from 3-9 MeV and to match these smoothly with the calculated values from 9-30 MeV.

The reduction of the kinetic energies of correlated fission fragment mass pairs is currently near completion. From these spectra, fragment mass and kinetic energy distributions for a single fissioning nucleus (^{236}Np) as a function of excitation energy will be extracted using the previously described fission probability calculations to unfold contributions of other than 1st chance fission.

1) J. R. Boyce et al., Phys. Rev. C10, 231 (1974)

2) Gavron et al., Phys. Rev. C13, 2374 (1976)

3) V. F. Weisskopf, Phys. Rev. 52, 295 (1937)

4) The LLL Evaluated Nuclear Data Library, UCRL-50400 Vol. 15 Part C (1976)

5) A. Gilbert and A. G. W. Cameron, Can. J. Phys. 43, 1440 (1965)

B. NEUTRON POLARIZATION STUDIES

1. Analyzing Power Measurements for n-p Scattering from 10 to 18 MeV (W. Tornow, P. O. Lisowski, R. G. Byrd, S. S. Skubic, R. L. Walter)

a. Measurements

To complement the recent accurate measurement¹⁾ of the analyzing power A_y measurements for p-p scattering, we have undertaken a project to make the most accurate determinations of A_y for n-p scattering. The region between 10 and 18 MeV is being studied and the source of polarized neutrons is the $D(d,n)^3\text{He}$ reaction induced by a polarized deuteron beam. The reaction angle is 0° and the neutron polarization is approximately 60%. The target for n-p scattering is hydrogen contained in an organic scintillator. Data are buffer stored on magnetic tape for off-line analysis and about 10^6 counts will be obtained at each point measured. The data reported at the Zurich Polarization Conference²⁾ has been repeated with improved accuracy. The most recent data are compared in Fig. B1-1 to earlier results and to calculations using the three available sets of n-p phase shifts. Although these data are not yet considered final, we do not expect any corrections that will shift the data significantly closer to the theoretical values. (See part B1-b.) These measurements will be rechecked and additional points will be obtained in the near future before final publication. These data were reported at the Lowell Tech. International Neutron Conference (1976).

1) J. D. Hutton, W. Haerberli, L. D. Knutson, and P. Signell, Proc. of the Zurich Polarization Conference, Birkhäuser Verlag (1976) p. 448

2) W. Tornow, P. W. Lisowski, R. C. Byrd, S. E. Skubic, R. L. Walter and T. B. Clegg, Proc. of the Zurich Polarization Conference, Birkhäuser Verlag (1976) p. 439

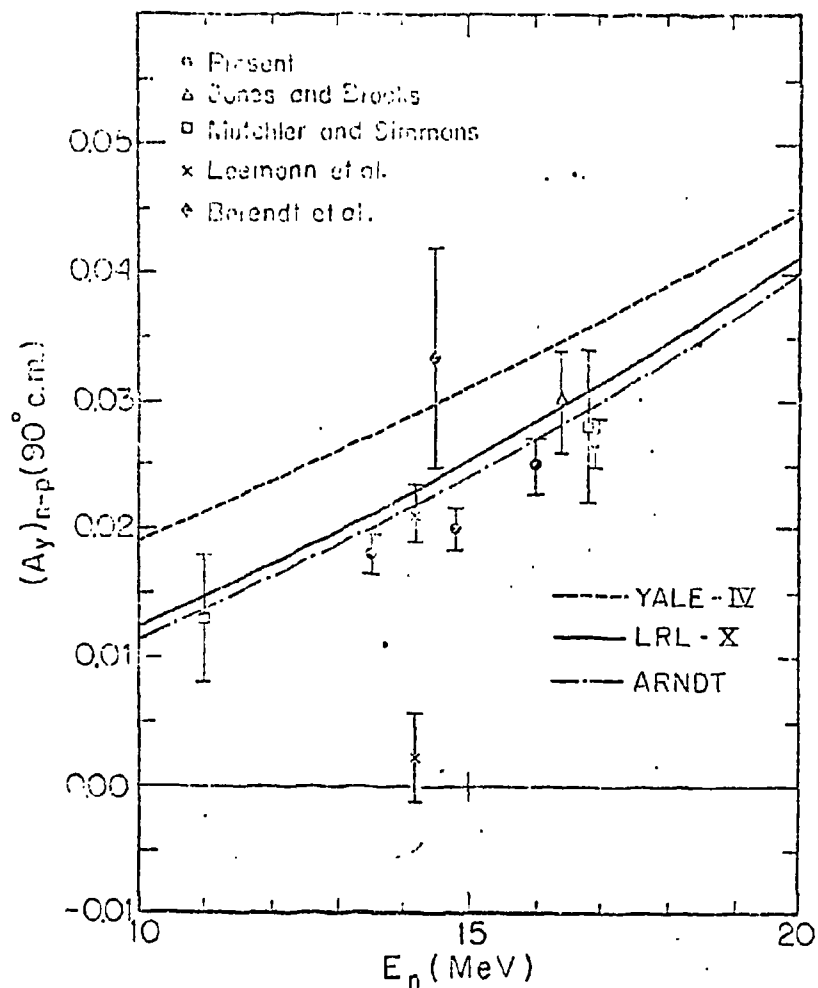


Fig. B1-1. Analyzing power for n-p scattering at 90° c.m. The theoretical predictions are represented by the three curves. The present results fall systematically lower than the theoretical curves.

b. Corrections to The A_y Data

A Monte Carlo code which incorporates the exact dimensions of the components (i.e., D_2 gas cell, shadow bars, center-scatterer, and side detectors) has been written to enable a determination of the best design for n-p scattering experiments using the above neutron source, and neutron time-of-flight (TOF) discrimination for the center-to-side detector scatterings. Multiple scattering backgrounds are generated and by placement of time-windows on the TOF spectra, the best choice of geometrical parameters is obtained. Furthermore, for the final choice, the code will have already generated the corrections to be applied to the raw data to compensate for the dilution of the A_y values for these effects. The code employs available cross-section information. One can also calculate the effect of multiple scattering from ^{12}C and ^1H existing in the center detector. Currently, an attempt is being made to incorporate the polarization effect caused by the ^{12}C in the central scatterer, although this effect is anticipated to be less than the size of the present error bars. The code is written in a flexible manner such that variations of it can be utilized for other experimental situations as described below.

The measured spectra compare favorably to those obtained with the code, but additional (unpolarized) backgrounds are exhibited in the measured spectra. The corrections for these unknown sources of pulses are small, and the error bars on the data exhibited in Fig. B1-1 include uncertainties due to these backgrounds.

2. Analyzing Power Measurements for n-d Scattering at 12 MeV (W. Tornow, P. W. Lisowski, R. G. Byrd, R. L. Walter)

An angular distribution of the analyzing power $A_y(\theta)$ for n-d scattering has been obtained at 12 MeV with greatly improved accuracy and over a wider angular range than has previously been available. Data were collected for ten angles between 40° to 140° (lab) to an accuracy ranging from ± 0.007 to 0.015. Such data are expected to reflect the differences between p-d (for which a large amount of $A_y(\theta)$ data have been accumulated) and n-d scattering. The neutron data are now comparable in accuracy to the proton data³⁾ and to within these accuracies, the two sets of data agree with one another. This finding is in agreement with some of the recent results at higher energies and contradicts the earlier comparisons that showed significant differences between $A_y(\theta)$ functions for the two systems. A preliminary report of these findings was given at the Lowell Tech. International Neutron Conference (1976). Corrections to the data for neutron multiple scattering from all sources were calculated using the above mentioned Monte Carlo code. The data are nearly finalized and a paper is being prepared.

3. Analyzing Power for $^{12}\text{C}(n,n)^{12}\text{C}$ Scattering

Because the central scatterer in the n-p and n-d experiments above contains ^{12}C , the effects of multiple scattering involving ^{12}C must be known. It was originally planned to perform measurements of $A_y(\theta)$ for $^{12}\text{C}(n,n)^{12}\text{C}$ over the range of interest,

³⁾ T. B. Clegg and W. Haerberli, Nucl. Phys. A95 (1967) 608

i.e., about 6 MeV to 18 MeV. Preliminary tests employing a ^{12}C scintillator (diamond) showed that the experiment using the $^2\text{H}(\vec{d}, \vec{n})^3\text{He}$ as a source of polarized neutrons was feasible. However, parallel tests conducted with enhanced ^{12}C scattering for the n-p study (Zurich Polarization Conference²⁾ suggested that the effects were negligible. Until the version of the Monte Carlo code which includes the $A_Y(\theta)$ for $^{12}\text{C}(n, n)^{12}\text{C}$ is functional, further ^{12}C experiments will be postponed unless there is a demand for such data to complement the existing TUNL ^{12}C cross-section information.

4. Neutron Polarization and Analyzing Power in the $\text{H}(\vec{t}, \vec{n})^3\text{He}$ Reaction Using a Polarized Triton Beam (R. A. Hardekopf, * G. G. Ohlsen, * P. W. Lisowski, R. L. Walter)

The measurements of $A_Y(\theta)$ and the polarization transfer coefficients K_Y^i which were conducted at LASL for the $\text{H}(t, n)^3\text{He}$ reaction from 6.5 to 16 MeV have been reported preliminarily at Zurich⁴⁾ and have been given to the LASL theorists who are involved in the 4-nucleon system calculations. A final report of this experiment will follow the theoretical analyses.

5. Similarities between $A_Y(\theta)$ and $P_Y(\theta)$ for the $^3\text{H}(p, n)^3\text{He}$ Reaction (W. Tarnow, P. W. Lisowski, R. C. Byrd, R. L. Walter, T. R. Donoghue* *)

Concern over the inequalities of the analyzing power A_Y for an incident polarized beam and the polarization P_Y for an incident unpolarized beam for (p, n) reactions began in 1971 with the reaction $^3\text{H}(p, n)^3\text{He}$. A large difference in these two quantities was interpreted to mean that the lowest 2^- state in ^4He was an admixture of p- and f-waves which caused some interest. Furthermore, as other P_Y and A_Y comparisons that we were conducting for other (p, n) reactions showed near similarity (at that time) we began to question the accuracy of previous A_Y and P_Y data for the $^3\text{H}(p, n)^3\text{He}$ reactions. Donoghue's group at Ohio State University remeasured the $A_Y(\theta)$ values below 6 MeV and at TUNL we independently verified the accuracy of the earlier $A_Y(\theta)$ data. Next we performed a careful measurement of the $^3\text{H}(p, n)^3\text{He}$ $P_Y(\theta)$ distributions, and after careful off-line scrutiny found the earlier data to be too low by about 20% in the region of the largest disparity. Examples of the new $A_Y(\theta)$ data (obtained at OSU) and the new $P_Y(\theta)$ data (obtained at TUNL) are shown in Figs. B5-1 and B5-2. Comparisons are also made to the earlier A_Y and P_Y values. The curves in Figs. B5-1b, B5-2b, and B5-2d represent fits to the $A_Y(\theta)$ data! Clearly the new $P_Y(\theta)$ data do not exhibit statistically significant differences from $A_Y(\theta)$. Hence, the f-wave admixture in the lowest 2^- state in ^4He is no longer required. This work was reported in Phys. Rev. Letters 37 (1976) 981 and is being written up for a more complete publication.

* Staff member at Los Alamos Scientific Laboratory

** Visiting professor from Ohio State University

4) R. A. Hardekopf, G. G. Ohlsen, P. W. Lisowski, R. L. Walter, Zurich Polarization Conference, Birkhäuser Verlag (1976) p. 528

5) P. W. Lisowski, R. C. Byrd, R. L. Walter, T. B. Clegg, Zurich Polarization Conference, Birkhäuser Verlag (1976) p. 573

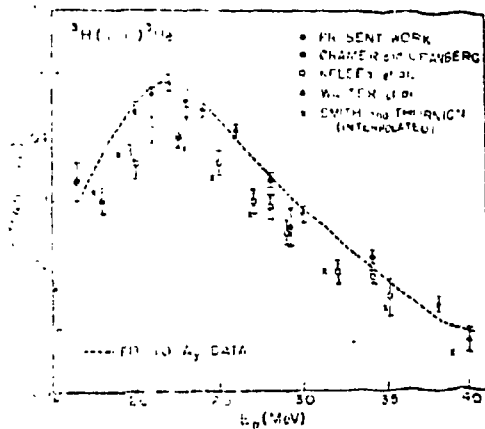
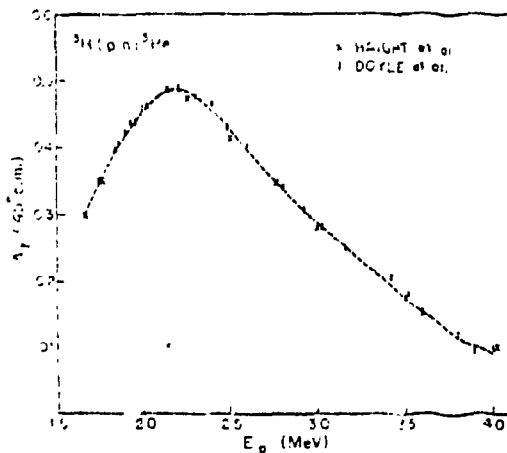


Fig. B5-1. Comparison of $A_y(45^\circ)$ and $P_Y(45^\circ)$ for the ${}^3\text{H}(p,n){}^3\text{He}$ reaction between 1.5 and 4 MeV. Note that the new P_Y data are significantly higher than the older data, and that P_Y and A_y are in good agreement to one another.

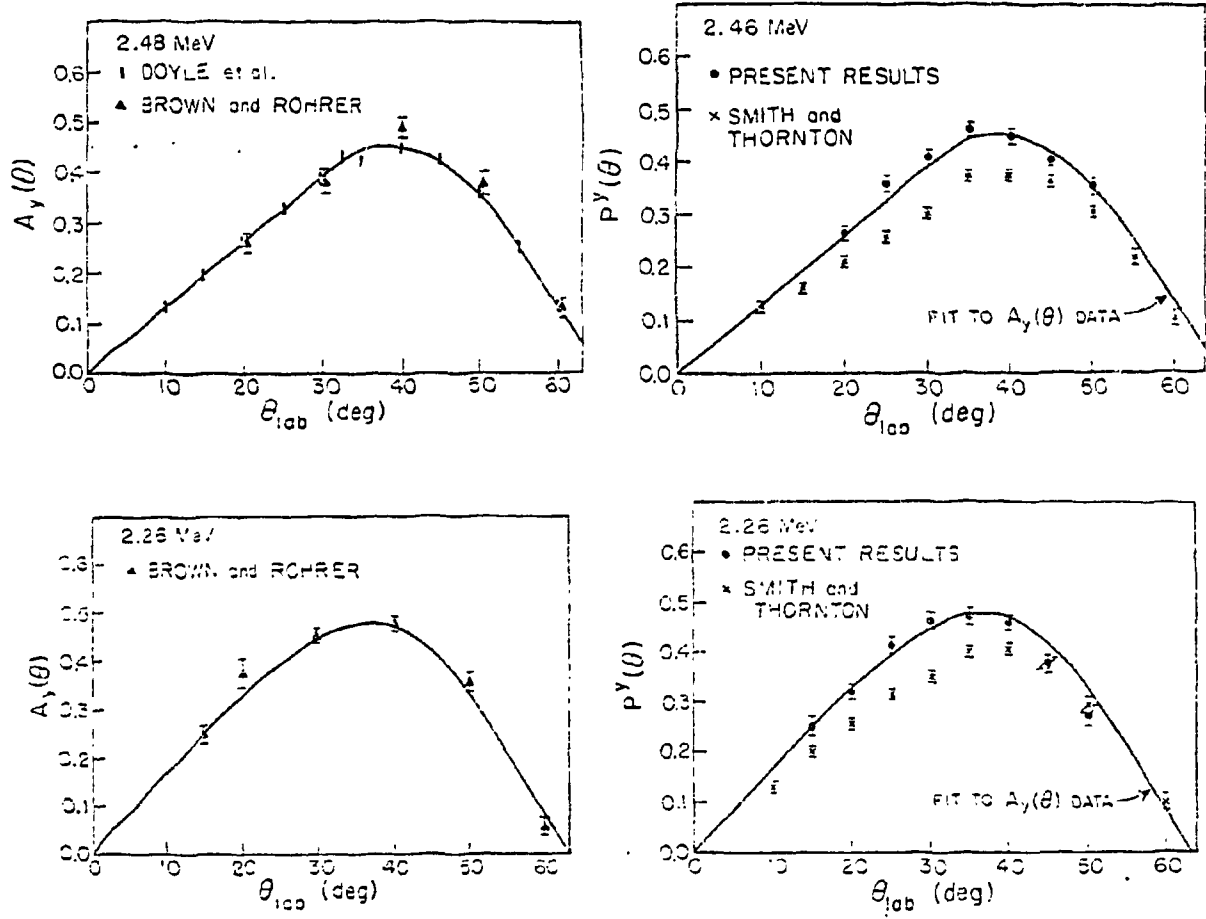


Fig. B5-2. Comparison of new $A_y(\theta)$ data to $PY(\theta)$ for the ${}^3\text{H}(p,n){}^3\text{He}$ reaction for two low energies. Note the agreement of the newer PY data to the curve which is a fit to the A_y data.

6. Remeasurement of P_Y for the ${}^2\text{H}(d, \vec{n}){}^3\text{He}$ Reaction and Its Implication to the f-wave Admixture of the 2- State at 22 MeV in ${}^4\text{He}$ (W. Tornow, S. S. Skubic, R. C. Byrd, P. W. Lisowski, R. L. Walter)

One indication that existing $P_Y(\theta)$ data for the ${}^3\text{H}(t, n){}^3\text{He}$ reaction may be in error (see Section B5) came from a remeasurement at TUNL of $P_Y(\theta)$ at 2.44 MeV for the ${}^2\text{H}(d, n){}^3\text{He}$. The results of this latter experiment and its implications were described in a paper titled with the heading above. It appeared in Phys. Rev. C13 (1976) 2080.

7. Neutron Polarization Produced by the Breakup of Vector Polarized Deuterons on ${}^2\text{H}$ and ${}^4\text{He}$ (P. W. Lisowski, R. C. Byrd, T. B. Clegg, R. L. Walter)

The polarization of neutrons produced in the breakup of vector polarized deuterons on ${}^2\text{H}$ and ${}^4\text{He}$ has been measured at 0° reaction angle at 8.7, 11.4 and 14.4 MeV. The values obtained for K_Y for the ${}^4\text{He}$ reaction at all energies and the ${}^2\text{H}$ reaction at the highest energy are about 10% in magnitude below the value of 2/3, a result one expects in a simple stripping picture where one assumes little perturbation due to other effects. Other models which describe breakup might be able to show similar predictions, but no calculations have been made to date. The data appeared in the Zurich Polarization Conference Proceedings⁵⁾ and are in final form for a more complete paper.

8. Polarization Transfer in the ${}^2\text{H}(\vec{t}, \vec{n}){}^4\text{He}$ Reaction (G. G. Ohlsen,* R. A. Hardekopf,* R. L. Walter,** P. W. Lisowski**)

Measurements have been made of the neutron polarization from the ${}^2\text{H}(\vec{t}, \vec{n}){}^4\text{He}$ reaction with polarized tritons incident. The experiment which was conducted at Los Alamos Scientific Laboratory involved a study of the polarization transfer coefficient K_Y at 0° from 5 to 16 MeV and from 0° to 120° at 10.5 MeV. The data showed the inadequacy of the current R-matrix parameterization of the mass-5 system in the energy range above about 25 MeV. The data appeared in Phys. Rev. Letters 14 (1976) 1688.

9. A Calibrated Source of High Energy Polarized Neutrons Obtained from $A_{zz}(0^\circ)$ Measurements for the ${}^3\text{H}(d, n){}^4\text{He}$ Reaction (P. W. Lisowski, R. L. Walter, R. A. Hardekopf, G. G. Ohlsen)

For the ${}^3\text{H}(d, n){}^4\text{He}$ measurement, G. G. Ohlsen et al. showed that if one knows $A_{zz}(0^\circ)$, one can know the value for the longitudinal polarization transfer $K_Z^Z(0^\circ)$ and hence, can predict (or calibrate) the neutron polarization produced in this reaction from knowledge of the magnitude of the incoming (longitudinal) deuteron polarization. $A_{zz}(0^\circ)$ was measured to better than ± 0.02 from 4 to 12 MeV at LASL. This yields a neutron source of known polarization for E_n from 20 to 30 MeV. This work was also published in Phys. Rev. Letters 13 (1976) 809.

* Staff member at Los Alamos Scientific Laboratory

** Visiting staff member at Los Alamos Scientific Laboratory (June 1975)

10. Elastic Scattering of Polarized Neutrons from ^3He (P. W. Lisowski, T. C. Rhea, C. E. Busch, T. B. Clegg, R. L. Walter)

Polarized neutrons obtained in the $^2\text{H}(\vec{d}, \vec{n})^3\text{He}$ via polarization transfer at 0° were scattered from ^3He contained in a gas scintillator. The $P_Y(\theta)$ values obtained at 8 and 12 MeV were included in a global phase shift search for the $^3\text{He}(n, n)^3\text{He}$ reaction. The results have appeared in Nuclear Physics A259 (1976) 61.

11. Elastic Scattering of Nucleons from ^4He

Because elastic scattering of nucleons from ^4He is the most effective method for measuring the magnitude of the polarization P_Y in a nucleon beam, there has been a continuing effort to improve the accuracy of our understanding of the mass-5 system. The status of several parts of our program is as follows:

- a. Cross-Section Measurements for $^4\text{He}(n, n)^4\text{He}$ (G. Mock,* R. C. Byrd, P. W. Lisowski, R. L. Walter)

Analysis of the spectra for ^4He recoil distributions from 8 to 16 MeV has been completed. However, after all the combinations of spectra (several gas mixtures and varied container configurations for each of six neutron energies) were manipulated to obtain the final angular distributions for $^4\text{He}(n, n)^4\text{He}$, it was apparent that a systematic problem exists in some of the data. The origin of such is not understood, although it is known to exist in the spectra themselves. As this measurement was (presumably) the most accurate and careful one to have been done to date, the data may shed some light as to what the problems with cross-section data reported earlier might be. The data as they now stand are of no value for new cross-section values, and if we can sense what the difficulties with this type of recoil measurements are, a paper on these pitfalls will be submitted for publication. If we return to measurements of cross sections in the 8 to 16 MeV region, we probably will avoid using the gas-scintillation-cell recoil method.

- b. $^4\text{He}(\vec{n}, n)^4\text{He}$ Analyzing Power Measurements at 14 and 17 MeV (P. W. Lisowski, T. C. Rhea, R. L. Walter, T. B. Clegg)

The accurate values for $A_Y(\theta)$ at 14 and 17 MeV for $^4\text{He}(n, n)^4\text{He}$ have not been published yet because they were intended to appear along with the cross-section data from above and the global R-matrix analysis underway at our laboratory for the mass-5 system. Since the cross-section data will not be forthcoming immediately, we will probably publish the data separately in the near future.

* University of Tuebingen, Tuebingen, West Germany

- c. $^4\text{He}(\vec{n}, n)^4\text{He}$ Analyzing Power Measurements from 20 to 29 MeV with a Calibrated Source of Polarized Neutrons (R. L. Walter,* P. W. Lisowski,* G. G. Ohlsen,* * R. A. Hardekopf* *)

Using the calibrated source of polarized neutrons obtained via the $^3\text{H}(\vec{d}, \vec{n})^4\text{He}$ as described in Section B9, a calibration for the analyzing power of $^4\text{He}(n, n)^4\text{He}$ was obtained with the apparatus available at the LASL tandem laboratory. The neutron energy ranged from 20 to 29 MeV and the concentration was on data near the maxima in $A_y(\theta)$. The results are particularly significant because little solid information existed in this energy range for this quantity previously and because $^4\text{He}(n, n)^4\text{He}$ is the only analyzer for polarized neutron beams above 20 MeV. The data were compared to $^4\text{He}(p, p)^4\text{He}$ information and, when the results are shifted to account for Coulomb energy effects (in first order), both sets of $A_y(\theta)$ values for the charge symmetric systems are identical to within statistics. The data were recently published in Phys. Rev. Letters 13 (1976) 809.

- d. $^4\text{He}(\vec{p}, p)^4\text{He}$ Analyzing Power Measurements (P. W. Lisowski, T. B. Clegg, W. Jacobs, R. L. Walter)

As part of a program to determine the accuracy with which the quench-ratio method is able to predict the beam polarization at TUNL, precision angular distributions of the $^4\text{He}(p, p)^4\text{He}$ asymmetry were measured at 3.6, 6.3 and 12.2 MeV. At each energy the data cover an angular range from 25.0° to 157.5° (lab), generally in 2.5° steps. Analyzing power values deduced from the asymmetry data have a statistical accuracy in the range 0.001 to 0.003. Because of the low uncertainty of the results it was felt that the relative angular dependence of these data would be useful in improving the phase shift solution for the $p + ^4\text{He}$ system in addition to providing information about the quench-ratio method. The details of the latter point were covered in last year's progress report. The data are included in our data bank for the mass-5 system and their status is described in the next part.

- e. Phase Shift Analysis of the $^4\text{He}(n, n)^4\text{He}$ and $^4\text{He}(p, p)^4\text{He}$ Scattering Processes (P. W. Lisowski and R. L. Walter)

The accurate values for $A_y(\theta)$ for $p + ^4\text{He}$ and $n + ^4\text{He}$ discussed above have been included in a detailed study of phase shifts for the mass-5 system parameterized in an R-matrix formulation. No progress has been made in the past months because the cross-section data for $^4\text{He}(n, n)^4\text{He}$ was anticipated. Now that this data will not be available, and in light of other mass-5 analyses, the next step in our global approach to these systems must be reconsidered.

* Visiting staff member at Los Alamos Scientific Laboratory (June 1975)

** Staff member at Los Alamos Scientific Laboratory

12. Polarization Transfer Studies in (\vec{p}, \vec{n}) Reactions (P. W. Lisowski, G. Mack, R. C. Byrd, C. E. Busch, T. B. Clegg, R. L. Walter)

Polarization transfer coefficients have been deduced from measurements of the outgoing $\theta = 0^\circ$ neutron polarization for (\vec{p}, \vec{n}) reactions on a variety of targets. The parameter investigated was the transverse (vector) polarization transfer coefficient K_Y^1 which relates the magnitude of the component of the (transverse) proton polarization to that along the same (transverse) direction for the neutron polarization. This coefficient is identical to the old Wolfenstein depolarization coefficient D for elastic scattering of a polarized beam of spin 1/2 particles.

a. Polarization Transfer in the $D(\vec{p}, \vec{n})2p$ Reaction from 10 to 15 MeV

Data were obtained on the values of $K_Y^1(0^\circ)$ for the $D(\vec{p}, \vec{n})2p$ reaction from 10 to 15 MeV for the entire region of neutron energies. Since the last report the data have been reanalyzed and prepared for final publication. Some calculations to compare with one model of the interactions were believed to be possible in the immediate future, but because of personnel shifts between laboratories, the computer code is no longer functioning, and getting it running again appears insurmountable in the reasonable future. Therefore we plan to publish the data imminently so that they will be more widely available.

b. Polarization Transfer Effects in (\vec{p}, \vec{n}) Reactions on Light Nuclei at $\theta = 0^\circ$

Data on $K_Y^1(0^\circ)$ has been obtained for the ${}^9\text{Be}(\vec{p}, \vec{n}){}^9\text{B}$, ${}^{11}\text{B}(\vec{p}, \vec{n}){}^{11}\text{C}$, and ${}^{13}\text{C}(\vec{p}, \vec{n}){}^{13}\text{N}$ reactions from 7 to 15 MeV. The results and their significance have been published in Nuclear Physics A264, 188 (1976).

13. Comparison of the Polarization and Analyzing Power in (p, n) Mirror Reactions on ${}^{15}\text{N}$ and ${}^9\text{Be}$ (R. C. Byrd, P. W. Lisowski, G. Mack, S. S. Skubic, W. Tornow, T. B. Clegg, R. L. Walter)

In elastic scattering processes, parity and time-reversal arguments require that the polarization $p_Y(\theta)$ produced in the scattering of an unpolarized beam be equal to the left-right counting-rate asymmetry $A_Y(\theta)$ that results when a beam with unit polarization is scattered from the same nucleus. Recently the comparison of $p_Y(\theta)$ and $A_Y(\theta)$ has been under theoretical discussion for (p, n) mirror reactions. (Earlier in the report we described our work on the ${}^3\text{H}(p, n){}^3\text{He}$ reaction.) Conzett⁶⁾ presents arguments that differences in A_Y and p_Y must result from charge-symmetry breaking components in mirror reactions, or more fundamentally, in the nucleon-nucleon force. As $p_Y(\theta)$ data existed⁷⁾ for the reactions ${}^9\text{Be}(p, n){}^9\text{B}_{G.S.}$ and ${}^{15}\text{N}(p, n){}^{15}\text{O}_{G.S.}$ it was decided to investigate the differences around 8 to 11 MeV for these reactions. Large differences were indeed observed in each reaction, particularly at those angles where

⁶⁾ H. E. Conzett, Phys. Rev. Lett. 51B (1974) 445; see also, L. G. Arnold et al., Phys. Rev. Lett. 32 (1974) 310.

⁷⁾ B. D. Walker, C. Wong, J. D. Anderson, and J. W. McClure, Phys. Rev. 137 (1965) B1504

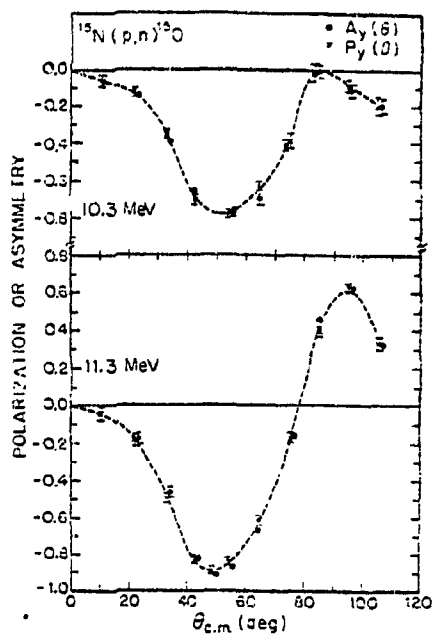
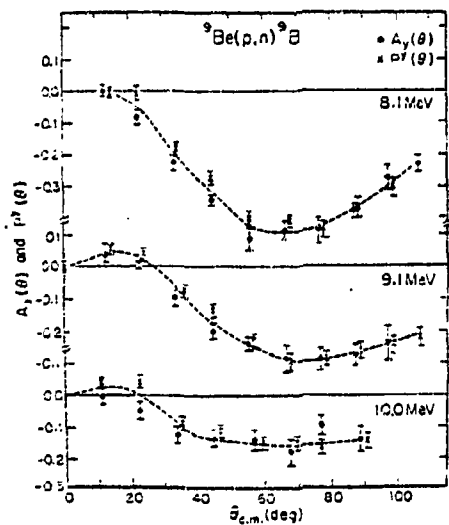


Fig. B13-1. Comparison between $P_Y(\theta)$ and $A_Y(\theta)$ for several energies for the ${}^9\text{Be}(p,n){}^9\text{B}$ reaction. The curve is a guide to the eye.

Fig. B13-2. Comparison between $P_Y(\theta)$ and $A_Y(\theta)$ for two energies for the ${}^{15}\text{N}(p,n){}^{15}\text{O}$ reaction. The curve is a guide to the eye.

$p_y(\theta)$ and $A_y(\theta)$ peaked. To be sure of these effects the earlier polarization data was checked and found to be in error. Also, better statistics were accumulated on the $A_y(\theta)$ data. Some of the comparisons are shown Figs. B13-1 and B13-2. The data sets typically now have statistical errors of less than ± 0.03 , sufficient to show that the remaining differences between these parameters is quite small, if any exists at all! Hence from these data above 8 MeV, it does appear that the charge-symmetry breaking component in this reaction is small (or else it has only a small effect on comparisons of these observables).

In order to determine if this agreement between $PY(\theta)$ and $A_y(\theta)$ was a basic constraint on (p,n) reactions, we extended the measurements for $PY(\theta)$ and $A_y(\theta)$ down to 3 and 5 MeV respectively for ${}^9\text{Be}$ and ${}^{15}\text{N}$. Of course, it was believed that at some stage, Coulomb effects would break this agreement. Surprisingly, for ${}^9\text{Be}$, to within our accuracy, $PY(\theta)$ and $A_y(\theta)$ agree exactly. Hence, nowhere in the ${}^9\text{Be}(p,n){}^9\text{B}$ reaction is any difference exhibited! On the other hand, in one small region between 5 and 6 MeV, violent dissimilarities were found for the ${}^{15}\text{N}(p,n){}^{15}\text{O}_{G.S.}$ reaction. At one energy the magnitudes are large, but the signs are opposite. At this stage we are extending our discussions with theorists with the hope of stimulating some interpretation (and calculation) of these unique findings.

14. Cross Sections and Polarizations in $({}^3\text{He},n)$ Reactions from ${}^{12}\text{C}$ and ${}^{13}\text{C}$ from 8 to 22 MeV (T. C. Rhea, R. A. Hardekopf, P. W. Lisowski, J. M. Joyce, R. Bass,* R. L. Walter)

As stated in the last report, polarizations and cross-section data were obtained on $({}^3\text{He},n)$ reactions on ${}^{12}\text{C}$ and ${}^{13}\text{C}$ from 8 to 22 MeV. Furthermore, the DWBA calculations had been completed but due to the higher priority given to the other neutron polarization experiments in this section, no progress has been made toward publication of these data. However, because these data are the only existing ones of this type in the 8-20 MeV range, it is still our intention to submit them eventually.

15. Polarization Transfer Studies of ${}^{12}\text{C}(\vec{d},\vec{n}){}^{13}\text{N}$, ${}^{14}\text{N}(\vec{d},\vec{n}){}^{15}\text{O}$, ${}^{16}\text{O}(\vec{d},\vec{n}){}^{17}\text{F}$ and ${}^{28}\text{Si}(\vec{d},\vec{n}){}^{29}\text{P}$ at $\theta = 0^\circ$ (P. W. Lisowski, R. C. Byrd, G. Mack, T. B. Clegg, R. L. Walter)

The study of polarization transfer in (\vec{d},\vec{n}) reactions has recently been of increasing interest for both theoretical and experimental reasons. Theoretically, analysis of polarization transfer information is useful in the study of reaction mechanisms and offers new possibilities for investigating the D-state of the deuteron. Previously experimental studies had been carried out for only the lightest nuclei. (See ref. 9 for example.) As reported previously, we have investigated the ${}^{12}\text{C}(\vec{d},\vec{n}){}^{13}\text{N}$, ${}^{14}\text{N}(\vec{d},\vec{n}){}^{15}\text{O}$, ${}^{16}\text{O}(\vec{d},\vec{n}){}^{17}\text{F}$ and ${}^{28}\text{Si}(\vec{d},\vec{n}){}^{29}\text{P}$ reactions. The energy range studied was about 6 to 15 MeV. Since the last report we have made an off-line reanalysis of most of these data and have prepared a

* Institut für Kernphysik der Universität, Frankfurt, West Germany

9) F. D. Santos, Nucl. Phys. A236 (1974) 90 and private communication

report for publication. The conclusion stands that for the ^{28}Si , ^{16}O , and ^{14}N and the $^{12}\text{C}(d,n)^{13}\text{N}$ reactions $K_{\gamma'}$ is very close to the $2/3$ value expected from a simple stripping picture which ignores the deuteron D-state.

16. Depolarization Effects in Stripping a Polarized Negative Ion Beam in The Terminal of a Tandem Van de Graaff (P. W. Lisowski, R. L. Walter, T. B. Clegg, G. G. Ohlsen,* P. A. Lovoi,* R. A. Hardekopf)

In performing proton and deuteron polarization experiments in tandem laboratories, polarized negative ion beams are stripped in carbon foils in the high voltage terminal of the accelerator with no loss in nuclear polarization because the time interval for stripping both electrons is negligibly small. However, if there is residual gas in the stripper region, it is possible for the electrons to be removed in successive steps that are separated by a non-negligible time, i.e., non-negligible in comparison to the precession time during which the atom is neutral. The problem here is that the spin of the single electron and the spin of the nucleus precess around each other and depolarization results. This depolarizing effect is known to be small and really does not matter when the polarization is measured in the target area after full acceleration. However, at our laboratory (as well as at LASL) we use the "quench-ratio" method to measure the shift polarized ion sources, but it primarily measures the polarization of the beam prior to acceleration. At TUNL our concern about depolarization grew as experiments were conducted with increasing accuracy and decreasing energy. The results of a measurement with and without an evaporation pump in the terminal at LASL have now been published in Nucl. Instr. and Methods 131 (1975) 489. Data obtained for relative angular distributions of $A_{\gamma}(\theta)$ for $^4\text{He}(p,p)^4\text{He}$ will also give information about depolarization effects, but this requires an accurate knowledge of $p\text{-}^4\text{He}$ phase shifts. The aforementioned mass-5 system analysis will lead to a scaling parameter that yields the depolarization factor. Although the mass-5 analysis is not complete yet, the preliminary results now show that the terminal depolarization is less than 1% all the way down to $E_p = 4$ MeV.

17. Pulsed Polarized Beam Studies (P. W. Lisowski, S. Wender, R. L. Walter, T. B. Clegg, F. O. Puser)

As described in our last report, we would like to initiate a program of neutron reaction studies with pulsed-polarized beams. No additional tests of the method reported there were made this past year, but beam time has been scheduled during January 1977 for successive developmental experimentation.

18. Sources of Polarized Fast-Neutron Beams--A Status Report (R. L. Walter, P. W. Lisowski)

In order to bring the current status for the production of polarized neutron beams into the forefront, a special paper related to this topic was delivered at the Lowell Tech. International Neutron Conference (1976) and has been published in the Proceedings. One purpose was to point out our use of the transfer polarization source of neutrons, i.e.,

* Staff member at Los Alamos Scientific Laboratory

the ${}^2\text{H}(\vec{d}, \vec{n}){}^3\text{He}$ reaction. In addition, we cautioned against the acceptance of polarization values published more than a few years ago, since we now have evidence that the reported values for $PY(\theta)$ for ${}^2\text{H}(\vec{d}, \vec{n}){}^3\text{He}$, ${}^3\text{H}(\vec{p}, \vec{n}){}^3\text{He}$, ${}^9\text{B}(\vec{p}, \vec{n}){}^9\text{B}$, and ${}^{15}\text{N}(\vec{p}, \vec{n}){}^{15}\text{O}$ are in error. This is particularly upsetting as some of the previous measurements appeared to have been performed with extreme care and outstanding techniques. The final purpose of the paper is to review the recent calibrated sources of polarized neutrons obtained under special polarization transfer conditions and also to provide a recent up date of the comparison of all methods of producing polarized neutrons.

C. HIGH RESOLUTION STUDIES

1. High Resolution Elastic Scattering (E. G. Bilpuch, G. E. Mitchell, M. Bleck, D. Flynn, D. A. Outlaw, W. K. Wells, C. Westerfeldt)

The new efforts in elastic scattering measurements have been on ^{26}Mg (on the 3 MV accelerator) and ^{90}Zr (on the tandem). The ^{30}Si and ^{42}Ca data have been published, and the ^{54}Fe results submitted for publication. Our major review article on the fine structure of analogue states has been published.

a. Review Article

A review article "Fine Structure of Analogue States" by E. G. Bilpuch, A. M. Lane, G. E. Mitchell and J. D. Moses was published: *Physics Reports* 28 (1976) 145. The abstract of this paper follows:

"This article reviews all the high-resolution data on fragmented analogue states taken at the Triangle Universities Nuclear Laboratory, over a period of ten years. There are fifty analogue states observed by proton scattering on targets of masses between 40 and 64, and mass 92. The number of fragments may be only two or three, or as many as fifty. Of the total, only 18 states have a sufficient fine structure pattern where an analysis is attempted. In a few cases, inelastic widths and photon and neutron widths are observed besides proton elastic ones. The article discusses the optimum method of analysis of the data with a view to extracting the physical parameters of the analogue; the energy, proton spectroscopic factor, spreading width, shift and asymmetry parameter. The last three quantities are discussed from the viewpoint of the Robson model based on one-channel external mixing of the analogue by Coulomb forces. This model has qualitative success, particularly in describing the large asymmetry sometimes seen, but it is not quantitatively adequate. When the proton spectroscopic factors are compared to the neutron counterparts for the parent (as measured by (d,p) studies), after allowing for Coulomb effects, the proton ones are smaller by an amount which increases to 30% in the heavier nuclei (Ni, Mo). This is in line with the situation on ^{208}Pb . Thus it seems that the inadequacy of a Coulomb explanation of the analogue-parent energy shift (the Nolen-Schiffer anomaly) has a counterpart in the spectroscopic factors."

b. ^{26}Mg

Excitation functions at four angles for $^{26}\text{Mg}(p,p)$ have been measured from $E_p = 1.55$ to 3.05 MeV. The targets were $2-3 \mu\text{g}/\text{cm}^2$ of ^{26}MgO deposited on $5 \mu\text{g}/\text{cm}^2$ carbon foils; the overall experimental resolution was ~ 400 eV. Fifty eight resonances were observed. Processing and analysis of these data is now beginning.

c. ^{30}Si

A paper has been published on these results: "A High-Resolution Study of the $^{30}\text{Si}(p,p)$ Reaction", D. A. Outlaw, G. E. Mitchell and E. G. Bilpuch, Nuclear Physics A269 (1976) 99. The following is the abstract of that paper:

"The $^{30}\text{Si}(p,p)$ reaction has been measured at four angles from 1.1 to 3.0 MeV with an overall energy resolution of $350-450$ eV. Sixty-two resonances were observed and analyzed. Three analogues were identified and their Coulomb energies and spectroscopic factors determined. Proton strength functions were determined. There is an anomalous cluster of $3/2^-$ strength observed: about one half the single particle strength is within an energy range of less than one MeV. By combining the present values for Γ_p with the results of previous capture experiments, total γ -ray widths were determined for most of the resonances observed."

d. ^{34}S

Analysis of the $^{34}\text{S}(p,p)$ data is complete and a paper on these results is nearly ready for submission. In the bombarding energy range $E_p = 1.45$ to 2.82 MeV 59 resonances were analyzed. The analogue of the $3/2^-$ third excited state of ^{35}S is identified and other analogues are tentatively identified. Proton strength functions are determined and combined with our previous results in the $A = 40-64$ mass region. The present data are consistent with previous results: the $p_{3/2}$ and $p_{1/2}$ strength functions peak near $A = 40$, with the $p_{3/2}$ giant resonance slightly lower than the $p_{1/2}$ resonance. There are indications that the data follow separate curves for different target isospin; this serves as rather direct evidence for an isospin term in the nuclear potential. Results of earlier capture measurements are combined with the present elastic widths to evaluate Γ_γ for ~ 40 resonances.

e. ^{42}Ca

A paper has been published on these results: "High Resolution Proton Scattering from ^{42}Ca ", W. M. Wilson, E. G. Bilpuch and G. E. Mitchell, Nuclear Physics A271 (1976) 49. The following is the abstract of that paper:

"Differential cross sections were measured for $^{42}\text{Ca}(p,p)$ at four angles between $E_p = 1.2$ and 3.0 MeV, with an overall energy resolution of 325 eV. Spins, parities and proton widths

were extracted for 170 resonances. Two analogue states were identified and spectroscopic factors determined. The nearest neighbor spacing distributions were analyzed. Proton strength functions were determined for $1/2^+$, $1/2^-$ and $3/2^-$ resonances."

f. ^{54}Fe , ^{58}Ni , ^{60}Ni

A high resolution system has been developed for the 4 MV accelerator. A paper has been published on this system: "Energy Range Extension for an Electrostatic-Analyzer Homogenizer System", D. S. Flynn, E. G. Bilpuch, F. O. Purser, H. W. Newson, L. W. Seagondollar and G. E. Mitchell, Nuclear Instruments and Methods 137 (1976) 125. The following is the abstract of that paper:

"The energy range of an electrostatic-analyzer homogenizer system has been extended by the introduction of a molecular dissociator which operates on the diatomic hydrogen ions from a Van de Graaff accelerator. Energy resolutions of 300-400 eV with solid targets have been obtained routinely up to proton energies of 4.5 MeV with an electrostatic analyzer originally limited to measuring proton energies below 2.7 MeV. Improvements to the Van de Graaff accelerator are expected to permit this system to operate as high as 5-6 MeV. Since feedback for this homogenizer is obtained by modulating the voltage on the dissociator, a magnetic analyzer could be substituted for the electrostatic analyzer."

This system has been utilized in a series of experiments on ^{54}Fe , ^{58}Ni , ^{60}Ni . This work is described in the dissertation of D. S. Flynn, "A High Resolution Study of Proton Resonances in ^{55}Co , ^{59}Cu and ^{61}Cu ."

A paper on the ^{54}Fe results has been submitted for publication: "High-Resolution Proton Scattering from ^{54}Fe ", D. S. Flynn, E. G. Bilpuch and G. E. Mitchell. The following is the abstract of that paper:

"Differential cross sections were measured for $^{54}\text{Fe}(p,p)$, (p,p') at four angles between $E_p = 3.28$ and 4.53 MeV with an overall energy resolution of about 350 eV. Spins, parities, and widths were extracted for 131 resonances. Several analogue states were identified and several other analogues tentatively proposed. Spectroscopic factors and Coulomb energies were obtained for the analogues. Proton strength functions were determined and level densities compared with semi-empirical predictions."

g. ^{90}Zr

The $^{90}\text{Zr}(p,p)$ reaction has been measured at four laboratory angles with the terminal stabilized tandem Van de Graaff in the vicinity of the $1/2^+$ analogue states at $E_p = 5.41$ MeV. The data were taken in several sections of 30-50 keV, one section of which has been fitted with a resolution of 425 eV. Difficulties which probably stem from the drifts in the analyzing magnet power supplies have been encountered in the process of combining the different sections of the yield curves. We plan to study the $1/2^+$ analogue state at $E_p = 7.3$ MeV. For this latter analogue one or more inelastic channels will be measured in addition to the elastic channel. An array of BF_3 counters has been installed to monitor the (p,n) reaction.

2. High Resolution Proton Capture (G. E. Mitchell, E. G. Bilpuch, J. F. Wimpey)

A paper has been published on the ^{44}Ca results: "Electromagnetic Decay of Fragmented Analogue States in ^{45}Sc ", J. F. Wimpey, G. E. Mitchell and E. G. Bilpuch, Nuclear Physics A269 (1976) 46. The following is the abstract of that paper:

"The $^{44}\text{Ca}(p,\gamma)$ reaction was studied for 45 resonances for $E_p = 1.6-2.2$ MeV. The overall proton energy resolution was 300-350 eV; the γ -rays were detected with both $\text{NaI}(\text{Tl})$ and $\text{Ge}(\text{Li})$ detectors. Partial and total γ -ray widths were measured for each of the fine structure states of the $3/2^-$ and $1/2^-$ analogue states at $E_p = 1.65$ and 2.04 MeV, respectively. The data are examined for correlations between the partial widths ($\Gamma_p, \Gamma_{p'}, \Gamma_\gamma, \Gamma_\gamma^{\text{total}}$) in different channels. The γ -ray intensities are compared with (τ,d) spectroscopic factors."

3. High Resolution Inelastic Scattering (G. E. Mitchell, E. G. Bilpuch, J. Chandler, T. Dittrich, C. R. Gould, D. A. Outlaw, K. Wells)

This program of measurements of the (p,p') and $(p,p'\gamma)$ neutrons focusses on p-wave resonances. The combination of the two angular distributions provides a unique spin assignment and the value of both the magnitudes and relative phases of the inelastic decay amplitudes for the $3/2^-$ resonances.

a. Method

A brief paper on this approach has been published in Physics Letters. The method of analysis is described in detail in the Ph.D. dissertation of T. R. Dittrich, "Channel Spin Mixing Ratios in High Resolution Proton Inelastic Scattering on ^{50}Cr ".

b. ^{50}Cr

A paper on the ^{50}Cr results has been accepted for publication: "High Resolution Proton Inelastic Scattering from ^{50}Cr ", T. R. Dittrich, C. R. Gould, G. E. Mitchell, E. G. Bilpuch and K. Stelzer. The following is the abstract of that paper.

"Resonances in the $^{50}\text{Cr}(p,p'\gamma)$ reaction were investigated with the TUNL high resolution system. All previously observed p-wave resonances between $E_p = 2.00$ and 3.03 MeV were studied. Measurement of the p' and the γ -ray angular distributions provides sufficient information to determine unambiguously the J-value of the resonance and the magnitude and relative phase of the inelastic decay amplitudes. Expressions are given for the appropriate angular distributions and for the transformation between the channel spin and the total angular momentum representation. Experimental results are presented for 24 p-wave resonances in ^{51}Mn including decay amplitudes and relative phases for 16 $3/2^-$ resonances. Six resonances formerly assigned $1/2^-$ are reassigned $3/2^-$. Inelastic spectroscopic factors were determined for two analogue states. Proton strength functions were evaluated from both the elastic and inelastic data."

c. ^{56}Fe

Preliminary results were reported at an APS meeting: "High Resolution Proton Inelastic Scattering on ^{56}Fe ", W. K. Wells, D. A. Outlaw, E. G. Bilpuch and G. E. Mitchell, Bull. Am. Phys. Soc. 21 (1976) 662.

"Thirty-nine p-wave resonances in the $^{56}\text{Fe}(p,p'\gamma)^{56}\text{Fe}$ reaction between proton bombarding energies of 2.1 and 3.01 MeV were investigated using the high resolution beam of the TUNL 3 MV Van de Graaff accelerator. Four point angular distributions of both inelastic protons and de-excitation gamma-rays were measured. Spins, inelastic widths, and magnitudes and relative phases of the channel spin mixing ratios were extracted for those compound nuclear resonances with sufficient yield. The statistical implication of this data will be discussed."

Mixing ratios were obtained for 17 $3/2^-$ resonances. Most of the other resonances were either determined to be $p_{1/2}$ resonances, had insufficient inelastic yield (probably $p_{1/2}$ resonances), or were obscured by other resonances. Three resonances yielded inconsistent results; these will be remeasured. Further analysis is now in progress.

d. ^{44}Ca

The emphasis in this experiment is on the behavior of the magnitudes and relative phases of the decay amplitudes in the vicinity of the fragmented $3/2^-$ analogue state at $E_p = 2.62$ MeV. Preliminary results were reported at an American Physical Society meeting: "Channel Spin Mixing Ratios in High Resolution Proton Inelastic Scattering on ^{44}Ca ", T. R. Dittrich, C. R. Gould, G. E. Mitchell, E. G. Bilpuch, M. E. Bleck and K. Stelzer, Bull. Am. Phys. Soc. 21 (1976) 662.

The data are consistent with non-statistical behavior in the relative phases for the fine structure resonances. Additional measurements on resonances away from the analogue have also been performed. Analysis of these data is in progress.

4. Isospin-Forbidden $T = 3/2$ Resonances (T. B. Clegg, W. W. Jacobs, E. J. Ludwig, W. J. Thompson, S. A. Tonsfeldt, H. P. Wu)

The analysis of isospin-forbidden resonances in ^{21}Na , ^{25}Al , ^{29}P , and ^{33}Cl has been described in recent papers. A Physical Review Letter presents the trends of proton reduced widths with mass number (part a of Fig. C4-1). Shown below this plot is the trend of α -particle summed branching ratios for the same range of mass numbers. There is an unexplained periodicity in reduced widths plot which appears to a lesser extent in the branching ratios. The horizontal lines show least squares estimates for $A = 8n + 4$ targets (upper line) and for $A = 8n$ targets (lower line). In Fig. C4-2 are shown examples of fits to a resonance corresponding to the lowest $T = 3/2$ state in ^{25}Al populated by $^{24}\text{Mg}(p,p)^{24}\text{Mg}$ at $E_p = 5.866$ MeV and the next higher $T = 3/2$ state in ^{25}Al found at $E_p = 5.939$ MeV. A paper which will soon appear in Nuclear Physics describes in detail the experimental measurements and our analysis techniques.

Projects still in the analysis stage include a study of the lowest $T = 3/2$ state in ^{13}N which appears as a resonance in $^{12}\text{C}(p,p)^{12}\text{C}$ and the lowest two $T = 3/2$ states in ^{17}F seen through $^{16}\text{O}(p,p)^{16}\text{O}$. The ^{12}C work has resulted in the extraction of resonance widths in good agreement with the work of other groups. The analysis constituted the Master's degree project of H. P. Wu who reported the results at a recent American Physical Society meeting. The $^{16}\text{O}(p,p)^{16}\text{O}$ data is still being evaluated and further measurements will be made. All of these data are analyzed to determine the extent to which isospin mixing occurs in the target ground state and/or states in the compound nucleus.

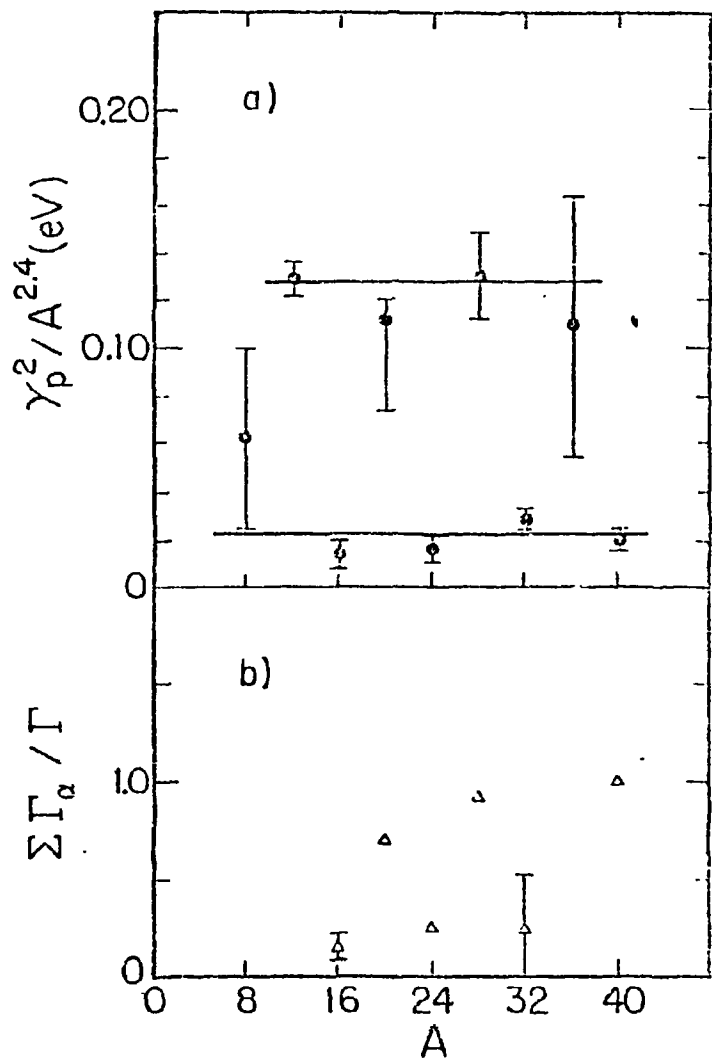


Fig. C4-1. a) Proton reduced width vs. mass number.
 b) Alpha particle summed branching ratios vs. mass number.

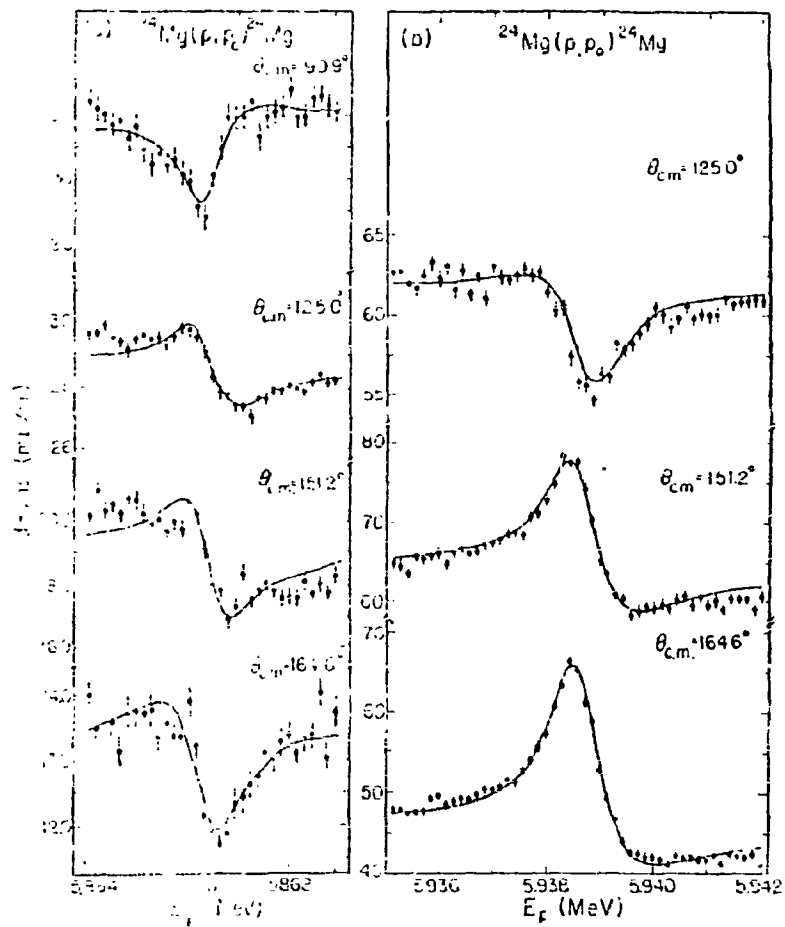


Fig. C4-2. Fits to a resonance corresponding to the lowest $T = 3/2$ state in ^{25}Al .

D. GAMMA RAY SPECTROSCOPY

1. Mean Lifetimes of Excited States in ^{38}Ca (E. C. Hagen,* S. Maripuu, N. R. Roberson, D. R. Tilley)

No new experimental work has been undertaken since the last report. The analysis of the data is in final form and a paper is being prepared for publication.

2. Mean Lifetimes of Levels in ^{55}Co (R. O. Nelson,** J. R. Williams,+ D. R. Tilley, D. G. Rickel,†† N. R. Roberson, S. Maripuu, C. P. Cameron, R. D. Ledford)

A paper by this title has been published in Nucl. Phys. A261 (1976) 427. The abstract is presented below.

"The mean lifetimes of levels in ^{55}Co below 5.2 MeV have been investigated with the Doppler-shift attenuation method and the $^{54}\text{Fe}(^3\text{He},d)^{55}\text{Co}$ reaction at 12 MeV. Scattered particles were detected in two E-ΔE telescopes at $\pm 55^\circ$ with respect to the beam axis, in coincidence with γ -rays observed at 90° and 130° in a 50 cm³ Ge(Li) detector. Mean lifetimes are reported for the following levels (energy in keV, lifetime in fs): 2166 (139±18), 2566 (680±200), 2923 (>245), 2939 (190±65), 3303 (99±22), 3323 (54±15), 3642 (680⁺⁴⁰⁰₋₃₀₀), 3943 (>170), 4164 (54±15), 4180 (<16), 4722 (<33), 4749 (<70) and 5174 (<40). The experimental results are compared with a detailed shell-model calculation."

3. Measurement of Gamma-Ray Angular Distributions and Linear Polarizations for ^{48}V (D. G. Rickel, N. R. Roberson, C. P. Cameron, R. D. Ledford, S. G. Buccino,‡‡ D. R. Tilley)

A paper by this title has been published in Nucl. Phys. A256 (1976) 152. The abstract follows.

"Levels of ^{48}V were populated by the $^{48}\text{Ti}(p,n\gamma)$ and the $^{34}\text{S}(^{16}\text{O},pn\gamma)$ reactions. Proton energies of 5.5, 6.0, 6.4 and 7.0 MeV and a ^{16}O energy of 34 MeV were used. Gamma rays were measured in singles. The J^π assignments for eight of these levels follows from γ -ray angular distribution and linear polarization measurements when combined with presently available lifetime and nucleon transfer data."

* E. G. and G., Los Alamos, New Mexico

** Los Alamos Scientific Laboratory, Los Alamos, New Mexico

+ Physics Department, Auburn University, Auburn, Alabama

†† EPA, Durham, N. C.

‡‡ Visiting scientist from Tulane University

4. Studies of The Gamma-Ray Decay of Excited Levels in ^{117}Sb
(C. Schiffel, * ** C. P. Cameron, C. R. Gould, R. D. Ledford,
J. D. Turner, M. Jensen, D. G. Rickel, N. R. Roberson, K.
Stelzer,* D. R. Tilley)

No new experimental work has been undertaken. The previously reported data is being analyzed and mean lifetimes or limits have been obtained for several low lying levels. We hope to prepare a paper for publication.

5. A Study of The Low Lying Levels of ^{77}Kr (S. A. Wender, C. R. Gould,
D. R. Tilley, P. Von Behren, J. D. Turner, N. R. Roberson)

The decay scheme and the electromagnetic properties of neutron deficient ^{77}Kr are being studied using the $^{74}\text{Se}(\alpha, n)^{77}\text{Kr}$ reaction. So far the results of n- γ coincidence and γ - γ coincidence experiments confirm the level diagram proposed by Liptak and Hohernichth⁽¹⁾ up to 500 keV excitation. Also a preliminary analysis shows that the lifetime of the first excited state is on the order of 100 nsec. This result is in agreement with Roghven and Roghven.⁽²⁾ On the basis of the lifetime of the level it is difficult to understand the tentative spin assignment of $5/2^-$ ⁽¹⁾ which would allow E1 radiation. A more likely assignment would be $3/2^-$.

We are continuing to analyze the γ - γ data above 500 keV to search for new levels and confirm the previous β decay work.⁽¹⁾ We also plan to measure γ -ray angular distributions to determine the spins and parities of these low lying states. In addition, we plan to measure the lifetime and g-factor of the first excited state.

6. Spin and Parity of The 11.86 MeV Level in ^{24}Mg (S. A. Wender, C. R. Gould, D. G. Rickel, J. D. Turner, D. R. Tilley)

Previous investigators,⁽³⁾ suggested that the spin and parity of the 11.86 MeV level in ^{24}Mg is 8^+ . However, their results were unable to rule out the possibility of $J^\pi = 6^+$ with $\delta \simeq 0.8$. The 8^+ assignment is somewhat surprising since the state is lower in energy than the 8^+ member of the ground state rotational band. Fig. D6-1 shows a partial level scheme of ^{24}Mg . In order to remove the ambiguity in the spin assignment we have measured linear polarization of the γ -rays.

The 11.86 MeV state was populated using the $\text{C}^{12}(0^{16}, \alpha)^{24}\text{Mg}$ reaction at 42 MeV. The γ -rays were detected with a Compton polarimeter in coincidence with the outgoing α particles at 0° . The polarimeter consisted of a 4" x 7" NaI center crystal surrounded by a 2-1/2" thick NaI annulus sectioned into four quadrants. Compton events in the vertical and horizontal plane were routed into separate regions of memory and the data were stored event by event on magnetic tape. The final analysis

* Visitor from Frankfurt, Germany

** Deceased

1) Ya. Liptak, W. Habernichth, Izvestia Akademii Nauk SSSR Seriya Fizicheskaya 39 (1975) 501

2) P. Roghven and R. S. Roghven, Rutgers University Progress Report 1975, p. 119

3) D. Bronford, M. J. Spooner, I. F. Wright, Particles and Nuclei 4(1972) 231

was performed off line. The polarization sensitivity was determined using the $C^{12}(p,p')$ reaction and was measured to be approximately 6% at 4.0 MeV.

The results of a preliminary experiment supported the 8^+ assignment. The statistical errors on this measurement however were too large to exclude the 6^+ option, so a second experiment with improved statistics was performed. The data are presently being analyzed.

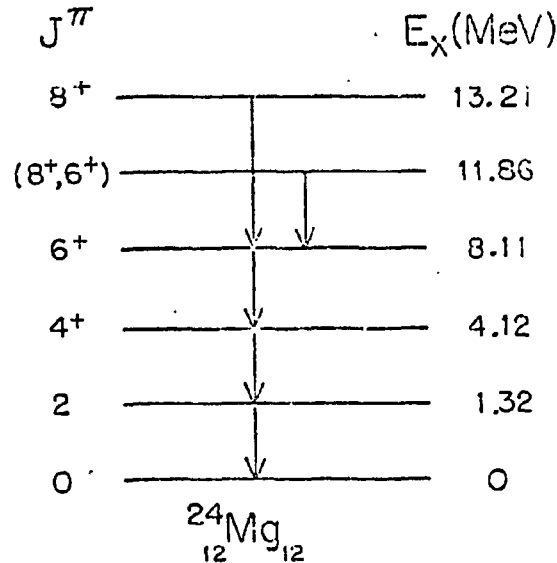


Fig. D6-1. Partial level scheme of ^{24}Mg .

7. Magnetic Moment of 738 keV Level in ^{43}K (S. A. Wender, C. R. Gould, D. R. Tilley, D. G. Rickel, J. D. Turner, N. R. Roberson)

The first result obtained with the recently developed perturbed angular correlation apparatus (see TUNL XIV) was the measurement of the g factor of the 738 keV level in ^{43}K . This state was previously¹⁾ assigned a spin and parity of $7/2^-$ based on its relatively long (184 nsec) lifetime. To further investigate this level we have measured its magnetic moment.

The state was populated using a 15.0 MeV pulsed He^{4+} beam with the $^{40}\text{Ar}(\alpha,p)^{43}\text{K}$ reaction. A small gas cell filled with 7 atmospheres of natural argon was placed between the pole tips of a conventional electromagnet, and the spin precession was measured in an external field of 5.4 and 3.8 kg. Two 3" x 3" NaI detectors placed at 45° and 135° detected the γ -rays. The direction of the field was reversed periodically. The ratio

$$R(t) = \frac{N(+H, \theta, t) - N(-H, \theta, t)}{N(+H, \theta, t) + N(-H, \theta, t)}$$

for each field value is shown in Fig. D7-1. This ratio was fitted with the expression

¹⁾ E. Bozek, C. Gehring, C. Jaeger, J. C. Merdenger, Nucl. Phys. A250 (1975) 257

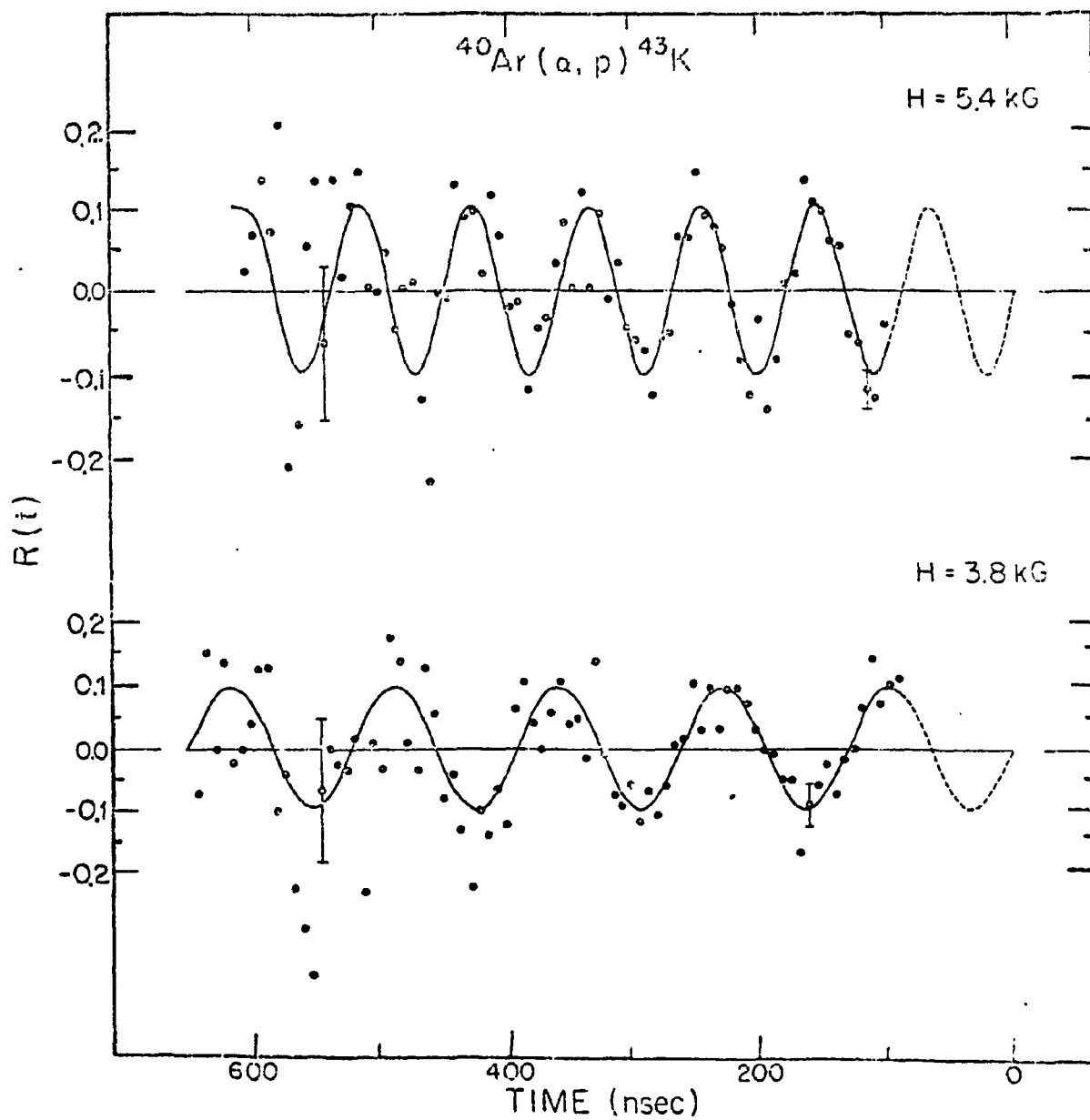


Fig. D7-1. $R(t)$ for one detector with an applied magnetic field of 3.8 and 5.4 kG.

$R(t) = \frac{3A_2}{4+A_2} \sin 2\omega t$ where $\omega = g \mu_N H/\hbar$. We measure $g = 1.28 + .04$, which corresponds to a magnetic moment of $(4.48 \pm .14)\mu_N$, assuming the spin is $7/2$. In addition we measured the half life $\tau_{1/2} = 182 \pm 4$ ns which is approximately 10% smaller than the previously measured value.⁽¹⁾

Table D7-1 lists the magnetic moments of the $7/2^-$ levels in the odd potassium isotopes, and the ground state magnetic moments of the odd scandium isotopes. On the basis of the single particle shell model, the similarity of these magnetic moments suggest that the 738 keV level in ^{43}K is predominantly a single particle $f_{7/2}$ state.

TABLE D7-1

Nucleus	$\mu_{\text{exp}}(\mu_N)$	Nucleus	$\mu_{\text{exp}}(\mu_N)$
^{39}K	$5.3 \pm 1.1^{(2)}$	^{41}Sc	$5.43 \pm .02^{(3)}$
^{41}K	$4.41 \pm .05^{(3)}$	^{43}Sc	$4.62 \pm .04^{(3)}$
^{43}K	$4.48 \pm .14^{(a)}$	^{45}Sc	$4.7562 \pm .0004^{(3)}$

(a) Present work assuming $J^\pi = 7/2^-$

-
- 1) E. Bozek, C. Gehringer, C. Jaeger, J. C. Merdenger, Nucl. Phys. A250 (1975) 257
 2) E. Bozek, A. Z. Huynkiewicz, J. C. Merdenger, J. P. Vivien, Phys. Rev. C12 (1975) 1873
 3) P. M. Endt and C. Von der Leun, Nucl. Phys. A214 (1973) 10, 11

E. CHARGED PARTICLE REACTIONS WITH POLARIZED BEAMS

1. The Hamburger Effect in $^{207}\text{Pb}(\vec{d}, p)^{208}\text{Pb}$ and $^{207}\text{Pb}(\vec{d}, d)^{207}\text{Pb}$ (S. A. Tonsfeldt, T. B. Clegg, W. W. Jacobs, E. J. Ludwig, W. J. Thompson)

Vector polarized deuterons have been used to study the $^{207}\text{Pb}(\vec{d}, p)^{208}\text{Pb}$ and $^{207}\text{Pb}(\vec{d}, d)^{207}\text{Pb}$ reactions in the energy range corresponding to $T = 45/2$ single-particle states in ^{209}Bi . The object of this work is to understand the mechanism responsible for structures in the (\vec{d}, p) cross section and vector analyzing power excitation functions.

A computer program has been written to analyze the (d, d) excitation function so as to extract an upper limit on the deuteron partial width for these resonances. This case of spin 1 particle incident on a spin 1/2 target generally involves several partial widths contributing to a given resonance formation and so particular attention will be paid to the $J^\pi = 1/2^+$ resonance data at 90° which involves only one partial width. An oral presentation regarding this work was made at the East Lansing meeting of the Division of Nuclear Physics.

2. The Study of The $^{207}\text{Pb}(\vec{d}, t)^{206}\text{Pb}$ Reaction (R. D. Willis, M. Kaitchuck, T. B. Clegg, W. W. Jacobs, E. J. Ludwig)

Improved cross section and vector analyzing power data were taken for the $^{207}\text{Pb}(\vec{d}, t)^{206}\text{Pb}$ reaction using 15 MeV deuterons. These data were incorporated with already-existing measurements to provide more precise data at forward angles for about 10 levels in the residual nucleus. Since the l - and j -values are not unique for the transferred particles in this reaction, a least-squares fit of the cross sections and analyzing powers is being used to extract spectroscopic factors for each l - and j -value transferred in forming a given final state. Several of the revised distributions have been reanalyzed and spectroscopic factors extracted.

3. The (\vec{d}, α) Reaction on ^{28}Si , ^{32}S and ^{40}Ca (E. J. Ludwig, T. B. Clegg, W. W. Jacobs, S. A. Tonsfeldt)

Cross section and vector analyzing power (VAP) data have been obtained at angles $\leq 100^\circ$ for 6 states populated in the $^{28}\text{Si}(d, \alpha)^{26}\text{Al}$ reaction, for four states populated in the $^{32}\text{S}(d, \alpha)^{30}\text{P}$ reaction and for three states reached in the $^{40}\text{Ca}(d, \alpha)^{38}\text{K}$ reaction. The VAP distributions for the strongest of these states (which have a known l value but different j values transferred) are being compared to determine the extent to which these distributions depend on j transfer. Angular distributions have been taken at several energies in the neighborhood of 16 MeV for each target nucleus to establish whether compound-nucleus processes are involved. Where possible, energy-averaged distributions have been prepared for theoretical analysis. Preliminary results show a dependence on j transfer for $l = 4$ and $l = 2$ angular distributions. The agreement with DWBA calculations is reasonably good for VAP distributions obtained with targets of ^{28}Si and ^{32}S .

4. The Mechanism of ($\vec{d}, {}^6\text{Li}$) Reactions on Light Nuclei (W. W. Jacobs, E. J. Ludwig, S. A. Tonsfeldt)

Cross section and vector analyzing power angular distributions have been measured for targets of ${}^{12}\text{C}$, ${}^{16}\text{O}$ and ${}^{19}\text{F}$. Data have been obtained at several energies for the ($\vec{d}, {}^6\text{Li}$) reactions populating the ground states of the residual nuclei. The energy averaged VAP angular distributions are oscillatory with regions of large analyzing powers. Theoretical calculations assuming a cluster transfer show good agreement with the data when optical model potentials using weak absorption are used. The ($\vec{d}, {}^6\text{Li}$) analyzing cross sections (σA_y) have been obtained for the $\ell = 0$ transfers and compared to (\vec{d}, d) analyzing cross sections for the same nuclei at the same energy. Similarities exist between these distributions which suggests that the α particle may act as a spectator during the interaction. The ${}^{19}\text{F}(\vec{d}, {}^6\text{Li}){}^{15}\text{N}_{G.S.}$ cross section is smaller than that for targets of ${}^{16}\text{O}$ and ${}^{12}\text{C}$ and appears to change more with energy. It is possible that this reaction is less "direct" in nature perhaps because of the absence of a large α particle cluster transfer component. Spectroscopic factors are being extracted for the energy-averaged data which should be of value since the optical model parameters used have provided a measure of agreement with both cross section and VAP data. Errors for the spectroscopic factors can be estimated from the standard deviations extracted from the energy-averaged data. A report on this work was presented at the Washington American Physical Society meeting (see Appendix III).

F. RADIATIVE CAPTURE REACTIONS

1. General Discussion of The Program

The program to study phenomena associated with giant resonances (GR) in light and medium weight nuclei continues to be a productive area of research at TUNL. In this work we have utilized radiative capture reactions induced by protons (polarized and unpolarized), deuterons, alpha particles and neutrons. The 25.4 x 25.4 cm NaI crystal and anti-coincidence shield continues to be the main system used in this research and it provides high resolution (2.5 to 3.5%) for the gamma rays observed in the GR regions. Work completed to date includes a detailed study of the $^{14}\text{C}(\vec{p},\gamma)^{15}\text{N}$ reaction and studies of the isospin splitting of the giant dipole resonance (GDR) in the nuclei ^{56}Fe , ^{55}Co , ^{57}Co and ^{59}Co . Experiments nearing completion are studies of the reactions: $^{30}\text{Si}(\vec{p},\gamma)^{31}\text{P}$, $^{88}\text{Sr}(\vec{p},\gamma)^{89}\text{Y}$ and $\text{T}(\vec{p},\gamma)^4\text{He}$. The general aims of these investigations are (1) to decompose the GDR in terms of the various T-matrix elements and their phases, (2) to search for the electric quadrupole (E2) isoscalar and isovector resonances, and (3) to study the isospin splitting of the GDR.

To compliment our charged particle work, we have established in the past year a program of fast neutron capture investigations. Preliminary results on the reaction $^{40}\text{Ca}(n,\gamma)^{41}\text{Ca}$ were reported at the International Conference on Neutron Interactions, Lowell, Mass. The neutron cross section program at TUNL provides the basic facilities. The neutron source in the $\text{D}(d,n)^3\text{He}$ reaction with a pulsed and bunched beam incident on a gas target. The spectrometer consists of a 4" x 7" NaI anti-coincidence shield. The second experiment planned for this system is to compare the yield from the reaction $^{14}\text{N}(n,\gamma)^{15}\text{N}$, which can populate only $T = 1/2$ components of the GDR, with the yield from the $^{14}\text{C}(p,\gamma)^{15}\text{N}$ reaction, where both $T = 1/2$ and $T = 3/2$ components are populated. A preliminary run with a beryllium nitride target indicated that the experiment is quite feasible.

2. Giant Resonance Region of ^{15}N Studied by Polarized and Unpolarized Proton Capture Measurements (H. R. Weller, R. A. Blue, N. R. Roberson, D.G. Rickel, S. Maripuu, C. P. Cameron, R. D. Ledford, D. R. Tilley)

The abstract for a paper published in Phys. Rev. 13C (1976) 922 follows.

"We have measured the cross sections and the analyzing powers for the $^{14}\text{C}(\vec{p},\gamma)^{15}\text{N}$ reaction for proton energies from 4.0 to 16.2 MeV. The corresponding range in excitation energies, 13.94 to 25.33 MeV, covers the region of the giant dipole resonance in ^{15}N . The five-angle angular distributions measured with unpolarized and with polarized beams at eight energies over this region were analyzed to determine the magnitudes and relative phases of the transition matrix elements. The analysis included E1, M1, and E2 transitions. The observed E1 strength exhausts only about 6% of the classical dipole sum rule. The dominant E1 strength is compared to a shell-model calculation which includes 3p-3h excitations. A fairly uniform distribution

of E2 strength is observed which exhausts about 7% of the total energy-weighted sum rule. Although large uncertainties on this result could allow the existence of a giant E2 resonance, the most probable values indicate that no appreciable concentration of E2 strength is observed."

3. Giant Dipole Resonance in ^{56}Fe Observed via (p, γ) and (α, γ) Reactions
(D. G. Rickel, C. P. Cameron, R. D. Ledford, N. R. Roberson, H. R. Weller, D. R. Tilley)

The abstract for a paper published in Phys. Rev. 14C (1976) 338 follows.

"A comparison is made between the yield curves of the measured $^{52}\text{Cr}(\alpha, \gamma_0)$ and $^{55}\text{Mn}(p, \gamma_0)$ reactions in the giant dipole resonance region of ^{56}Fe ($E_x = 14.0$ to 21.5 MeV) to determine if the gross differences can be interpreted as being due to isospin effects. Above 18 MeV the yield of (γ, α_0) , determined by the principle of detailed balance, is observed to drop below the value obtained when the energy dependence of the transmission coefficients is removed. This leads to the conclusion that while the diminished yield in the (γ, α_0) channel may be due to the failure to populate the isospin forbidden $T >$ states, other effects cannot be ruled out."

4. Giant Dipole Resonances in $^{55,57,59}\text{Co}$ Using Polarized Proton Capture
(C. P. Cameron, N. R. Roberson, D. G. Rickel, R. D. Ledford, H. R. Weller, R. A. Blue, D. R. Tilley)

The abstract for a paper published in Phys. Rev. 14C (1976) 553 follows:

"The angular distributions of cross sections and analyzing powers have been measured for the $^{54,56,58}\text{Fe}(\vec{p}, \gamma_0)$ reactions throughout the giant dipole resonance regions of $^{55,57,59}\text{Co}$. In addition, the 90° yield curve has been measured for the $^{58}\text{Fe}(p, \gamma_0)^{59}\text{Co}$ reaction for E_p from 5.0 to 16.0 MeV in 100 keV steps. The data are analyzed to deduce the amplitudes and phases of the T matrix elements involved. The preferred solution indicates that the major change occurring in crossing the giant dipole resonance occurs in the relative phase between the $d_{5/2}$ and $g_{9/2}$ amplitudes. The implications of these results are discussed vis à vis the isospin splitting of the giant dipole resonance."

5. Study of The Giant Dipole Resonance Region of ^{31}P (C. P. Cameron, R. D. Ledford, N. R. Roberson, J. D. Turner, D. G. Rickel, H. R. Weller, R. McBroom, D. R. Tilley)

The measurements in the giant dipole resonance (GDR) region of ^{31}P which were reported in our last progress report have been extended with the Cyclo-Graff to an excitation energy of 34 MeV ($E_p = 28$ MeV). The excitation curves of both $^{30}\text{Si}(p, \gamma_0)^{31}\text{P}$ and $^{30}\text{Si}(p, \gamma_1)^{31}\text{P}$ were obtained and are shown in Fig. F5-1. The structure observed is typical for this mass region. The photo-neutron measurements of Berman and his co-workers¹⁾ and of Gellie et al.²⁾ indicate that the main strength of the giant dipole resonance starts around $E_x \cong 16$ MeV. One obvious feature of our (p, γ_0) data is the large strength below 16 MeV, a feature which is also observed with the $^{31}\text{P}(p, \gamma_0)^{32}\text{S}$ and $^{88}\text{Sr}(p, \gamma_0)^{89}\text{Y}$ reactions. If we look above $E_x \cong 16$ MeV, the $^{30}\text{Si}(p, \gamma_0)$ data suggests two broad "peaks" centered at ≈ 17.7 and 21 MeV, respectively. An integration of the cross section from 16 to 19.4 MeV and from 19.4 to 23 MeV gives ~ 4.6 and 3.9 mb-MeV, respectively. If we take the $^{31}\text{P}(\gamma, n_0)^{30}\text{P}$ data of Gellie et al. and integrate the same regions we find ~ 10.9 and 1.7 mb-MeV. These results suggest isospin splitting of the GDR with the lower energy region being associated with $T = 1/2$ component and the upper with $T = 2/3$ component. This is one of the few cases where both the (γ, p_0) and the (γ, n_0) reactions have been studied and which permits a simple comparison of the $T_<$ and $T_>$ regions. While the $^{30}\text{Si}(p, \gamma_1)$ yield should also show the same structure but shifted by ~ 1.3 MeV (E_{x_1} of ^{31}P), the results of our work (Fig. F5-1) do not indicate this feature.

Angular distributions of cross section and analyzing power have been measured at 12 energies with polarized proton beams, and at seven angles from 42° to 142° . The angular distributions of the cross section and analyzing power were fit to Legendre and associated Legendre polynomials, respectively, and a transition matrix analysis has been applied to the a_k and b_k coefficients. As a first step, only E1 radiation, which is expected to be the major component in the decay, was included in the analysis. Since the ground state of ^{31}P is $1/2^+$, only $p_{1/2}$ and $p_{3/2}$ amplitudes are involved in the E1 decay of this GDR. The results, shown in Fig. F5-2, indicate two possible solutions; one with $\sigma(p_{1/2}) > \sigma(p_{3/2})$ and the other $\sigma(p_{3/2}) > \sigma(p_{1/2})$. The relative phases were calculated from the optical model using global parameters and the results are shown in Fig. F5-2 as the dashed line. The phase difference, which is expected to come from the spin-orbit splitting, is observed and calculated to be rather small.

We have also obtained the E2 strength from an extended T-matrix analysis. The results of the analysis indicate an appreciable E2 strength which appears as a broad peak centered between 17-18 MeV excitation and with a width of ≈ 5 MeV. Unfortunately, the magnitude of the E2 cross section is rather uncertain. The source of the uncertainty comes from both the question of whether or not to include M1 radiation in the analysis and from the large errors in the a_4 coefficients. We have recently remeasured the angular distributions of cross sections over an angular range to include the zeros of $P_5(\cos\theta)$. A preliminary analysis of these new data indicates a significant reduction in the a_4 errors. A new T-matrix analysis is underway.

1) Berman et al.,

2) Gellie et al., *Asilomar* (1973) 171

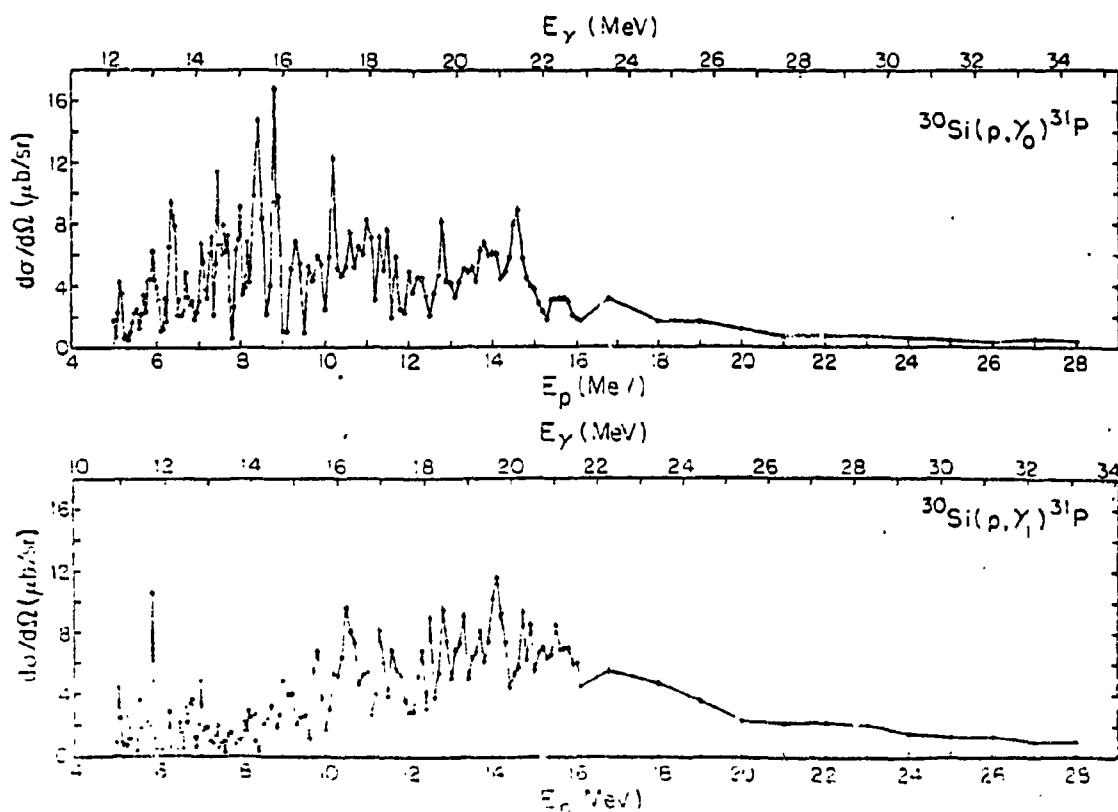


Fig. F5-1. The excitation functions for $^{30}\text{Si}(p, \gamma_0)^{31}\text{P}$ and $^{30}\text{Si}(p, \gamma_1)^{31}\text{P}$ measured at a laboratory angle of 90° . The solid line is composed of straight lines connecting the data points.

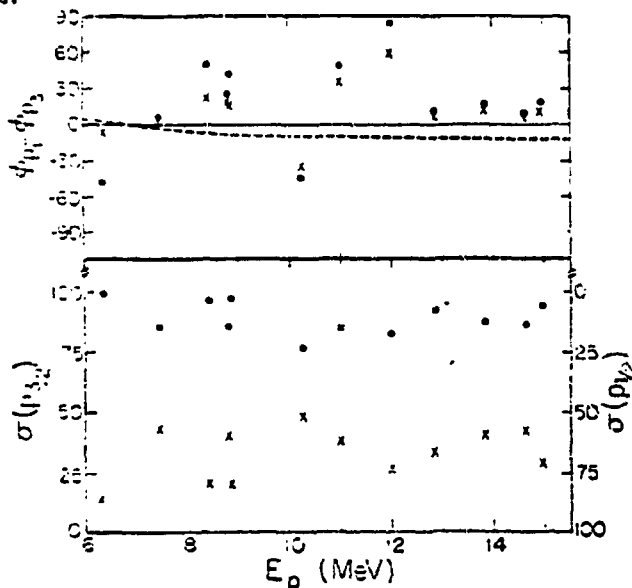


Fig. F5-2. The two solutions from a pure $E1$ analysis of the coefficients a_1 , a_2 and b_2 obtained from fitting the $^{30}\text{Si}(p, \gamma_0)$ data. The σ 's are expressed as a percentage of a_0 .

6. Study of The Radiation in The Giant E1 Resonance Region of ^{89}Y with The Reaction $^{88}\text{Sr}(\beta, \gamma)^{89}\text{Y}$ (R. D. LeFord, C. P. Cameron, N. R. Roberson, D. Turner, D. G. Rickel, H. R. Weller, R. A. Blue, R. McBroom, D. R. Tilley)

The Cyclo-Graaff beam has been used to extend the yield curves for the $^{88}\text{Sr}(p, \gamma_0)$ and $^{88}\text{Sr}(p, \gamma_1)$ reactions to an excitation energy of ≈ 34 MeV ($E_p = 27$ MeV). The results are shown in Fig. F6-1. A suggestion of isospin splitting in this nucleus has been made by Vergados and Kuo¹⁾ (based on unpublished data extending only to $E_p = 16$ MeV). Our extended measurements make the separation of the GDR into $T_<$ and $T_>$ components much more complicated. This is especially true for the (p, γ_1) yield where we now observed three broad "peaks" rather than two.

Angular distributions of cross section and analyzing power have been taken at 14 energies through the GDR region. The data for gamma-rays going directly to the ground state were fitted with Legendre and associated Legendre polynomial in order to extract a_k and b_k coefficients. A T-matrix analysis assuming pure E1 radiation (i.e., using only a_0 , a_2 and b_2) has been carried out as a first step in understanding the data. Fig. F6-2 shows the results in terms of the amplitudes $s_{1/2}$ and $d_{3/2}$ (l_j refers to the incoming proton since $J^{\pi} = 0^+$ and $1/2^-$ for ^{88}Sr and ^{89}Y , respectively). As expected, two solutions are found, one of which corresponds to $s_{1/2}$ being the major amplitude and the other to $d_{3/2}$ being the major component. As opposed to the cases of $^{30}\text{Si}(p, \gamma_0)$, the two solutions have significantly different relative phases. The dashed line is an optical model calculation of the phase difference and seems to suggest that the solution with major $s_{1/2}$ is the correct one. This is in contradiction to the expectation²⁾ that the component with the largest value of J will provide the major contribution to the decay of the GDR.

In an attempt to resolve this question, we have carried out a detailed study of the two IAS at $E_p = 6.06$ and 7.50 MeV, respectively. The $\theta = 70^\circ$ cross sections and analyzing powers were measured in small energy steps over these IAS. The results for the 6.06 MeV state are given in Fig. F6-3. The analysis assumed an interference of an isobaric analogue state with a GDR background. Since the energy interval is small, we assumed the GDR amplitudes, $s_{1/2}$ and $d_{3/2}$, were constant and used a Breit-Wigner resonance shape for the IAS. The fits shown in Fig. F6-3 indicate that $s_{1/2}$ is, in fact, the major component of the GDR (curves A and B). However, the fits (not shown) for the 7.50 MeV IAS yield $d_{3/2}$ as the major component. Since the E1 analysis shown in Fig. F6-2 does not suggest a crossing of the major components, our study of these two IAS has led to a new uncertainty rather than solving the original problem. More work is clearly needed before these problems can be understood.

1) Vergados and Kuo, Nucl. Phys. A168 (1971) 225

2) E. Hayward, Nat. Bur. of Stand. (U.S.) Monograph 118, 1970.

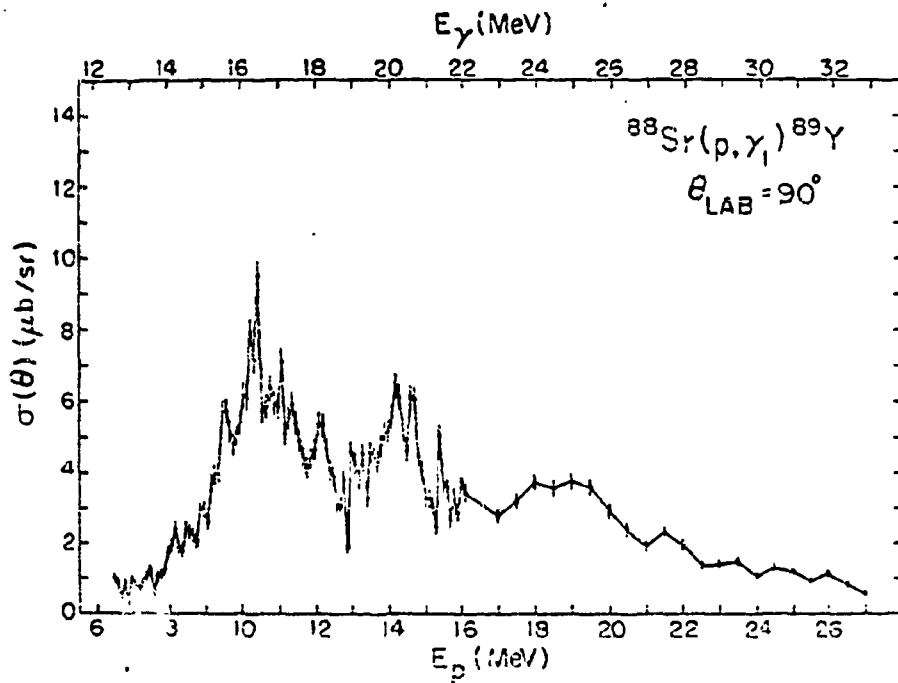
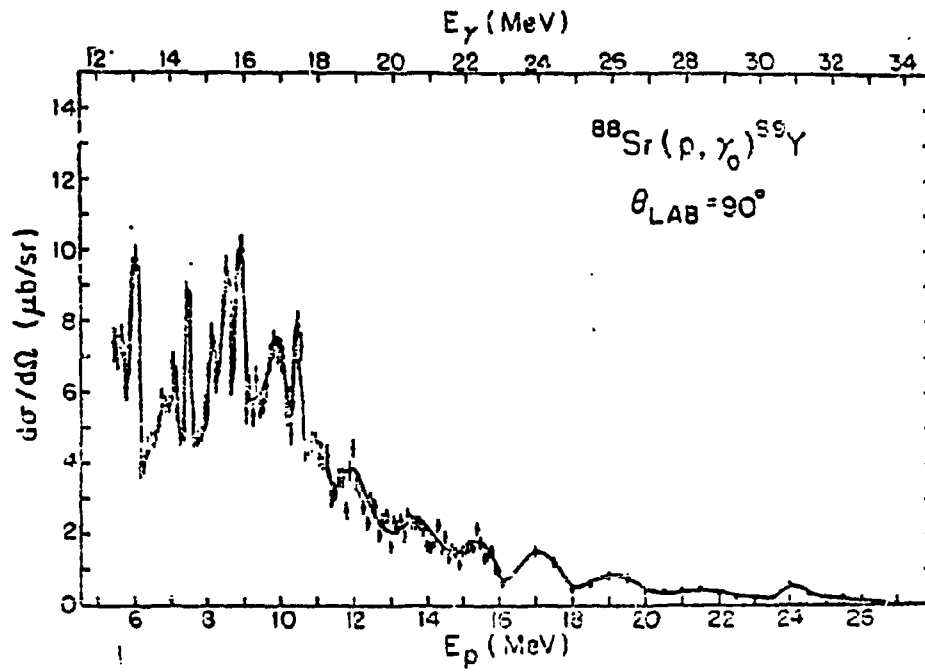


Fig. F6-1. The yield curves for $^{88}\text{Sr}(p, \gamma_0)$ and $^{88}\text{Sr}(p, \gamma_1)$. The solid lines are smooth curves through the data points.

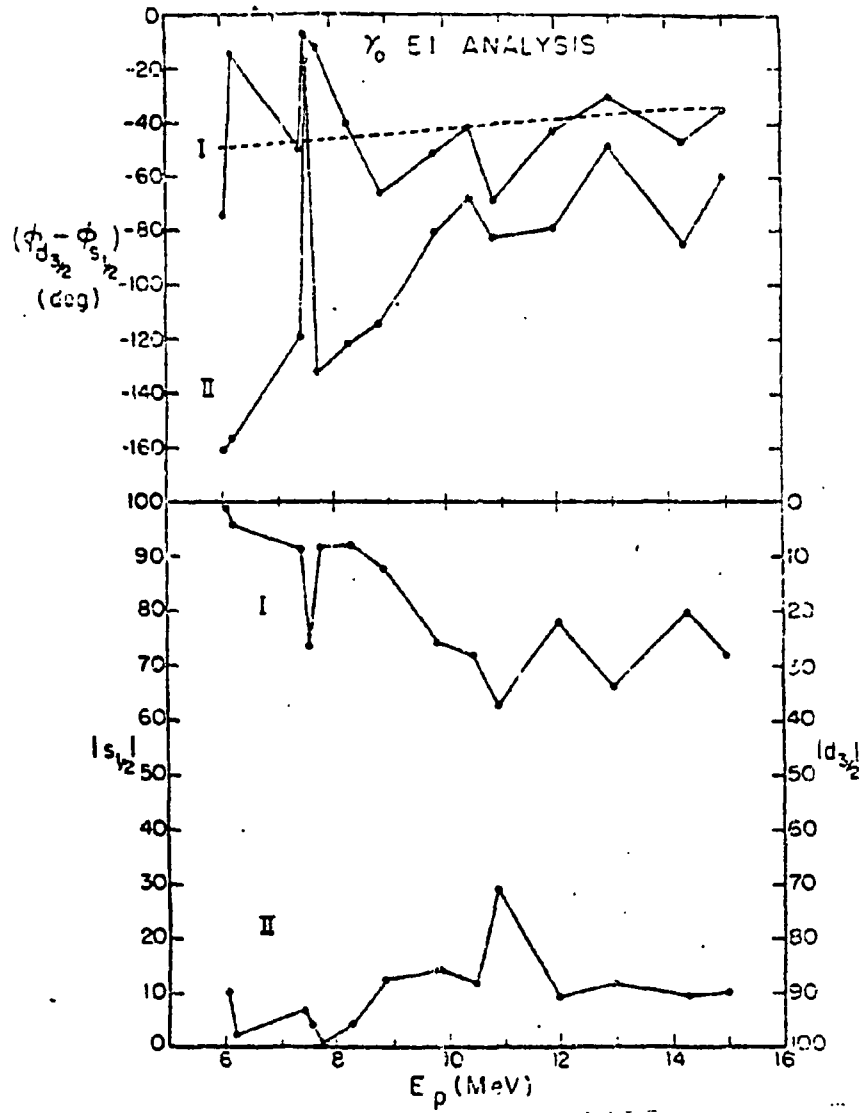


Fig. F6-2. The two solutions obtained from a pure EI analysis for the $^{88}\text{Sr}(p, \gamma_0)$ data. The amplitudes are expressed as a percentage of a_0 . The dashed line is an optical model calculation of the phase difference.

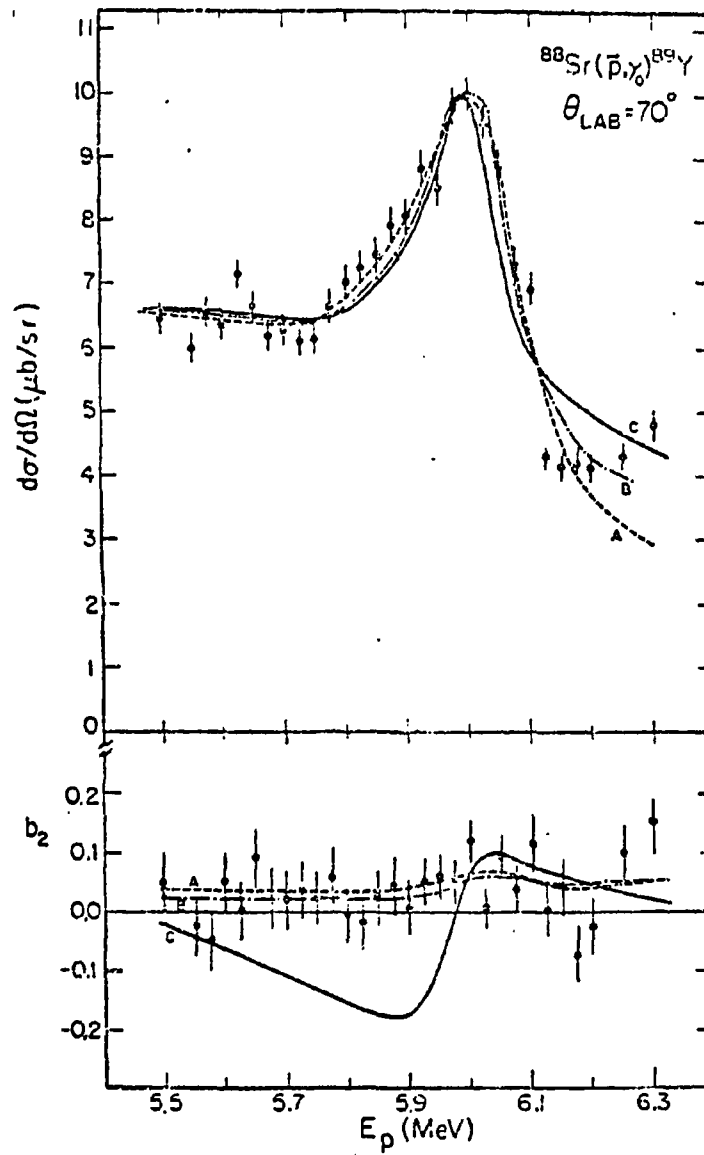


Fig. F6-3. The cross section and b_2 coefficients for the IAS at 1.06 MeV. The curves are simultaneous fits. Curves A and B represent $\Phi_{\text{IAS}} - \Phi_{\text{GDR}} \approx 0^\circ$ or 90° , respectively but both with $s_{1/2}$ as the major GDR amplitude. Curve C is a fit which is found to have $d_{3/2}$ as the major GDR amplitude.

7. A Study of The $D(p,\gamma)^3\text{He}$ Reaction (D. Skopik,* P. Von Behren, C. P. Cameron, N. R. Roberson, S. Wender, H. R. Weller, R. A. Blue, D. R. Tilley*)

Although some recent experiments on the (γ, p) and (p, γ) reactions have been performed, the experimental situation involving the two-body channel in ^3He remains confused. (Near the peak of the giant resonance.) There exists a wide choice of cross section magnitudes ranging from a low of $\sigma(\theta = 90^\circ) \approx 90_\mu \text{ b/sr}$ to a high of $\sigma(\theta = 90^\circ) \approx 120_\mu \text{ b/sr}$.

In addition there have been no measurements made with polarized beams which yield information on the importance of spin-flip amplitudes in the two-body channel, and also may allow one to extract the E2 cross section. The E2 cross section is especially interesting inasmuch as re-scattering effects are expected to be much more pronounced than in the E1 cross section.¹⁾

We have started a measurement of the $D(\vec{p}, \gamma)^3\text{He}$ reaction using a CD_2 target. At proton energies $E_p \gtrsim 11 \text{ MeV}$ a gas cell will be employed to avoid contamination of the gamma-ray spectrum with other reactions such as $^{12}\text{C}(p, \gamma)$. The data taken at $E_p = 8.0 \text{ MeV}$ are shown in Fig. F7-1. Preliminary analysis of these data indicates (a) that there is essentially zero phase between the E1 and E2 amplitudes and (b) there is some interference between different E2 amplitudes since fitting the data to associated Legendre polynomials gave a finite value for the $\ell = 4$ coefficient.

Further work is planned, extending the measurements to both lower and higher excitation energies.

8. Fast Neutron Capture Progress Report (P. Von Behren, S. Wender, H. R. Weller, R. A. Blue, N. R. Roberson, D. R. Tilley and C. R. Gould)

The fast neutron capture program is continuing in development and has produced experimental data during the past year. Modifications have been made to the original shield which have reduced the background count rate by a factor of ≈ 8 . We have replaced the original outer shield of copper with a combination of copper and polyethylene and have also added two more inches of lead shielding around the detector. Also, we have doubled the volume of our calcium target. These improvements have allowed us to take data with better statistics and lower background counting rates. Our detector is 4" diam. x 7" long and gives only 8-10% resolution for a 16 MeV γ -ray. Therefore, we have recently looked at both the full-energy peaks and escape peaks separately by setting appropriate coincidence windows in the anticoincidence shield. This gives us a better effective resolution. One further development will be to replace the present detector with a 5" diam. x 6" long NaI center in the hope of improving our resolution.

Fig. F8-1 shows the asymmetry data which we have measured at 8, 9, 10, and 12 MeV incident neutron energies (the 14 MeV point is by Arthur, et al.). The asymmetry is

* Visiting scientist from the University of Saskatchewan, Saskatchewan, Canada

1) J. M. Barbour and J. E. Hendry, Phys. Lett. 38B (1972) 151

2) E.D. Arthur, D.M. Drake, and J. Hallper, Phys. Rev. Lett. 35, No. 14, Oct. 6, 1975

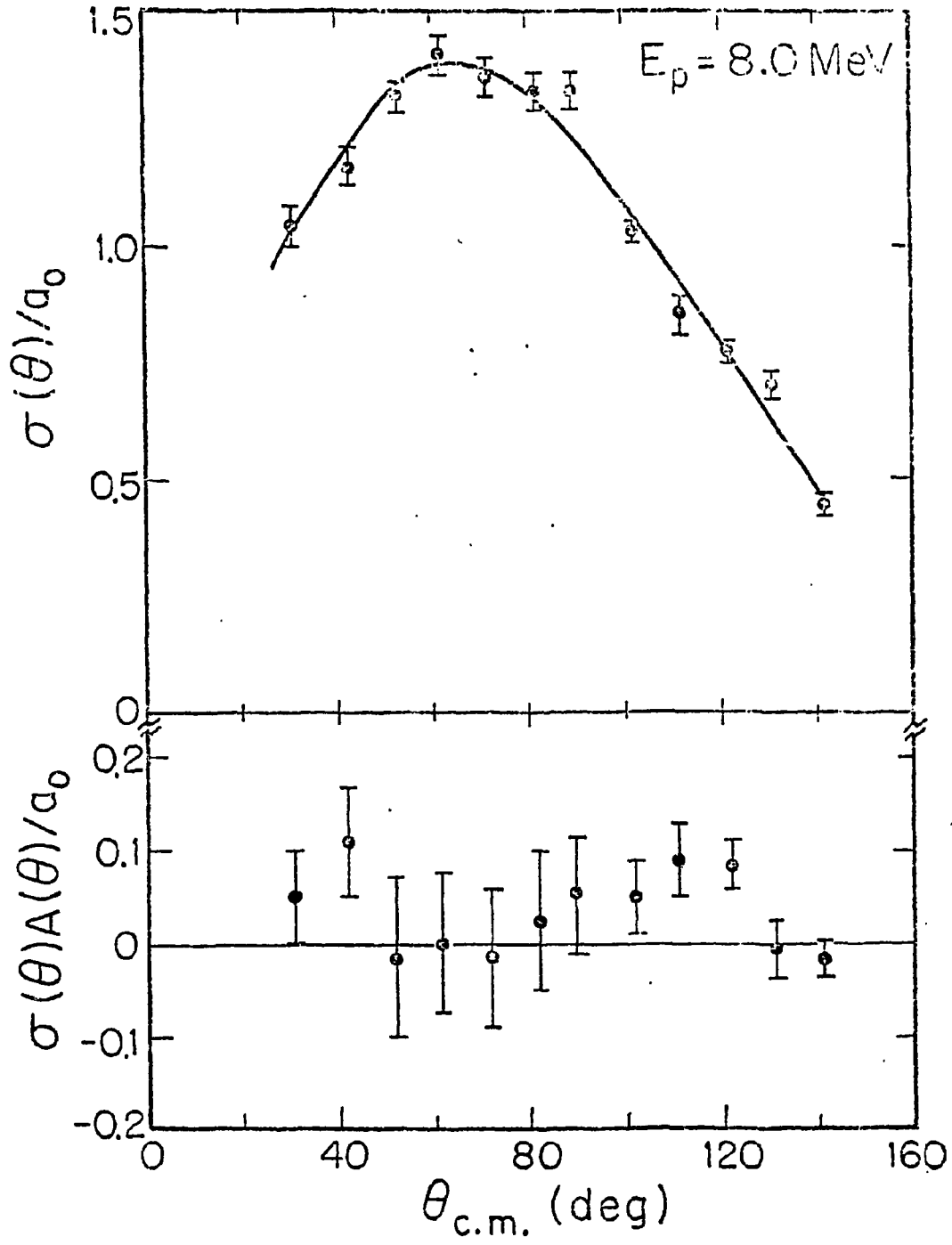


Fig. F7-1. Angular distribution of cross section and analyzing power for the $D(p, \gamma)^3\text{He}$ reaction.

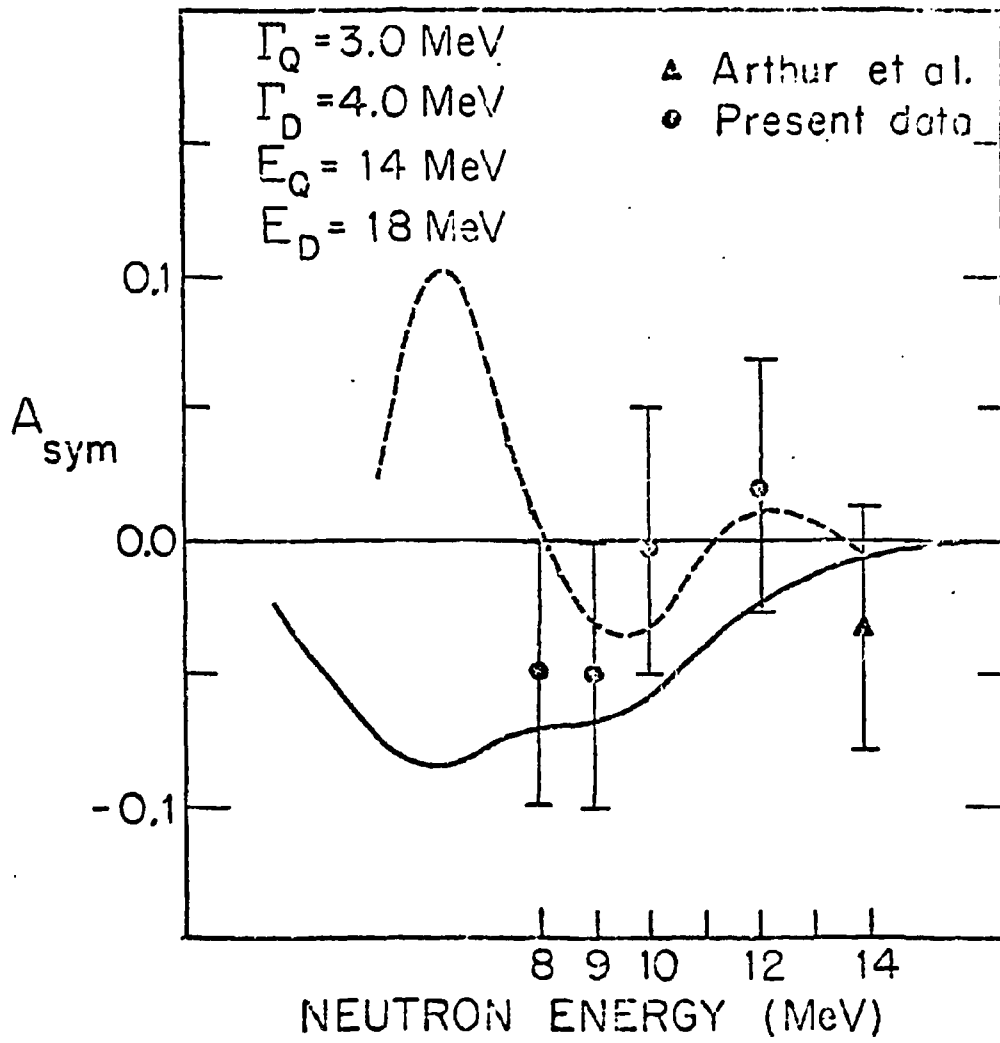


Fig. F8-1. The asymmetry obtained with the $^{40}\text{Ca}(n, \gamma)^{41}\text{Ca}$ reaction as discussed in the text.

$$A_{\text{sym}} = \frac{Y_{55^\circ} - Y_{125^\circ}}{Y_{55^\circ} + Y_{125^\circ}}$$

where Y_{55° and Y_{125° are the $^{40}\text{Ca}(n, \gamma_0)$ yields at 55° and 125° to the $^{41}\text{Ca} f_{7/2^-}$ ground state. The solid line in the figure is an attempt to fit the data by considering capture through broad resonances, a giant dipole resonance at 18 MeV excitation and 4 MeV wide, and a giant isoscalar quadrupole resonance at 14 MeV excitation and 3 MeV wide. We have assumed that the E2 radiation occurs primarily through $p_{3/2}$ capture, and the E1 radiation occurs primarily through $d_{5/2}$ and $g_{9/2}$ capture.

Recently, M. Potokar²⁾ has calculated the asymmetry data for $^{41}\text{Ca}(n, \gamma)$ using the direct-semidirect model and the same resonance parameters as used in the above calculation. His calculations are shown as the dashed line in the figure for a real quadrupole form factor.

Further measurements are planned to reduce the uncertainties of the asymmetry data.

9. Study of The Giant Dipole Resonance Regions of ^{60}Ni (J. David Turner, C. P. Cameron, N. R. Roberson, H. R. Weller, R. A. Blue, D. R. Tilley)

The GDR of ^{60}Ni as studied via the $^{59}\text{Co}(p, \gamma_0)^{60}\text{Ni}$ has been presented as a clear example of isospin splitting with two broad "peaks" corresponding to $T = 2$ and $T = 3$. The proposed $T_<$ peak is centered near 17 MeV excitation energy while the $T_>$ one is near 20 MeV. In order to further investigate this proposed isospin splitting, we have started a study of the $^{59}\text{Co}(\vec{p}, \gamma_0)^{60}\text{Ni}$ reaction with polarized protons from the TUNL Lamb shift ion source. A T-matrix analysis of the data should allow us to obtain more information on the structure of the GDR as one moves through the peaks corresponding to $T_<$ and $T_>$.

The 90° yield curve has been remeasured from 8-13 MeV in 100 keV steps and from 13-16.4 MeV in 200 keV steps. Three preliminary angular distributions of cross sections and analyzing power have been measured at 8.8, 10.1 and 10.6 MeV. The results for $E_p = 10.1$ MeV are shown in Fig. F9-1. The experiment is continuing.

10. A Study of The $^3\text{H}(p, \gamma)^4\text{He}$ Reaction from $17 < E_p < 30$ MeV. (R. McBrook, R. D. Ledford, C. P. Cameron, N. R. Roberson, J. David Turner, D. G. Rickel, H. R. Weller, R. A. Blue, D. R. Tilley)

In our last report, we presented data, obtained with the TUNL Cyclo-Graaff, for the $^3\text{H}(p, \gamma)^4\text{He}$ reaction. Specifying a 90° excitation curve which extended to an excitation in ^4He of 42 MeV and a number of angular distributions were shown. As this work has continued, the exciting result has been the apparent observation of a relatively narrow resonance in ^4He at about 40 MeV with

2) M. Potokar, private communication

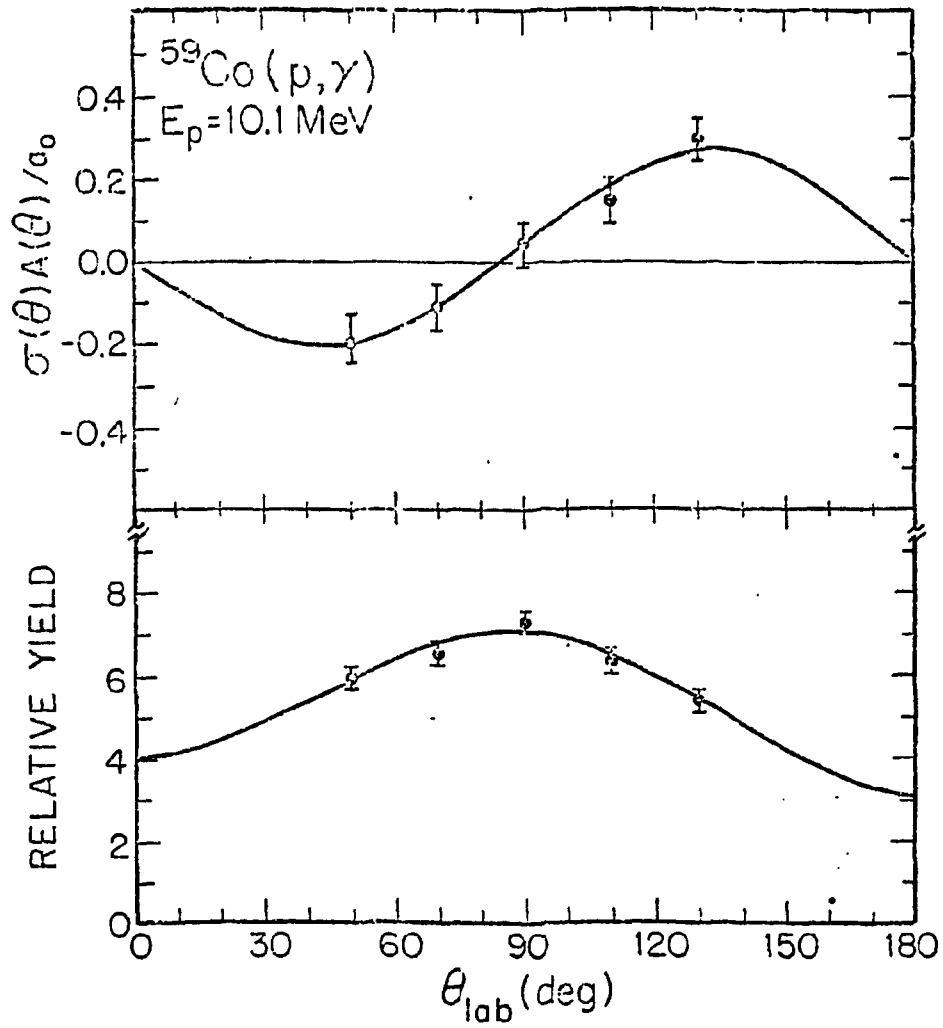


Fig. F9-1. Angular distribution and analyzing power for $^{59}\text{Co}(p, \gamma)^{60}\text{Ni}$.

$\Gamma \cong 3.5$ MeV. As we will see below, 94 coefficients appear to be required to fit the data--a result which suggests the resonance is E2 (i.e., a 2^+ state).

Fig. F10-1 shows the 8 angular distributions of cross sections that have been obtained since our last report. For six of these, the angular range extends in 20° , which is well beyond the zero of $P_5(\cos \theta)$ and which allows us to determine very accurately the a_k coefficients for $k \leq 4$. The a_k coefficients are shown in Fig. F10-2.

We have also measured the fore-aft asymmetry (see Sec. 12 above) from $E_x = 25$ to 43 MeV. These results along with other measurements are shown in Fig. F10-3. The solid lines in Figs. F10-2 and F10-3 are the results of a calculation which includes a smoothly varying E1 component which was determined so as to fit the data. The E2 strength is assumed to include a direct turn¹⁾ plus two 2^+ resonances. The first 2^+ resonance has previously been established²⁾ at 34 MeV with $\Gamma \approx 10$ MeV. The second 2^+ resonance which has the parameters given above is the result of this experiment. More work is underway to check our conclusions.

11. Measurement of E2 Strength for The Capture Radiation from ^{56}Fe via The (α, γ) Reaction (D. G. Rickel, N. R. Roberson, H. R. Weller, C. P. Cameron, R. D. Ledford, D. R. Tilley)

No new work has been done on this reaction. A paper is being prepared for publication.

12. A Search for the Isovector E2 Resonances in ^{31}P , ^{89}Y and ^{60}Ni (H. R. Weller, R. A. Blue, C. P. Cameron, R. D. Ledford, J. David Tumer, N. R. Roberson, D. R. Tilley)

A recent experiment of inelastic electron scattering from ^{89}Y has exhibited a broad state around 28 MeV excitation.³⁾ The location of this resonance is in reasonable agreement with the expected location of a collective isovector quadrupole resonance at $135/A^{1/3}$. Stimulated in part by these (e, e') results, we have used the TUNL Cyclo-Graaff to search for the effects of E2 resonances above the region of the GDR via the $^{30}\text{Si}(p, \gamma)^{31}\text{P}$, $^{88}\text{Sr}(p, \gamma)^{89}\text{Y}$ and $^{54}\text{Co}(p, \gamma)^{60}\text{Ni}$ reactions. The presence of radiation which can interfere with the E1 radiation from the tail of the giant dipole would produce finite a_1 and a_3 coefficients in the Legendre expansion of the cross sections. We have measured the fore-aft asymmetry

$$A = \frac{\sigma(55^\circ) - \sigma(125^\circ)}{2P_1(\cos 35^\circ)} = A_1 - 0.67 A_3$$

for the three reactions mentioned above. The results for ^{89}Y and ^{31}P are shown in Fig. F12-1. The solid lines in the figure were obtained by a rather simple calculation which assumed that the amount of direct E2-E1 interference could be expressed as a straight line and that the interference between a E2 resonance and the GDR tail could

1) Flower and Mandel, Proc. Roy. Soc. A206 (1951) 131

2) Meyerhof and Fiarman, Asilomar (1973) 385

3) F. R. Buskirk, private communication (1976)

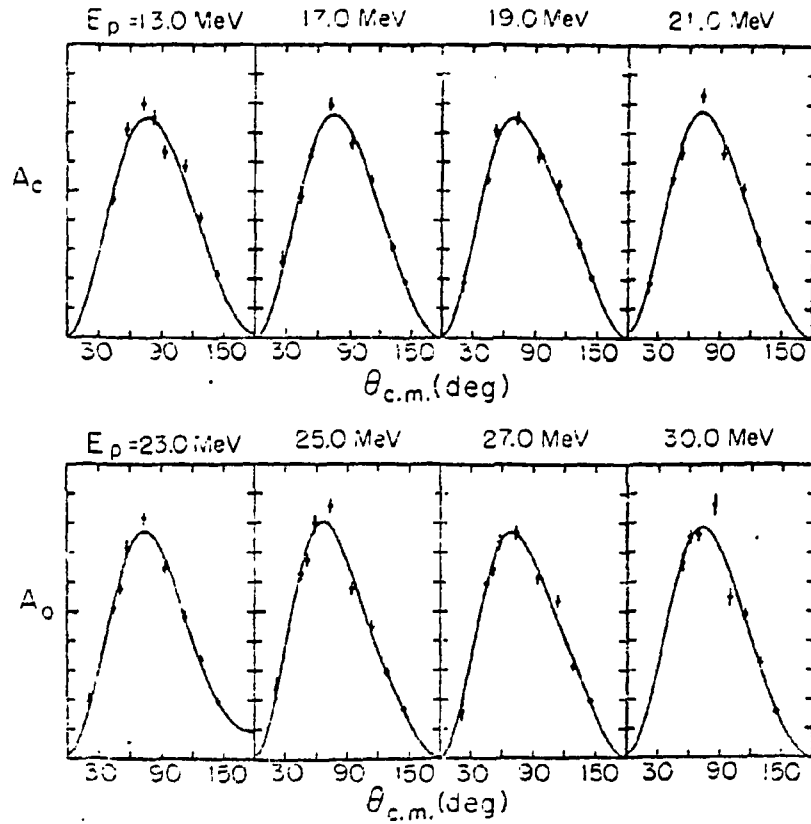


Fig. F10-1. Angular distribution for ${}^3\text{H}(p, \gamma){}^4\text{He}$.

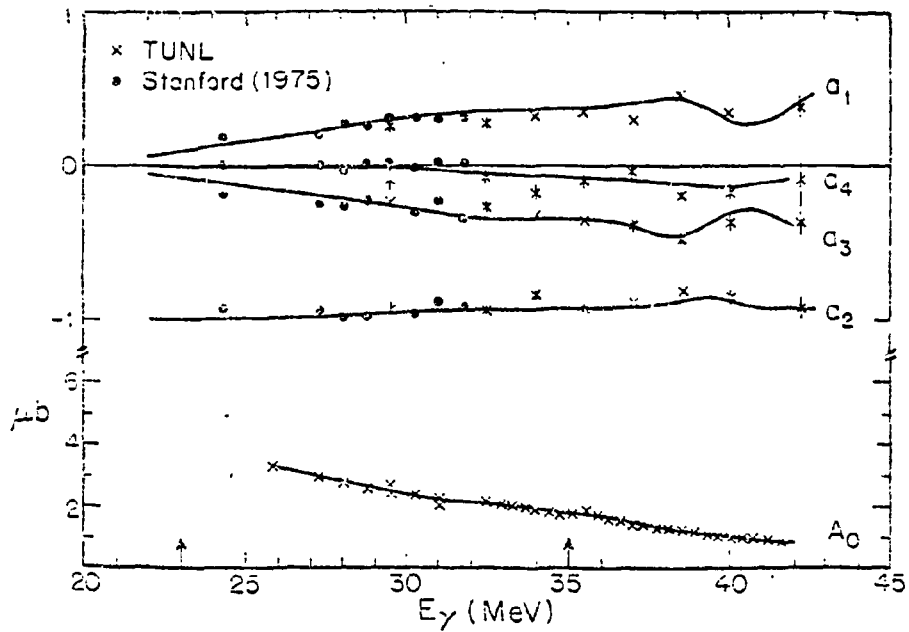


Fig. F10-2. Angular distribution coefficients for ${}^3\text{H}(p, \gamma){}^4\text{He}$.

be expressed as a Breit-Wigner shape (E2) times decaying exponential (E1).²⁾ The reasonable fits obtained and the fact that the resonance energy, width and approximate strength for the ^{89}Y case agree so well with the (e, e') measurements, give support to our conclusion that we have observed in ^{89}Y and ^{31}P the isovector E2 resonance. More extensive measurement will be made for these two cases as well as for ^{60}Ni , where the preliminary data was not extensive enough to analyze.

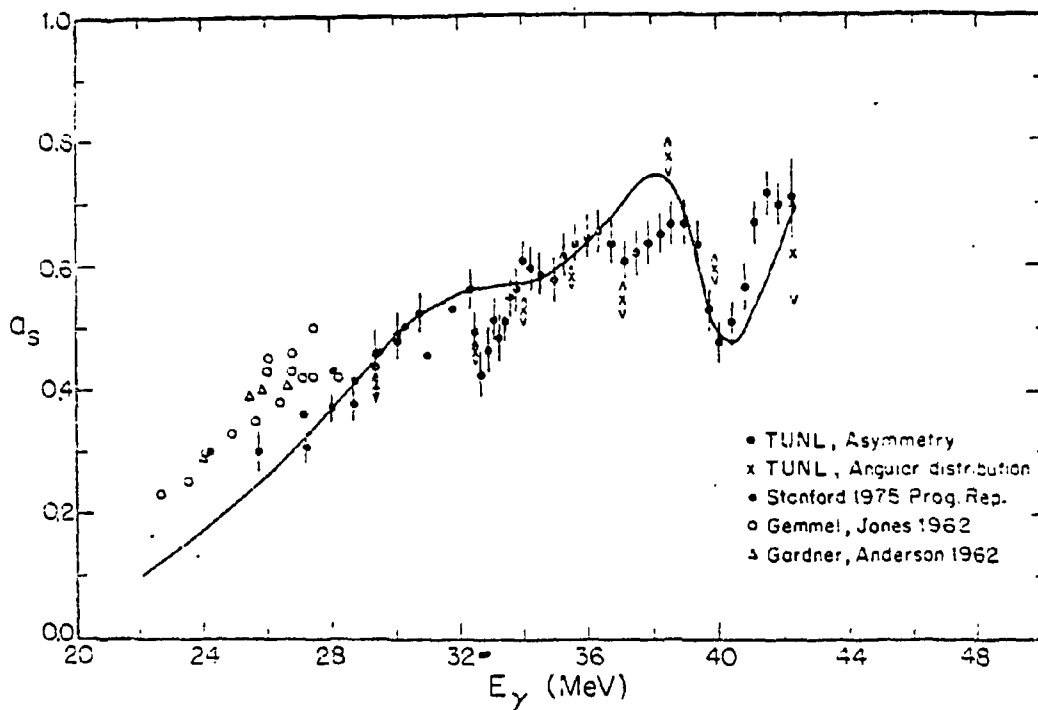


Fig. F10-3. Fore-aft asymmetry for $^3\text{H}(p, \gamma)^4\text{He}$.

¹⁾ K. A. Snover et al., Phys. Rev. Letts. 32 (1974) 317.

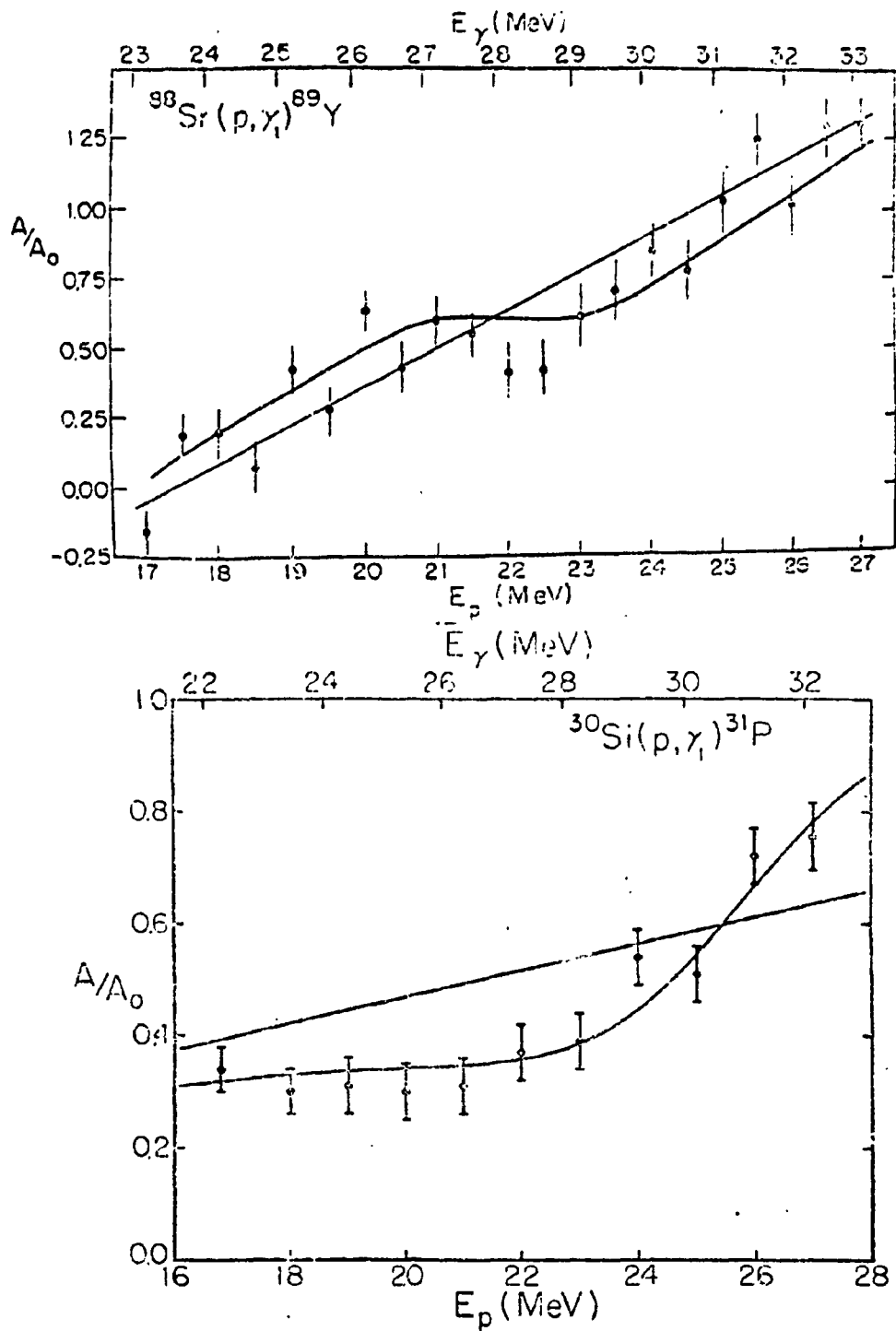


Fig. F12-1. The normalized asymmetry for the $^{88}\text{Sr}(p, \gamma)^{89}\text{Y}$ and $^{30}\text{Si}(p, \gamma)^{31}\text{P}$ reactions. The fits are described in the text.

G. ATOMIC COLLISION PHYSICS

1. Two Electron-One Photon X-ray Transitions (2e-1 γ) (B. Doyle, J. M. Feagin, S. M. Shafroth, J. A. Tanis, A. Waltner)

We have studied this process in considerable detail. The main features of interest were the energies of these x rays as a function of incident Cl^{n+} ion bombarding energy, the cross section for these rare x-ray transitions and the probability of one electron decay compared to two electron decay.

The study of the energies of these transitions lead to a better understanding of the effect of simultaneous L vacancy production on the transition energies and this has been submitted for publication to Physical Review Letters before the main paper. The title, authors and abstract of this paper are as follows:

Comment on The Comparison of Observed Two
Electron-One Photon Transition Energies with Calculated
Values

J. A. Tanis, J. M. Feagin, W. W. Jacobs, and S. M. Shafroth

"We describe a method for comparing observed two electron-one photon transition energies with theoretical values in order to determine the L-shell vacancy configuration at the time of x-ray emission. This method reduces the dependence on the particular computer code used in the calculation. Present calculations indicate a higher degree of L-shell ionization in the Fe and Ni data of Wölfli than that found by previous investigators."

Figure G1-1 illustrates the calculated results for energy shifts (ΔEK_{α}^h) of K_{α}^h (the 2e-1 γ transition) from the unshifted hypersatellite transition energies (K_{α}^{h0}) scaled by $Z(Z-1)$ where Z is the atomic number of the target or projectile as appropriate vs Z . One sees that at higher bombarding energy there is more multiple L shell ionization as in the case of calcium ($Z = 20$) for example. Furthermore in Wölfli's original experiments on Fe and Ni, the average L-shell ionization and the time of K_{α}^h emission is nearly 2 in contrast to conclusions of other workers who have claimed more nearly zero or one L-shell vacancy at the time of K_{α}^h emission.

We have taken data which will allow us to obtain absolute cross sections for this process. The Cl^{n+} ion energy dependence of these cross sections can be compared with electron promotion model calculations. This should give further insight into this important process for producing K vacancies. Finally, the ratio of 2e-1 γ to 1e-1 γ transition strengths as a function of target and projectile Z when two K vacancies are present has been the subject of considerable theoretical interest. One model says that the "first" transition is electric dipole and this shakes up the ionized atom in such a way that a subsequent 2s-1s monopole transition takes place giving rise to the 2e-1 γ photon. This model fits most of the existing data from Al-Ni.

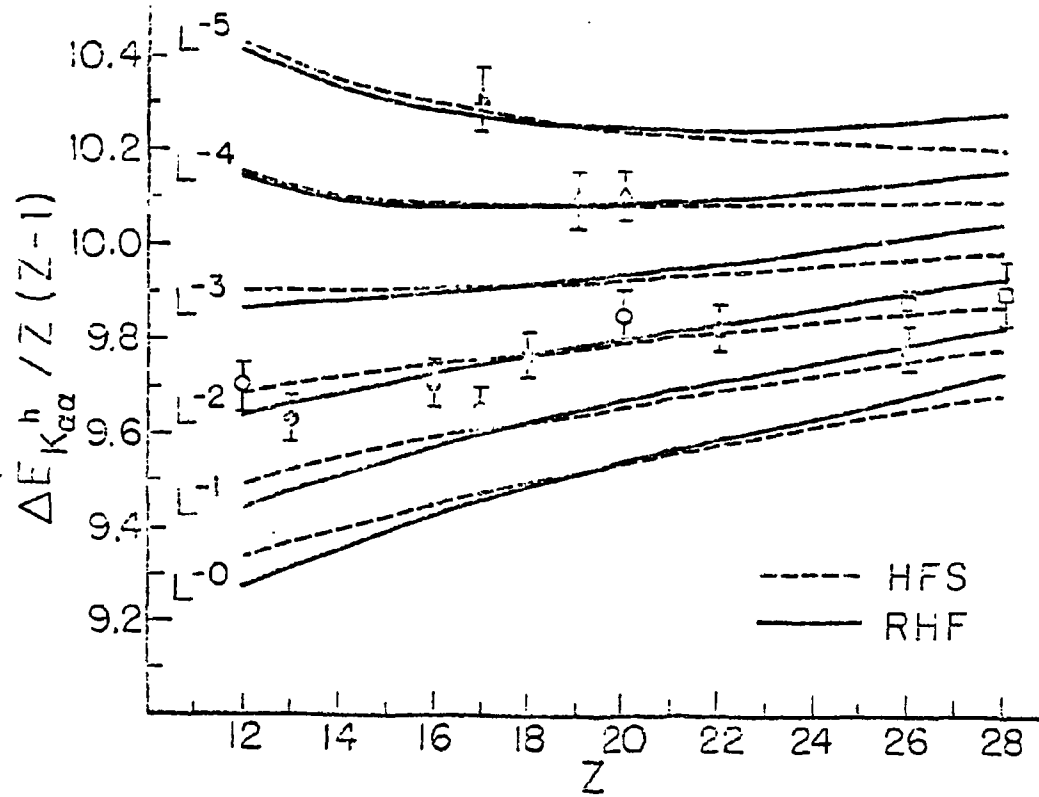


Fig. G1-1. Comparison of experiment and theory for $\Delta E_{K\alpha\alpha}^h / Z(Z-1)$ vs. Z where $\Delta E_{K\alpha\alpha}^h = E_{K\alpha\alpha}^h - E_{K\alpha}^{h0}$. RHF and HFS curves were calculated using the Desclaux program and the Herman-Skillman program, respectively. The circles represent data from N.R.L. obtained with 3.0 - 3.5 MeV projectiles; the triangles are from present work at TUNL for 50 MeV projectiles; and the squares are the 40 MeV measurements of W8ifli et al. The open symbols represent data obtained for target atoms while the closed symbols are for projectile atoms.

2. K X rays Arising from 20-80 MeV Ion Bombardment of Ti, Mn, Cu and KBr
(B. Doyle, W. W. Jacobs, S. M. Shafroth, J. Tanis)

Characteristic target K x-ray cross sections were determined at intervals of 10 MeV for the above listed targets and results were compared with theory. In the case of Cu we find fair agreement with corrected plane wave Born approximation calculations (PWBA) but in the case of potassium the experimental cross sections were an order of magnitude larger than corrected PWBA. This is due to "K Vacancy Sharing", where the projectile brings in a K vacancy which is transferred to the target in the collision. A detailed and systematic study has also been made of K x-ray energy shifts which for manganese ($Z = 25$) K_{β} range from 190 eV to 320 eV above the tabulated values as the Cl projectile energy varies from 20 to 80 MeV. Over this same projectile energy range, the Mn K_{β}/K_{α} ratio varies from 0.12 to 0.20. We are attempting to understand these results in terms of basic quantum mechanical calculations. We can tell approximately how many and which inner shell electrons must be ejected at the time of x-ray emission to explain the data from Hartree-Fock energy calculations but we have not yet gotten to the point where we can explain why these particular electrons are ejected at a given incident Cl^{n+} energy. In other words we can not yet predict very well what will happen if we change the Z of the projectile. Such information will be important if heavy ion beams are to be used for trace element analysis.

Recently we have been studying the effect of target thickness on these cross sections. Vacancy sharing and quenching effects must be taken into account to obtain primary electron removal cross sections suitable for detailed comparison with theory.

3. Radiative Electron Capture Resulting from 20-70 MeV Chlorine Ion Bombardment of C, Ti, Mn and Cu (B. Doyle, W. W. Jacobs, S. M. Shafroth, J. Tanis)

Radiative Electron Capture (REC) occurs when the projectile ion captures a target electron into its K shell and in so doing emits an x ray. The energy of this x ray is equal to the K shell binding energy of the projectile plus the center of mass kinetic energy of the captured electron in the projectile frame of reference. We have made a careful study of the energies of REC peaks vs Cl^{n+} energy and have found in the case where the target is a thin $20 \mu\text{g}/\text{cm}^2$ carbon foil that the REC peak energy varies nearly linearly from 3300 to 4600 keV when the Cl^{n+} ion energy is varied from 20-80 MeV. This variation can be expressed in terms of the multiple ionization state of the projectile which can be determined from Hartree-Fock calculations. Furthermore we have studied the width of the REC peak over this energy range and find it varies from 500 eV to 1 keV. Also we have measured the differential cross section for this process and find it to vary from 2-6 barns/sr. We obtained good agreement with the simplified theory of Bethe and Salpeter for the cross section assuming only one electron per carbon atom was available for capture and unit fluorescence yield. However, neither of these assumptions is easy to justify, so there is much more work to be done before the process is understood.

H. HEAVY ION REACTIONS

1. Recoil Ranges and Range Straggling of Nuclei Resulting from $^{59}\text{Co}(^{16}\text{O}, X)Y$ Reactions (A. W. Waltner, T. W. Godfrey, D. M. Peterson, S. M. Shafroth, W. Jacobs, J. A. Tanis)

This experiment was performed in order to determine the ranges of the recoil nuclei resulting from the $^{59}\text{Co}(^{16}\text{O}, X)Y$ reactions. This information was necessary in the analysis of a stacked foil experiment involving a set of 1 mg/cm^2 Co foils. It is necessary to determine the contribution of each foil to the activity of subsequent foils in order to determine the excitation function of each reaction. In this experiment the various $^{59}\text{Co}(^{16}\text{O}, X)Y$ reactions are identified through the gamma radiation associated with the residual nucleus. Although this type of reaction is expected to proceed by means of compound nucleus formation followed by evaporation of one or more nucleons and/or particles, the experiment should provide confirmation of this reaction mechanism. The experiment is of course insensitive to stable residual nuclei and to residual nuclei having very short half lives.

Two experiments were performed:

- (1) A stacked catcher foil experiment;
- (2) an angular distribution experiment .

The experimental arrangements are shown in Fig. H1-1.

The ranges of residual nuclei resulting from six of the major reactions were determined in a stacked catcher foil experiment, using Al foils with an areal density of about $0.28 \pm 0.03 \text{ mg/cm}^2$. The total stack of catchers was exposed to a beam of 56 MeV $^{16}\text{O}^{+7}$ ions at the TUNL tandem Van de Graaff. Each of the exposed foils was subsequently analyzed by Ge(Li) γ -ray spectroscopy to determine relative activity for each reaction product. The subsequent analysis was accomplished by fitting the relevant peaks to a Gaussian function and making appropriate decay corrections.

The mean range and straggling parameter for each residual nucleus was determined by plotting the activity transmitted through each of the foils on a probability scale. The mean range R_0 corresponds to the 50% reading; and the $R_0(1 + \sqrt{2P})$ value occurs at 7.87%. In the case of ^{73}Se resulting from $(^{16}\text{O}, \text{NP})$, the mean range is 1.04 mg/cm^2 and the straggling parameter is 0.203. This is equivalent to a Gaussian distribution about $R_0 = 1.04 \text{ mg/cm}^2$ with a standard deviation of 0.21 mg/cm^2 .

A summary for 6 major reactions is shown in Table H1-1. It is to be noted that the straggling parameter increases substantially with the number and mass of the evaporated particles, but the range remains essentially constant. (1.01 ± 0.05)

The range values as determined by this method represents only the component in the direction of the beam. It is necessary to have some information regarding

the angular distribution of the recoil nuclei. A separate experiment was set up to measure this distribution. The Al catcher foil was punched into 6 concentric annuli about the beam spot, and counted in the usual way. Results for three reactions and the total activity are shown in Fig. H1-2. The results of the experiment showed that the 86% of the recoils fall within a cone with a half-angle of 18° hence the recoils are predominantly in the forward direction.

The range of the residual nuclei from the $^{59}\text{Co}(^{16}\text{O}, X)Y$ reaction are compatible with a compound nucleus model. It is thus possible to use the measured ranges to calculate the contribution of each foil in the original ^{59}Co stacked foil experiment to subsequent foils and in this way determine the excitation function for each reaction.

TABLE H1-1

	R_0	$R_0(1+\sqrt{2P})$	P
^{73}Se	1.04	1.338	.203
^{72}Se	0.99	1.30	.221
^{72}As	1.025	1.33	.211
^{71}As	0.95	1.29	.254
^{69}Ge	1.01	1.45	.308
^{67}Ga	1.065	1.62	.368
	1.013 ± 0.040		

(Units in mg/cm^2)

R of CN = $1.058 \text{ mg}/\text{cm}^2$

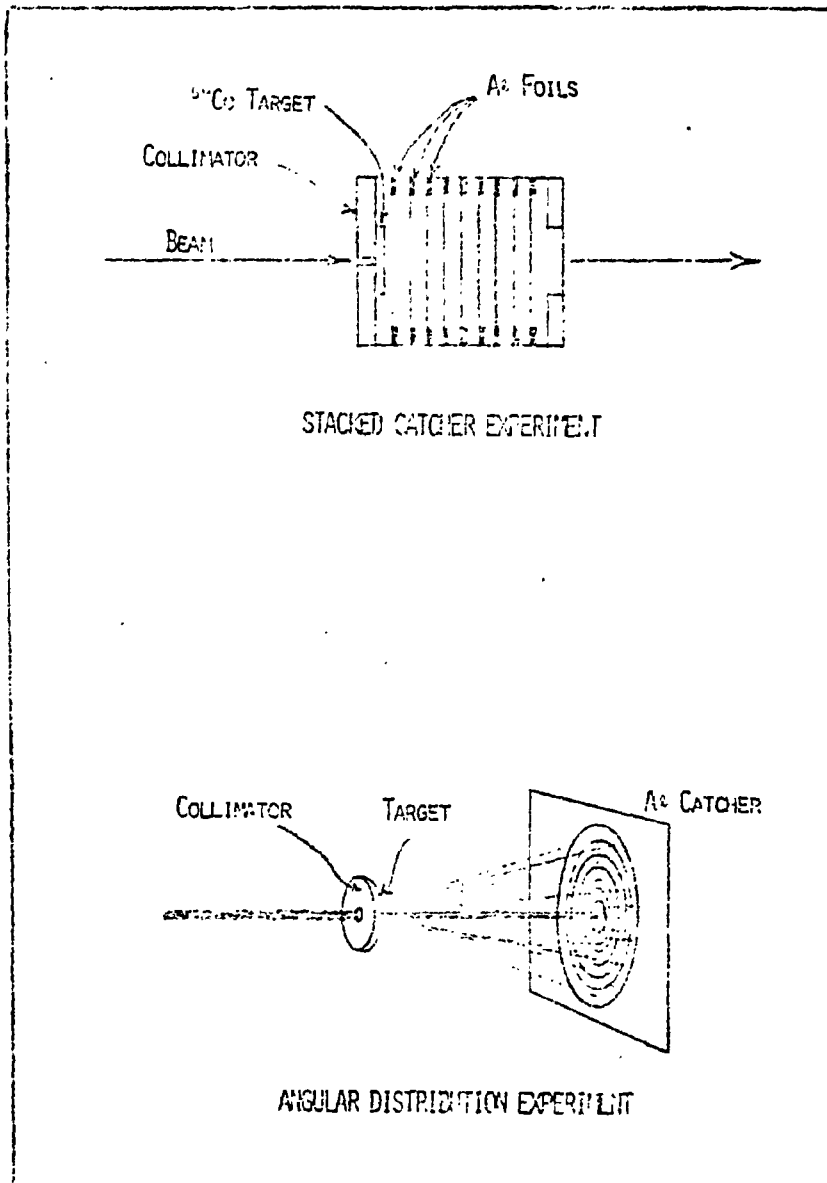


Fig. H1-1. Experimental arrangements for catcher foil and angular distribution measurements.

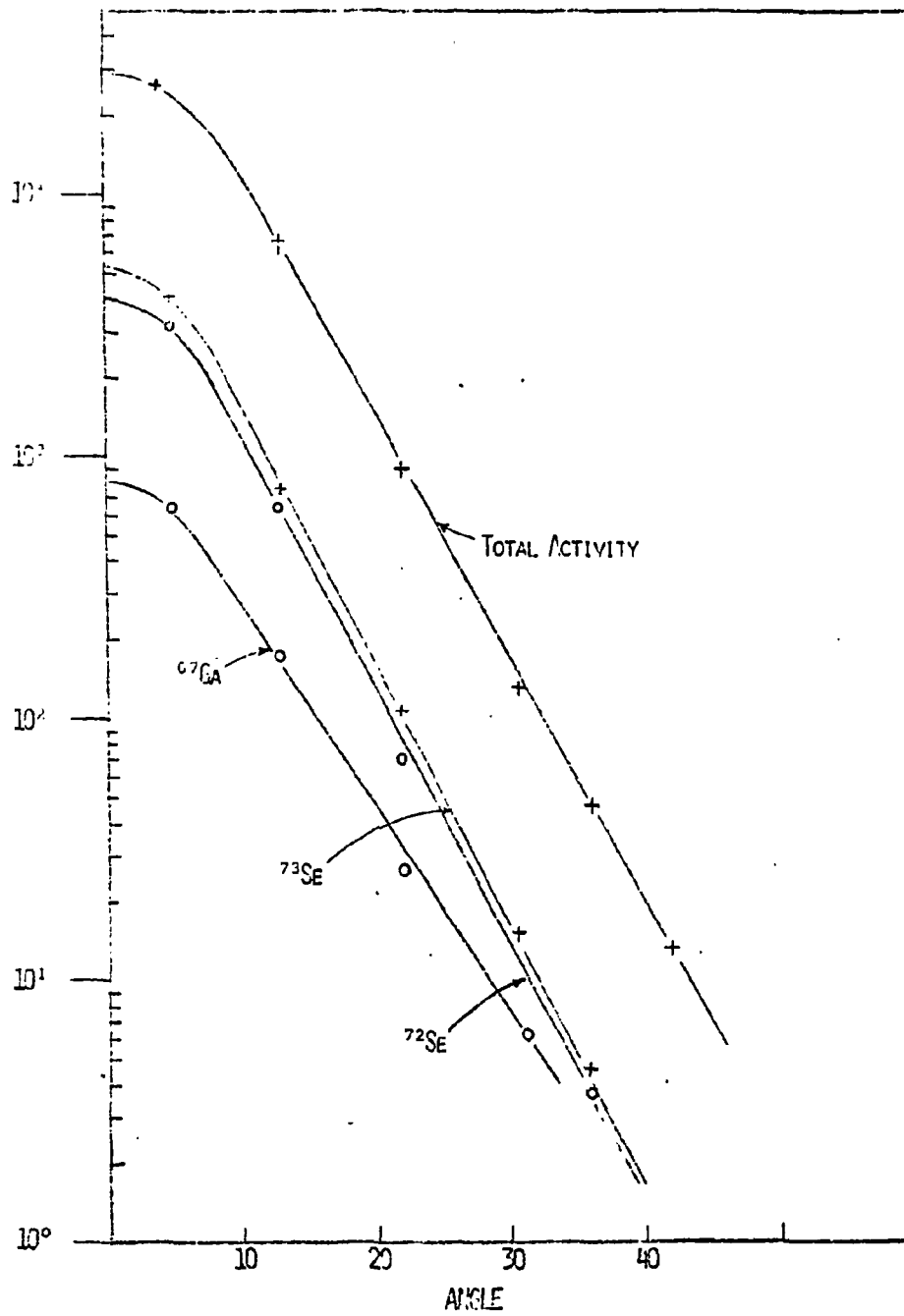


Fig. H1-2. Angular distributions of recoil nuclei.

I. APPLICATIONS

1. Neutron Spectra from Deuteron and Proton Bombardment of Thick Lithium Targets (C. E. Nelson,* F. O. Purser, P. Von Behren, H. W. Newson)

The suitability of thick lithium targets as sources of fast neutrons for cancer therapy has been investigated. Incident particle-energy combinations available to the small, "medical" cyclotron source used to determine if such beams when used to bombard lithium targets, lead to an improvement, vis a vis tissue penetration, in the resultant fast neutron spectra. Previous measurements were either non-existent (${}^7\text{Li} + p$) or yielded conflicting results (${}^7\text{Li} + d$).¹⁻³⁾

The relative energy sensitivity of the TUNL neutron time-of-flight facility main neutron detector was measured from .7 MeV to 24 MeV neutron energy using the well-known $T(p, n){}^3\text{He}$ and $T(d, n){}^4\text{He}$ neutrons at several charged particle energies,⁴⁾ and by scattering neutrons from hydrogen. The absolute efficiency was obtained by normalizing this relative efficiency curve at $E_n = 4.0$ MeV to a Monte Carlo calculation of the efficiency of the detector done at Oak Ridge National Laboratory.⁵⁾

Fig. 11-1 shows the neutron energy spectra obtained at zero degree for 8, 12 and 15 MeV deuterons and 15 MeV protons incident on the thick lithium target. These spectra were integrated for $E_n \geq 1.0$ MeV to obtain the neutron yield versus laboratory angle data shown in Fig. 11-2.

Calculations of the average neutron energy for each zero degree spectra showed $\bar{E}_n \cong .44E_d$ for the deuteron reactions while $\bar{E}_n \cong 4.7$ MeV for the proton reaction. The results of Weaver indicated that $\bar{E}_n \cong .42 E_d$ for deuterons on beryllium. Thus the lithium target offers essentially no improvement over beryllium with respect to average neutron energy. Since an average neutron energy of at least 8 MeV is required for adequate tissue penetration, the lithium target small cyclotron combination appears to be unsuitable for fast neutron cancer therapy.

This work has been submitted for publication to Physics in Medicine and Biology and has been presented at the following conferences: Interaction Conference on the Interactions of Neutrons with Nuclei, University of Lowell, Lowell, Mass., July 5-9, 1976; Fourth International Conference of Medical Physics, Ottawa, Canada, July 31-Aug. 4, 1976.

* Supported by National Cancer Institute Research Fellowship No. 1 F22 CA00332-01

1) A. Pinkerton, et al., Radiology 96 (1970) 131

2) F. M. Edwards, et al., Medical Physics 1 (1974) 317

3) A. N. Goland et al., Proceedings of the Charged Particle Accelerator Conference, Washington, D. C. 1975, IEEE N521

4) D. K. McDaniels et al., Physical Review C (1973) 882

5) G. Morgan, private communication

6) K. A. Weaver, et al., Nuclear Science and Engineering 52 (1973) 35

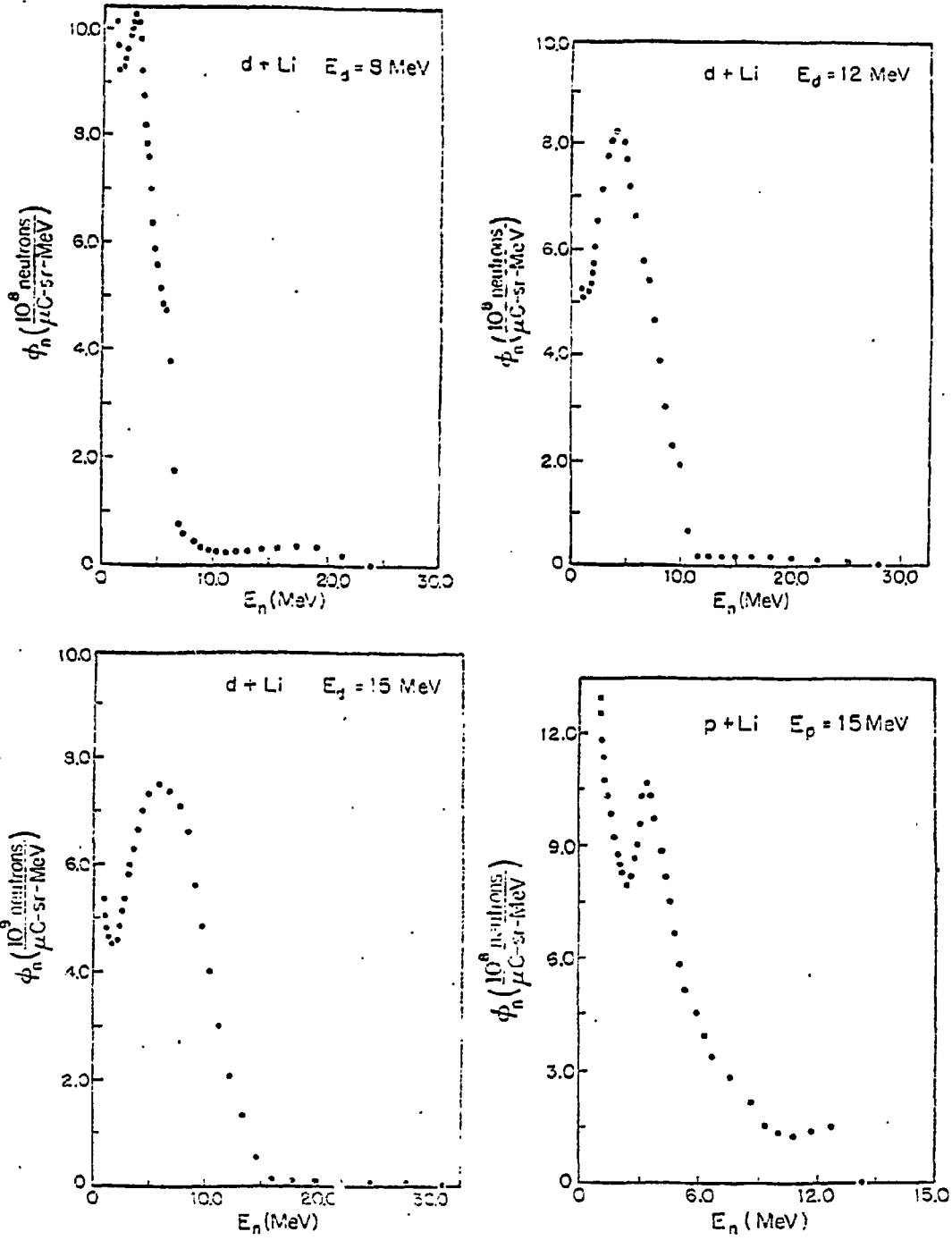


Fig. 11-1. Neutron energy spectra at zero degrees for thick Li target.

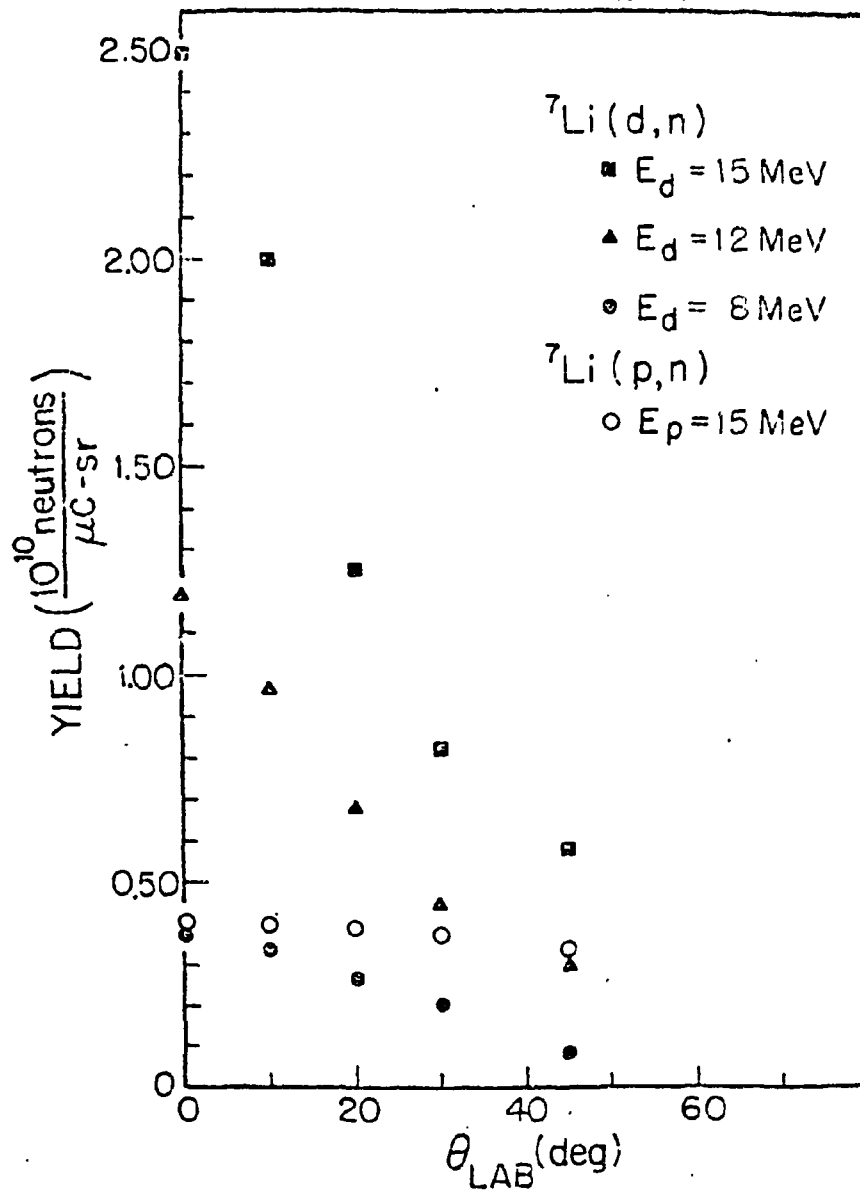


Fig. 11-2. Integrated neutron yield vs. laboratory angle.

2. Development of a Facility for Production of ^{15}O (C. E. Nelson, H. W. Newson, Robert H. Jones*)

A facility for the production and transport of short lived radioactive tracers is being developed in response to Duke University Medical Center interest in pulmonary-cardiovascular research. A specific interest is the use of the Oxygen-15 labelled carbon dioxide for the non-invasive detection of left to right cardiac shunts.

Recent work¹⁾ at the University of Wisconsin has shown the feasibility of producing ^{15}O via the $^{14}\text{N}(d,n)^{15}\text{O}$ reaction with $E_d = 8$ MeV in sufficient quantities such that it can be transported over substantial distances (up to 1/3 mile) if careful attention is paid to gas transport.

Relative yield measurements of the 511 keV coincident gamma rays have been made using the TUNL tandem Van de Graaff. The results indicate that ^{15}O yields similar to those obtained at the University of Wisconsin can be obtained with the 3.5 MeV deuteron beam of the 4 MeV Van de Graaff operating with beam currents of 20 to 25 μA .

In order to improve the operation of the 4 MeV Van de Graaff, particularly at such large beam currents, the former mercury diffusion pump has been replaced with a 10" oil diffusion pump, complete with a freon cooled baffle.

Preliminary work, including the testing of various foil-pressure-cell geometries is scheduled for Spring 1977. Also planned are studies done near the production site using animals and counting equipment supplied by Duke University Medical Center.

Further support for this work, including funds to extend gas capillaries to the Duke University Medical Center from the 4 MeV Van de Graaff laboratory are being sought by DUMC via a National Institute of Health Trauma Center Grant.

3. Continuation of PIXE Development for Multielemental Analysis with 3 MeV Protons (R. D. Willis, W. Gutknecht,** R. Shaw,** R. L. Walter)

Our effort to study the competitiveness of proton-induced X-ray emission (PIXE) as a multielemental analytical tool has continued, but at a reduced pace. The cooperation with the departments of medicine and chemistry and the USEPA and NIH still exists, but because of impending personnel changes, the project will be in a "hold" status for a period this Spring. Details of some of our findings, results, and innovations were presented at the First International Conference on PIXE held at Lund, Sweden. Four reports titled: (1) Proton-Induced X-Ray Emission Analysis of

* Assistant Professor, Department of Surgery, Duke University Medical Center

** Department of Chemistry, Duke University

1) R. J. Nickles, Bull. Am. Phys. Soc. 17 (1972) i37

Thick and Thin Targets, (2) Wavelength Dispersion Analysis of PIXE Spectra, (3) The Application of Proton-Induced X-Ray Emission to Bioenvironmental Analyses, and (4) Computer Analysis of Proton-Induced X-Ray Emission Spectra. Expanded versions of these talks will appear in Nuclear Instruments and Methods. The main direction for 1977 will probably be in animal toxicity studies and the flow of elements from mothers to fetuses, the accumulation of metals in human lung tissue, element balance for intravenously fed (hyperalimentation) patients, and microprobe developments.

J. ION SOURCE DEVELOPMENT

1. New Ion Sources for The Tandem Accelerator (F. O. Purser, H. W. Newson, E. G. Bilpuch, R. L. Rummel, A. G. Lovette, A. W. Lovette, D. H. Epperson, T. B. Clegg, S. S. Shafroth)

Installation of two new ion sources has been delayed. Funds have been made available to purchase and install a sputter heavy ion source. Installation of this source will have an effect upon the options available for the high current direct extraction source and the new lithium exchange helium source. Decisions on source installation have been held up pending a thorough restudy of the tandem low energy layout.

2. Intense Metastable Hydrogen Beams (T. B. Clegg ((with Lewis, Williams, and Dunford of the Univ. of Michigan at Ann Arbor)))

The ion source test bench consisting of a standard duoplasmatron, a cesium charge exchange canal, and the associated vacuum systems, which was on loan from UNC to the University of Michigan during the past year, has been returned to Chapel Hill and reassembled. During the year's loan period this ion source was in use at Michigan in the preliminary tests for an experiment to investigate parity violating effects in the electromagnetic interaction. The Michigan experimenters built, at the same time, an entirely new ion source test bench which was tested by Clegg in Ann Arbor in late August. This second ion source is now operating routinely to provide an intense metastable ($2S_{1/2}$ -state) hydrogen beam for the Michigan test of parity violation.

3. A New Polarized Ion Source for SATURNE II (T. B. Clegg ((with personnel from the Centre d'Etudes Nucléaires de Saclay, Gif-sur-Yvette, France)))

During the past year while on sabbatical leave in France, T. B. Clegg became deeply involved in the project to design, build, and install a new ion source for polarized proton and deuteron beams on the upgraded proton synchrotron at Saclay when it becomes operational in 1978. This new ion source will utilize a unique cryogenic electron beam ion source as an ionizer for the polarized atomic beam from a traditional dissociator-sextupole combination. Clegg's main contributions to this very large project were choosing the most suitable configuration for installing this new source on the injector Linac for the proton synchrotron and finding suitable American suppliers for several of the largest components for the ion source. Clegg was also invited to present a paper describing this new polarized source at the Symposium on High Energy Physics with Polarized Beams and Targets held at Argonne National Laboratory August 23-27, 1976.

4. Comparison of a Duoplasmatron and a Duopigatron Ion Source (T. B. Clegg ((with J. Aubert and C. Lejeune, Université de Paris - Sud, Orsay, France)))

Also while on sabbatical, T. B. Clegg initiated a program to compare in detail the plasma density distributions, the extracted beam intensities and the beam emittances for duoplasmatron and duopigatron ion source geometries. The first goal

of achieving a very uniform radial plasma distribution inside the expansion cup of the ion source was achieved using the duopigatron source with a symmetric four-hole, off axis system of apertures to allow the plasma to fill the cup more uniformly than in the case of a single central anode aperture. The second investigation showed, however, that this uniform plasma density did not translate into better output beam emittances, because the emittance patterns obtained for the extracted beams showed structure which reflected the four holes through which the plasma entered the expansion cup. The most significant finding was then that the plasma in the expansion cup cannot be considered separately from the plasma source which created it.

K. ACCELERATOR DEVELOPMENT AND INSTRUMENTATION

1. Injector Cyclotron (F. O. Purser, R. L. Rummel, A. G. Lovette)

During this period the injector cyclotron developed increasing problems with the stability of the main magnetic field. The cause has been traced to intermittent voltage breakdown between turns on one of the aluminum coil pancakes. By late October 1976 the instability had reached a degree incompatible with Cyclo-Graaff operation.

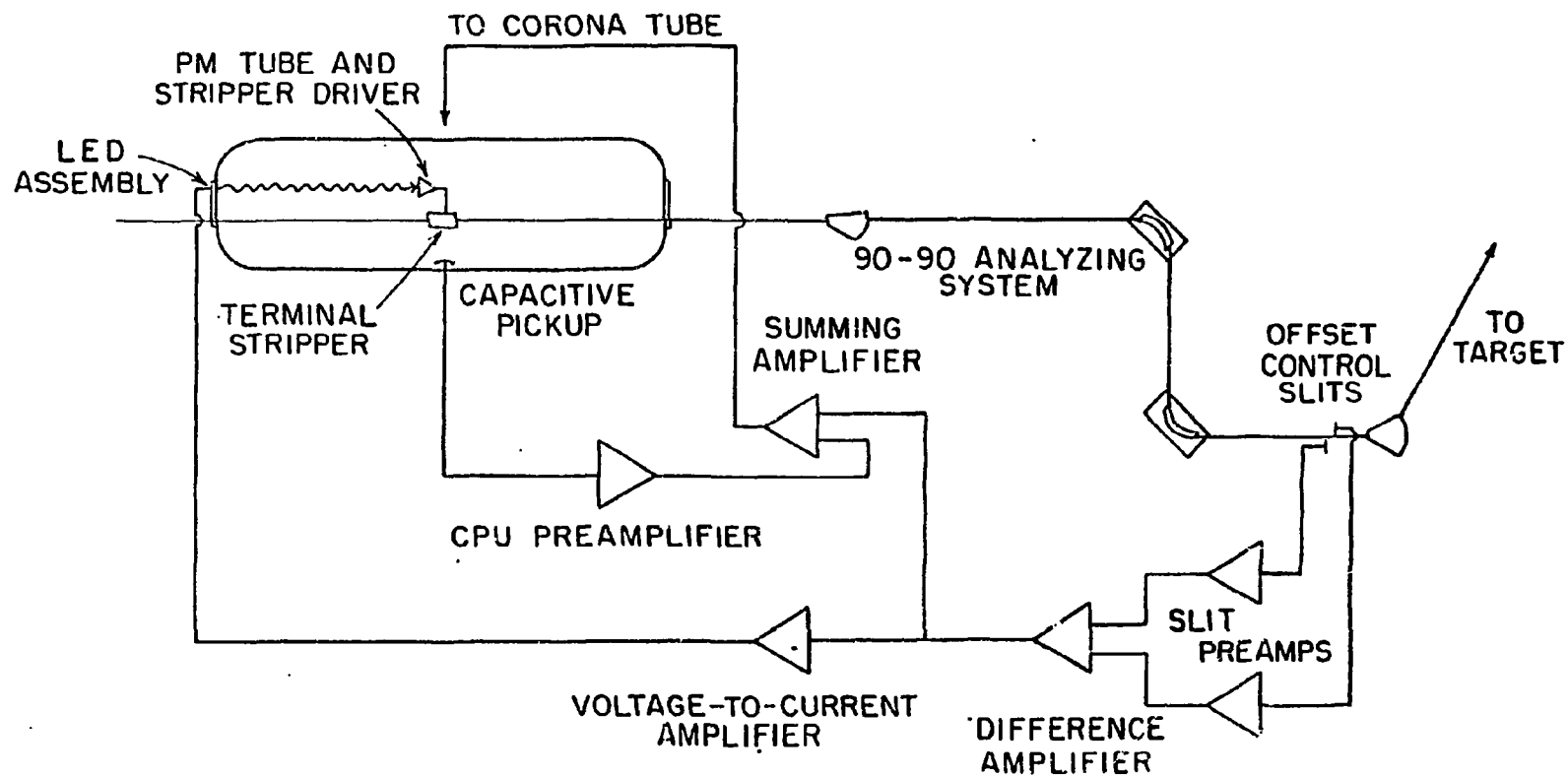
In addition the other coil in the main magnet windings had slowly developed a cooling problem, probably due to either radiation damage to or age hardening of the heat sink compound used to transmit coil heat flow to the cooling manifold.

At the time the cyclotron was constructed in 1967, the main magnet coils were made of 4" wide aluminum ribbon due to the scarcity and cost of copper. This design choice has resulted in operating problems in subsequent years. A proposal has been submitted to ERDA for funds to upgrade the cyclotron by replacing the present coils with coils wound with hollow copper conductors. Until this proposal has been acted upon, repairs to the present coils have been temporarily halted.

2. High Resolution Development on The Tandem Accelerator (M. E. Bleck, D. A. Outlaw, W. K. Wells, F. O. Purser, H. W. Newson, E. G. Bilpuch, G. E. Mitchell, T. B. Clegg)

a. Terminal Stabilizer

Development work on the energy stabilization system for the TUNL tandem Van de Graaff accelerator described in the 1975 progress report has continued during the past year. The neutral beam target correction technique has been abandoned in favor of the system shown in Fig. K2-1. In this configuration the control beam, which is also the target beam, is momentum analyzed by the 90-90 magnets. The focussing properties of these magnets render the control signal derived at the image slits insensitive to position fluctuations of the beam at the object slits. In addition, the superior analyzing power of the system increases the sensitivity of the control loop. It has been found that the control slits must be offset along the beam axis in order to prevent electron crosstalk which overloads the slit preamplifiers.



XV-72

Fig. K2-1. Triple loop control system for tandem accelerator.

An isolated $5/2^-$ resonance with $\Gamma_p = 65$ eV in the $^{54}\text{Fe}(p,p)$ reaction has been measured with this system and fitted with an asymmetric resolution function (FWHM = 375 eV). The result is shown in Fig. K2-2. The contribution to the overall resolution due to beam energy fluctuations is estimated at 250 eV or less.

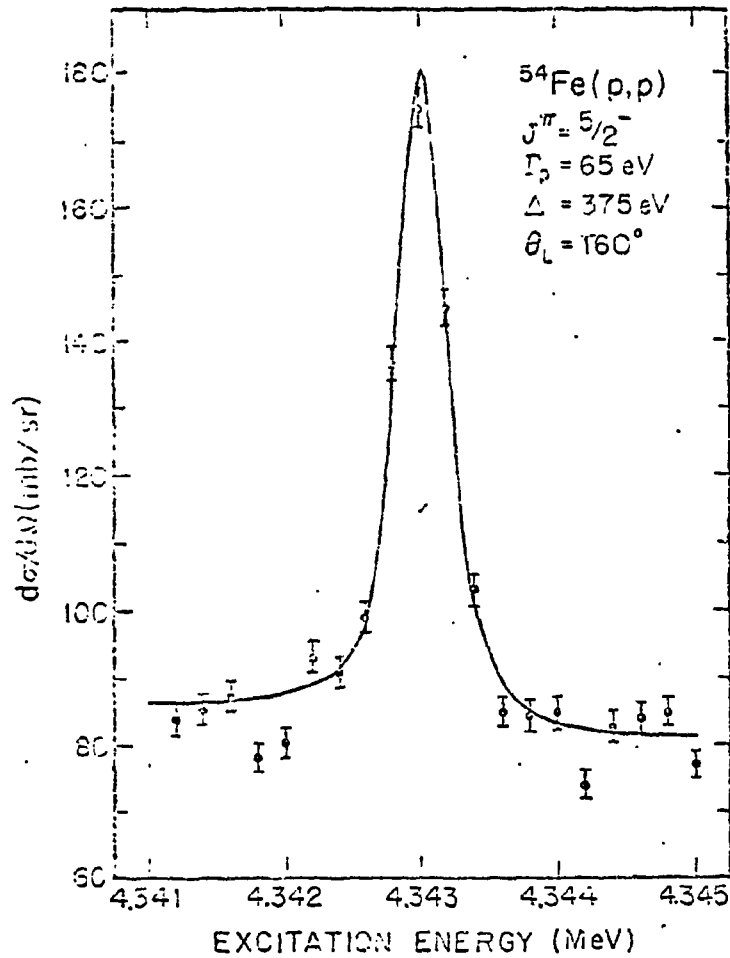


Fig. K2-2. Resonance in the $^{54}\text{Fe}(p,p)$ Reaction Using the Terminal Stabilizer.

b. 90-90 Analyzing Magnets

A computer controlled system for stepping the beam energy in a uniform manner has been developed in conjunction with the terminal stabilizer project. The remote master reference "fine" current potentiometer is driven, through a set of reduction gears, by a stepping motor commanded by the computer. The potentiometer is part of a voltage divider that provides a reference signal to the analyzing magnet power supply by scaling the voltage from a set of mercury batteries. These batteries reside in a styrofoam case to minimize temperature drifts. This system steps the master reference much more precisely than was possible by hand. However, preliminary analysis of $^{90}\text{Zr}(p,p)$ data taken over a period of several days indicates that significant drifts in the beam energy, with periods of a few minutes to several hours and with amplitudes of a kilovolt or more, may occur when the magnets are in the current regulated mode. The most attractive solution to this problem is to derive from the NMR fluxmeter a feedback correction signal for the magnet supply. In this way, the magnetic field would be regulated in addition to the current. The stability of such a system depends upon the stability of the RF oscillator which drives the NMR cavity. The existing fluxmeter and power supplies can be operated in this way, so a precision frequency synthesizer accurate to 1 part in 10^8 was obtained on loan for a system test. The beam energy at a given frequency was found to vary no more than ± 150 eV over a period of two days. Stepping the RF in 100 Hz increments provided 70 eV increments in beam energy. The frequency synthesizer is externally programmable and can be computer controlled, although this feature was not used in the test. The system is not without drawbacks, however. It has a range of control of only about 30 keV due to the extremely non-linear character of the error signal from the NMR discriminator. Recent advances in Phase-locked loop technology have made far superior field regulated magnets possible. Such systems are presently being investigated.

3. Polarization Monitoring and Beam Control (S. Tonsfeldt, E. J. Ludwig, W. K. Wells)

A beam control system which maintains the accelerator beam centered within the 60 cm diameter scattering chamber has been tested and used for experiments. This system consists of a magnetic steerer with current controlled by the difference signals generated by currents from segments of a split Faraday cup. The beam is maintained centered on this steerer by another control system consisting of beam slits and a magnetic steerer located further upstream. The system has been used to measure analyzing powers to an accuracy of .001. Plans for a new beam polarization monitor have been made which incorporate a similar control system.

4. Pulse Beam Time Pick-Off (S. A. Wender, P. W. Lisowski, R. L. Walter)

A time pick-off system is being developed to provide a time marker in pulsed beam experiments. A preliminary design consisted of a 1/16" piece of plastic scintillator placed in the beam line with an aperture for the beam to pass through. A phototube looking at the scintillator responded when the halo of the beam hit the scintillator. This technique has been generally successful and has the following

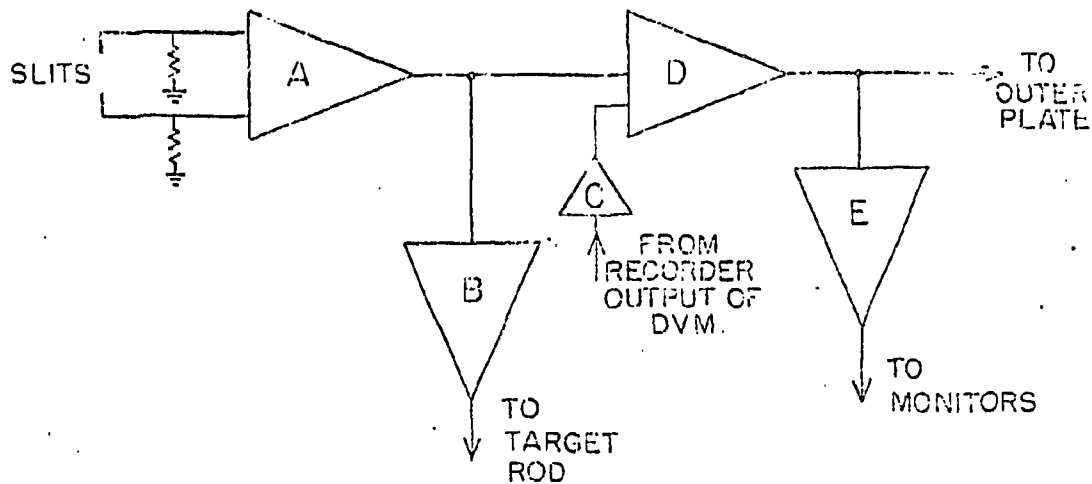
advantages over the conventional capacitive time pick-off unit. (1) It is useful when small beam currents are necessary such as some γ -ray experiments or when only small beam currents are possible such as polarized beam experiments. (2) It is useful when the timing is "sloppy". This is the case for heavy ion pulsing or for slow pulsing versus wide pulses.

The present design has the disadvantage in that the aperture in the scintillator must be changed for different beam currents. We plan to build a system which will permit adjustment of this aperture. We also plan to investigate different scintillators and different phototubes to further improve the timing characteristics of the pick-off system.

5. Improvements in Instrumentation in the 3 MeV Laboratory (W. K. Wells, D. A. Outlaw, M. E. Bleck, C. Westerfeldt, G. E. Mitchell, E. G. Bilpuch)

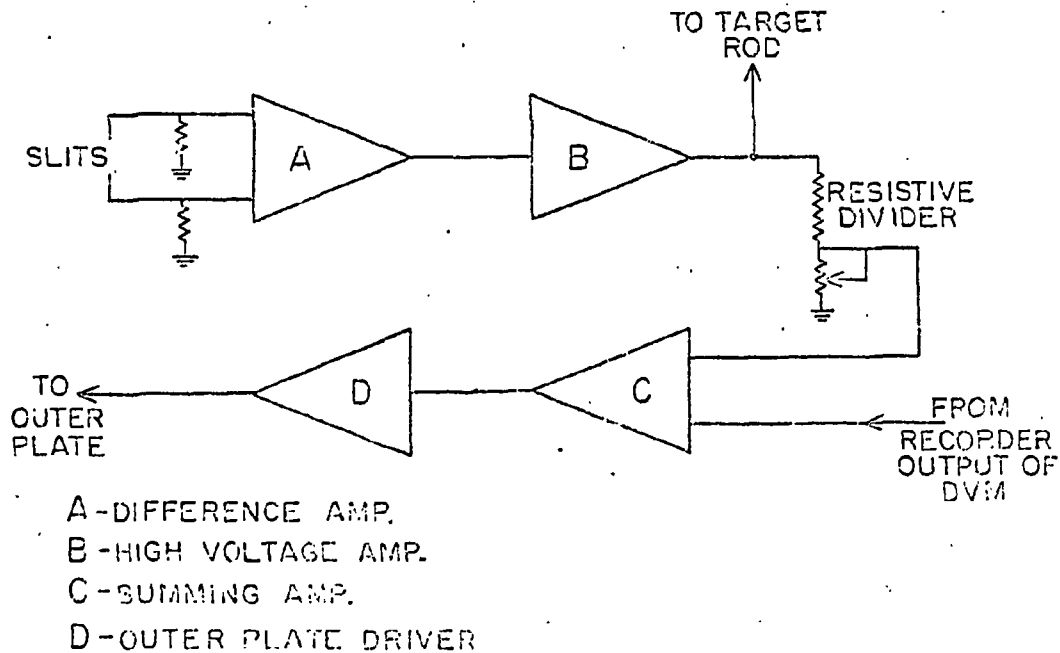
A new accelerator tube was installed in the TUNL KN Van de Graaff. Considerable improvement was achieved in performance in the energy range 2.5-3.0 MeV. During the 11 month operation of the machine no voltage breakdown was observed across the focus gap. This had been a serious problem with the old accelerator. The column resistors were replaced with a more uniform set. Corona control slits have been installed with a factor of 20 better isolation from environmental electrical noise.

A new beam homogenizer system has been constructed using information gained from a feedback analysis of the previous system. Higher gains and better linearity, especially in the high voltage amplifier have been realized. Figure K5-1 is a block diagram of the old system; Figure K5-2 is the corresponding diagram for the new system. The slit difference signal, which is proportional to the energy fluctuations in the beam, is derived in the same manner in both systems. This signal is then amplified and sent to the outer plate of the electrostatic analyzer. The new system has two fewer elements in this feedback path. The system may be run at higher gains because of the smaller phase shifts. The linearity and gain stability of the new high voltage amplifier is good enough to allow the amplifier to be used in an open loop configuration. The new system can regulate a beam with 2 keV peak to peak fluctuations and yield approximately 350 eV resolution with solid targets. The previous system was limited to 1 keV fluctuations for comparable resolution. Thus the new system makes experimental resolution less dependent upon accelerator operation.



- A - DIFFERENCE AMP
- B - HIGH VOLTAGE AMP
- C - VARIABLE GAIN AMP
- D - OUTER PLATE DRIVER
- E - UNITY GAIN BUFFER AMP

Fig. K5-1. Block diagram of new homogenizer circuit.



- A - DIFFERENCE AMP.
- B - HIGH VOLTAGE AMP.
- C - SUMMING AMP.
- D - OUTER PLATE DRIVER

Fig. K5-2. Block diagram of old homogenizer circuit.

L. COMPUTER RELATED DEVELOPMENTS

1. The Prime Computer (J. Chundler, W. K. Wells, N. R. Roberson, S. E. Edwards)

Within the past year, the Prime 300 computer has been upgraded in numerous areas. An additional 8K of memory was purchased, bringing the total memory to 32K. With 32K of memory, it is now possible to run in a "virtual" memory mode. This mode allows portions of user programs to be exchanged between memory and disk. It is therefore possible to run a program which normally requires 64K. In addition to "virtual" memory, software has been developed to read and write magnetic tapes compatible with the two DDP computers, thus allowing long listings to be performed on the high speed line printer of one of the DDP computers and permitting data taken on the DDP computer to be analyzed on the Prime computer.

Recently a remote teletype and display have been installed in the 3 MeV laboratory. Complete control of the computer can now be handled from the laboratory while data are being obtained. To handle data, a router has been built to route signals from up to eight different detectors into the CAMAC interface.

Items currently being developed include a light-pen, switch panel, and an interface card cage and pin board. The light-pen, which is almost complete, and the switch panel will facilitate both data acquisition and analysis by facilitating interaction with the user's program. The card cage and pin board are a necessity for data acquisition on a full scale basis. The card cage will provide a compact but easily accessible unit for the interface between peripherals and the CAMAC modules. The pin board will allow the user to set up his interrupt levels and possible coincidence data.

One final proposal has been raised, but is not yet being developed. With "virtual" memory, it is possible to connect teletypes to the CPU board and thus have simultaneous multiple users. The major drawback to this approach is the fact that "virtual" memory does not operate in the interrupt mode. If software can be developed to overcome this failing, the multiple users approach may be possible for off-line work.

2. Computer Program Development for Neutron Data Correction (H. H. Hogue, W. Tornow, C. E. Nelson, S. El Kadi, S. G. Glendinning, F. O. Purser)

Neutron scattering studies generally employ relatively large scattering samples to obtain adequate counting rates. Thus the measured data must be corrected for such effects as finite angular resolution, flux attenuation and multiply scattered neutrons. Monte Carlo simulation techniques are usually employed to calculate the necessary corrections for these effects.

The program Mulcat previously used at TUNL to make these corrections

was originally written to correct neutron scattering data for relatively heavy elements. For these cases, due to the negligible kinematic energy loss in scattering, the simplifying assumptions were made that: (1) the angular distributions of all scattered neutrons were constant with energy; and, (2) that all neutrons scattered into the detectors were counted. These assumptions are invalid for scattering from light elements, when kinematic energy losses can be substantial, and are totally inappropriate for measurements in which the continuum neutron spectra are of interest.

The following approach has been used at TUNL to attack this problem.

First: the program Mulcat¹⁾ has been extensively re-written to incorporate all kinematic energy loss effects exactly. A library of up to 80 distinct angular distributions covering the kinematic energy range applicable has been incorporated, together with appropriate interpolation procedures. In addition, simulated data are accumulated in a time of flight presentation so that the calculation can utilize the energy windows and/or bins corresponding to those used in the experiment. Final data analysis for ⁶Li, ⁷Li and ⁹Be is now in process utilizing this revised code.

Second: A new and faster version of the computer code MONTE SAMPLE^{2, 3)} has been acquired which contains the above mentioned requirements. In addition, this Monte Carlo code embodies a true analog of the scattering experiment without the assumptions inherent in the Mulcat logic. It is presently being modified to incorporate a finite, extended, non-isotropic neutron source routine and due to the longer computer running times required will be used to spot check results from Mulcat.

Third: A completely new Monte Carlo code similar in logic to MULCAT, except that all collisions are forced, has been developed. It has the features that the total calculation has been divided into several smaller calculations which permits the code to be run on our in-house off-line computer. The code is also designed to handle multi-element scattering samples. Results from this code have been exhaustively checked against results from MULCAT and are in excellent agreement. Data reduction with this code will produce substantial fiscal savings over analysis with MULCAT, which requires the use of off-site computer facilities.

3. Beam Optics Computer Code (T. B. Clegg, D. Stevenson)

The linear beam optics code TRANS for the interactive computer terminal at TUNL was documented fully before the departure of D. Stevenson in July. It now serves as a standard routine available to all the users in the laboratory.

1) W. E. Kinney, Nucl. Instr. and Meth. 83 (1970) 15.

2) P. Guenther, A. B. Smith, J. Whalen, Phys. Rev. 12 (1975) 1797.

3) A. B. Smith, private communication.

M. NUCLEAR THEORY AND PHENOMENOLOGY

1. Studies of Deuteron Scattering Potentials (J. A. Ramirez ((Inter-American University, Puerto Rico)), W. J. Thompson)

A report on the effects of non-locality in (d,d) scattering, investigated in the Ph.D. thesis project of J. A. Ramirez, has been prepared for publication. Selection of desirable cases for experiments to further test the folding model for deuteron scattering, including spin-orbit and tensor potentials, is being made in consultation with the experimental groups at TUNL and at ETH, Zürich.

2. Wave Functions and Wave Packets (E. A. Olszewski ((UNC-Wilmington)), W. J. Thompson)

Our calculations on the wavepackets produced in photo-ionization of hydrogen, part of the Ph.D. thesis of E. A. Olszewski, have been extended to describe the detailed behavior for small times. The documentation for a three-dimensional stereo-display program, TD PLOT2, written in consultation with J. D. Foley of the UNC Computer Science Department, has been completed. The wavepacket calculation results and a description of TD PLOT2 are being prepared for publication.

3. Polarization Phenomena in Nuclear Reactions (T. B. Clegg and W. J. Thompson)

We are preparing a review for non-specialists of the current concepts and techniques of polarization as used in nuclear physics. During a two-month visit at the University of Auckland, New Zealand, Dr. Thompson gave a series of ten review seminars on current polarization research: it is intended to incorporate some of the material from these seminars in the review.

4. Isospin-Consistent DWBA Analyses of (d,t) and (d,³He) Reactions (S. K. Datta ((Univ. of Wisconsin)), W. J. Thompson)

Calculation of finite-range effects in the isospin-coupled analysis of our polarized-beam data is being performed in collaboration with S. Cotanch (N. C. State University). A paper describing this work, which has a significance for the charge dependence of nuclear forces, is in preparation.

5. A DWBA Transfer-Reaction Code for Small Computers (W. J. Thompson)
The DWBA program which we have written for interactive use on small computers is being adapted to the display systems of the DDP-224 at TUNL.

6. Dissipative Forces in Quantum Mechanics (J. S. Eck ((Kansas State University)), W. J. Thompson)

The increased emphasis in heavy-ion physics of such classical concepts as friction and viscosity lead us to consider how dissipative forces could be accommodated in quantum mechanics. We have made a simple, but rigorous, derivation of the relation between dissipation and non-Hermitian terms in the interaction Hamiltonian. Examples

which are readily understood by beginners in nuclear physics have been presented. This work has been accepted for publication in the American Journal of Physics.

7. Survey of Nucleon-Nucleus Scattering Potentials (W. J. Thompson)

A survey of available data on nucleon-nucleus elastic-scattering cross section and polarization data is being made in order to determine targets and bombarding energies which would be important if a new global analysis of the nucleon-nucleus optical-model potential were made. The energy and isospin dependence of these potentials are particularly important. Such potentials are very useful for estimating interaction cross sections for neutron scattering from isotopes which are unstable or of low natural abundance.

8. Compound-Nucleus Effects and the Nucleon-Nucleus Spin-Spin Interaction (W. J. Thompson)

The effects of compound-elastic scattering on the determination of the spin-spin interaction V_{SS} have been calculated for two types of measurements: (1) Depolarization experiments. The case $^{14}\text{N}(\vec{p}, \vec{p})^{14}\text{N}$ at 16.2 MeV, for which a complete angular distribution of the depolarization parameter was recently measured at LASL, was shown to be dominated by compound-elastic spin-flip for all angles in the backward hemisphere. A report on this work has been published in Physics Letters. (2) Total spin-spin cross sections using polarized beams and targets at low bombarding energies have been shown to be consistent with compound-elastic effects arising from different level densities in the compound nucleus; $^{59}\text{Co}(\vec{n}, n)^{59}\text{Co}$ at energies $\lesssim 1$ MeV has been calculated in detail. This work, which was described at the American Physical Society Nuclear Division meeting in East Lansing, will be published in Physics Letters. The above considerations, together with the results of Blair and Sherif on the quadrupole spin-flip mechanism for targets with spin $I > 1/2$, make it unlikely that data obtained so far have lead to correct estimates of V_{SS} . Work in progress includes selection of the best $I = 1/2$ nuclei for determination of V_{SS} and design of depolarization experiments in collaboration with groups at Lawrence Berkeley Lab. and Texas A and M University.

9. Atomic Effects in Nuclear Resonances (F. M. Feagin, E. Merzbacher, W. J. Thompson)

The splitting of nuclear resonance levels due to excitations of the atomic electrons of the target atom during the collision may be observable for very sharp resonances observed with the resolution obtainable at TUNL. Sum rule methods for investigating discrete and continuum atomic-electron excitations have been developed and applied to early work on $^4\text{He} + \alpha$ scattering. The techniques are being applied to the narrow resonance near 14.2 MeV observed in $^{12}\text{C}(p, p)^{12}\text{C}$, and the design of experiments at TUNL and at Chalk River Laboratories is underway. This work is part of the Ph.D. research of Mr. Feagin.

10. Projectile-Size Effects in Deformation Measurements (W. J. Thompson, J. S. Eck ((Kansas State University)))

Intrinsic quadrupole and hexadecapole deformation parameters for ^{12}C , ^{20}Ne , ^{24}Mg and ^{28}Si have been extracted from deformation lengths for a wide range of projectiles from e to ^{16}O . The effects of finite projectile sizes have been included to second order in the deformations. The extracted values therefore give very reliable estimates of the deformation parameters, which can be compared with nuclear structure values and used in nuclear-scattering calculations. A preliminary account of this work was reported at the conference on Radial Shape of Nuclei, Krakow, Poland, June 1976. A full account has been submitted for publication.

11. Spin-Orbit Coupling in Heavy-Ion Scattering (W. J. Thompson)

A survey paper summarizing the theoretical predictions, and comparison with data for the few available cases (including ^6Li analyzing powers), is in preparation. Collaboration with the group of D. Fick at Max-Planck-Institut für Kernphysik in Heidelberg, which is performing the ^6Li experiments, is continuing.

12. Compound-Nucleus Fluctuation Theory for Polarized Beams (R. F. Haglund ((LASL)), J. M. Bowen, W. J. Thompson)

Investigations of statistical (Ericson) fluctuation effects for polarized beams are continuing by means of Monte-Carlo calculations using our code RANSACK. We have demonstrated that runs tests cannot be applied unambiguously to overlapping resonance data to reveal non-statistical (intermediate) structure. The results of this analysis have been published in Physical Review Letters as a comment on an analysis by a group at Rutgers University, in which it was claimed that an intermediate structure had been revealed by means of runs tests. Collaboration with the Rutgers group in the interpretation of their experiments has begun.

13. The Energy Splitting of the Lowest 6^- , $T = 0$ and $T = 1$ States in the (sd)-Shell (S. Maripuu, M. R. Meder ((Georgia State University)), G. E. Walker ((Indiana University)))

In contrast to present particle-hole interaction predictions the observed energy splitting between the lowest 6^- , $T = 0$ and $T = 1$ states in ^{24}Mg and ^{28}Si is almost 1.5 MeV.^{1,2)} (Most realistic interactions give an energy splitting of a few hundred keV in a simple particle-hole model.) Introduction of various perturbative corrections into the two-body Hamiltonian improves the situation somewhat but still does not provide enough energy splitting. We have tried to diagonalize large energy matrices in various sub-spaces with unperturbed two-body Hamiltonians derived from various realistic interactions. This method provides us with a stringent test of the nucleon-nucleon interactions deduced from free nucleon-nucleon scattering data.

1) G. T. Neal and S. T. Lam, Phys. Lett. 32B (1973) 127

2) G. S. Adams et al., Bull. Am. Phys. Soc. 21 (1976) 966

14. Spectroscopic Factors for the $^{28}\text{Si}(p,d)^{27}\text{Si}$ Reaction (S. Maripuu)

Recent measurements of the $^{28}\text{Si}(p,d)^{27}\text{Si}$ reaction at $E_p = 135 \text{ MeV}$ ¹⁾ have revealed new features not resolved in previous experiments. Strongly excited states with narrow widths have been observed in the $E_x = 10 - 18 \text{ MeV}$ range. A shell model calculation with the Sussex realistic interaction indicates considerable fragmented $1p_{3/2}$ strength in the region observed. The calculation predicts some $1p_{1/2}$, $1d_{5/2}$ and $1d_{3/2}$ strength at these excitation energies. It should also be possible to observe some weak $1f_{7/2}$ transitions. The $(1f_{7/2})^2$ admixture in the ^{28}Si ground state is predicted to be only a few percent.

15. 1975 Mass Predictions (S. Maripuu, K. Way)

A compilation of predicted masses has been undertaken for all nucleon-stable nuclides up to $A = 350$. A table of mass excesses including nine different entries of predicted values together with the Wapstra-Bos 1975 experimental values is published in Atomic Data and Nuclear Data Tables 17 (1976) 411.

16. Computer Codes for High Accuracy Single Particle States (R. Y. Cusson, E. G. Bilpuch, R. A. Hilko)

A computer program to compute single-particle states of finite nuclei in the spherical shell model, starting from the self-consistent K-Matrix model mentioned in the previous entry has been stored on disk and is available for general service usage. The code is useful to give very good first approximations to many single-particle properties of finite nuclei such as radii, density distributions, total and single-particle energies.

17. Realistic Single Particle Hamiltonian for Fission and Heavy Ion Calculations (R. Y. Cusson, R. A. Hilko, D. Kolb ((G. S. I. Darmstad)))

A paper on the use of our K-matrix model entitled "Realistic Heavy Ion Adiabatic Potentials" has appeared in Nuclear Physics A270 (1976) 437-470. The abstract follows.

"The K-matrix model of Cusson, Trivedi, Meldner and Weiss has been used to compute static adiabatic heavy-ion cluster potentials in a constrained self-consistent Brueckner-Hartree-Fock scheme. Heavy-ion potentials are found which can simultaneously reproduce the experimentally deduced heavy-ion potentials in the asymptotic region and the total energy versus quadrupole moment in the fused, compound nucleus region. Potentials for α - α , α - ^{12}C , α - ^{16}O , ^{12}C - ^{12}C , ^{16}O - ^{16}O are shown and compared with other work. The total energy of ^{12}C and ^{24}Mg versus deformation is also given."

¹⁾ D. W. Miller et al., Bull. Am. Phys. Soc. 21 (1976) 978

The detailed K-matrix model paper entitled "Self-Consistent K-matrix-model Calculation for Finite and Superheavy Nuclei" has appeared in Phys. Rev. C14 (1976) 1615, with authors, R. Y. Cusson, H. P. Trivedi, H. W. Meldner, M. S. Weiss, and R. E. Wright. The abstract follows.

"A model two-body K matrix is introduced which leads to simple Brueckner-Hartree-Fock equations similar to those resulting from Skyrme forces. The main features of the present model are determined by basic nuclear matter properties. Experimental nucleon removal energies for finite closed-shell nuclei are used as a criterion for setting the single-particle energy levels in our model. This is accomplished by parameterizing the Brueckner rearrangement potential which augments the single-particle potential producing single-particle level densities in better agreement with experiment than Skyrme-potential models or density matrix expansion theories. Good fits are also obtained to total binding energies, rms radii, and electron scattering form factors of the magic nuclei ^{16}O , ^{40}Ca , ^{90}Zr , ^{208}Pb . Extrapolated results for the magic superheavy nucleus $^{298}114$ are presented and discussed."

18. Realistic α -Particle Potentials (R. Y. Cusson, K. Sage, E. G. Bilpuch)

The heavy ion code discussed earlier has been used to study the adiabatic and sudden real parts of the α - α , α - ^{12}C and ^{16}O - ^{16}O optical potentials. Keith Sage is presently writing his thesis on this topic. A paper has been presented at the East Lansing American Physical Society meeting and the following abstract has appeared in Bull. Am. Phys. Soc. 21 (1976) 973.

"We have employed the two-body K-matrix model of Cusson, Hilko and Kolb¹⁾ in a constrained, self-consistent, Brueckner-Hartree-Fock iterative scheme to calculate a "sudden" cluster potential for the reactions $^{12}\text{C} + \alpha$ and $^{16}\text{O} + ^{16}\text{O}$. The resulting potential, together with the adiabatic cluster potential of Sage and Cusson²⁾, is used in optical model fits to experimental data on $^{12}\text{C} + \alpha$. The complex strengths of the potentials are adjusted to obtain best fits and yield a real and imaginary optical potential."

19. Applications of Group Theory to Rotational Vibrational Bands on Nuclei (R. Y. Cusson, L. C. Biederharn, O. L. Weaver ((Kansas State University)))

In a recent study we used the group $T_5 \otimes \text{SU}(2)$ to describe rotational bands in nuclei (Annals of Physics 77 (1973) 250) and we suggested to use the group $\text{CM}(3) = T_0 \otimes \text{SL}(3, \mathbb{R})$ to include vibrational excitations. This work has been carried

1) Cusson, Hilko and Kolb, to be published

2) Sage and Cusson, Bull. Am. Phys. Soc. 21 (1976) 512

out and a class of rotational-vibrational bands has been discovered. Each rotational-vibrational band is characterized by a fixed quantized vorticity, v . The $v = 0$ bands are the well-known SO(5) Bohr-Mottelson bands. The new $v \neq 0$ bands play the role of particle-rotational couplings, without the need to introduce explicitly the degrees of freedom of the decoupled particles. Applications to back bending rotational bands are envisaged. A paper on those results has been accepted for publication in Annals of Physics (N. Y.).

20. Exotic Configurations of Super Heavy Nuclei, Bubbles, Torus, etc.
(R. Y. Cusson, C. Y. Wong ((ORNL)))

A paper is being prepared on the results of a K-matrix calculation for the completely depleted bubble nuclei in the region $A = 900-1000$. A relatively low priority has been given to this project because there appears to be no way that these nuclei could have a long life time. However, the toroidal configurations near $A = 300-400$ could be stable or long-lived and might conceivably be produced in heavy ion reactions.

With this and other applications in mind, such as non-axial fission of the actinides, a new code has been written to adapt the Lanczos algorithm to the diagonalization of super large matrices, as encountered when constructing the eigenfunctions for superheavy nuclei without any conserved quantum numbers. The first 20 eigenvalues and eigenvectors of energy matrices having dimensions up to 5000×5000 have routinely been obtained. Some attempts at speeding up the calculation will be made before a detailed application to heavy nuclei is made.

21. Level Density Studies for a Reactions with Targets of $A \leq 40$ (K. Sage, R. Y. Cusson)

This program has been inactive during this progress report period.

22. Dynamics of Heavy Ion Reactions in a Realistic Time-Dependent Hartree-Fock Model (R. Y. Cusson, J. M. Bruhn ((ORNL)))

A letter entitled "Dynamics of $^{12}\text{C} + ^{12}\text{C}$ in a Realistic Time-Dependent, Hartree-Fock Model" has appeared in Phys. Lett. 62B (1976) 134 with the following abstract:

"A calculation of the dynamics of head-on collision for the ions $^{12}\text{C} + ^{12}\text{C}$, at initial energies of 1.6, 3.2, 4.8, 6.4, 8.0 and 12.3 MeV/A is described. A realistic phenomenological reaction matrix model is used in a T.D.H.F. scheme. Neutrons and protons are treated separately; direct and exchange Coulomb forces are included as well as spin-orbit forces. At the lowest energies, a molecular state of ^{24}Mg is observed.

In addition to this a detailed paper entitled "Time-Dependent Hartree-Fock Calculation of $^{12}\text{C} + ^{12}\text{C}$ with a Realistic Potential" has appeared in Nuclear Physics A270 (1976) 471, with the following abstract:

"We have used a realistic single-particle K-matrix model to compute the head-on scattering of $^{12}\text{C} + ^{12}\text{C}$ at incident projectile lab energies of 3.2, 6.4, 12.8, 19.2, 25.6, 32, 51.2 and 65 MeV/nucleon, above the Coulomb barrier, in the time-dependent Hartree-Fock approximation. Direct and exchange Coulomb forces as well as spin-orbit forces are included. A large deformed harmonic oscillator basis is used. Spatial density and current distributions at various times are shown. The outgoing energy is found to be $E_0 = 0.8E_{10} - 28$ (MeV), in the c.m. system. Fusion and fully relaxed scattering are observed at low energy. Some compression is seen at higher energies but no shock waves can be detected. Consequences for heavy-ion reactions are discussed."

23. Deep Inelastic Heavy Ion Cross Sections in a T.D.H.F. Model (R. Y. Cusson, J. Maruhn ((ORNL)), R. K. Smith, H. W. Meldner ((LLL)), M. S. Weiss ((LLL)), and A. K. Kerman ((MIT)))

A paper entitled "Time Dependent Hartree-Fock Calculation of the Reaction $^{16}\text{O} + ^{16}\text{O}$ in Three Dimensions" has appeared in Phys. Rev. Lett. 36 (1976) 1166 with the following abstract:

"We have solved the time-dependent Hartree-Fock equations in three dimensions for the heavy-ion reaction $^{16}\text{O} + ^{16}\text{O}$ at energies $E_{\text{lab}}/A_{\text{proj}} = 8, 16, \text{ and } 24$ MeV and impact parameters $b = 0, 2, 4, 6, \text{ and } 8$ fm. The potential used is a simplified form of the Skyrme interaction. An angular-momentum window for complete fusion is predicted. A multifluid flow pattern similar to that of atomic physics is observed and seems to cast doubts on the validity of the simplified axiality and rigid clutching assumptions currently made."

Further progress in this area has been made by including the Coulomb potential. Angular distributions for the quasi elastic scattering of ^{14}N by ^{12}C at 108 MeV have been obtained by a semiquantal method and reproduce the general exponential trend observed in the experimental data obtained in O. R. N. L. New methods to increase by nearly tenfold the computation speed are being studied and the study of much heavier ions is expected. A full length paper describing these results is in preparation.

24. Single Nucleon Induced Fission (R. Y. Cusson, H. W. Meldner ((LLL)), F. O. Purser, D. Epperson, H. W. Newson)

A new code to complete multiple chance single nucleon induced fission, called NIFTE has been written to replace an earlier version called PHROGNUM. The new version can take into account up to 9th chance fission and has a rapid recursive algorithm to include successive chances. Applications of these calculations to L. L. L. projects and to the proton induced fission experiments at TUNL are in progress.

25. Low Energy Behavior of Fusion Barriers in Heavy Ion Reactions (W. M. Howard (LLL), R. Y. Cusson)

Low energy fusion reactions such as $^{12}\text{C} + ^{12}\text{C}$ have considerable importance for astrophysical and other thermonuclear processes. Yet theoretical attempts at computing the $S(E)$ function have met with a systematic problem that the experimental $S(E)$ is usually several factors of two greater than the theoretical one at thermonuclear energies. A new method has been devised, based ultimately on a reinterpretation of the meaning of a fusion barrier for composite system, which shows good promise of allowing systematic and accurate predictions of $S(E)$ for a large variety of heavy ion fusion reactions. A letter describing this work is being readied.

26. The Griffin Model, Complex Particles and Direct Nuclear Reactions (C. Kalbach)

In the past, application of the Griffin preequilibrium model to nuclear reactions involving complex particles has led to certain apparent inconsistencies. The average two-body interaction matrix element showed an artificial projectile dependence when extracted from data analyses, and there seemed to be a need for underivable factors in the calculated rates for complex particle emission. This work shows that these problems may be largely attributed to an inadequate consideration of the influence of direct reactions.

In this work, the basic approximations of the Griffin model are reexamined. Proton-neutron distinguishability and the Pauli exclusion principle are treated in an improved way. The effects of the finite depth of the nuclear potential well and of the increasing density of single particle states with increasing well energy are included. Several improvements in the model input are also suggested. Direct reaction mechanisms are systematically considered, and semi-empirical descriptions are proposed for those not included in the Griffin model calculations (knockout and inelastic processes involving alpha particles, and stripping and pickup). When all of these points are considered, good agreement with experimental energy spectra for emitted particles are obtained without the artificial adjustments needed previously. A sample comparison between calculation and experiment is shown in Fig. M26-1.

This work has been written up for submission to Zeitschrift für Physik.

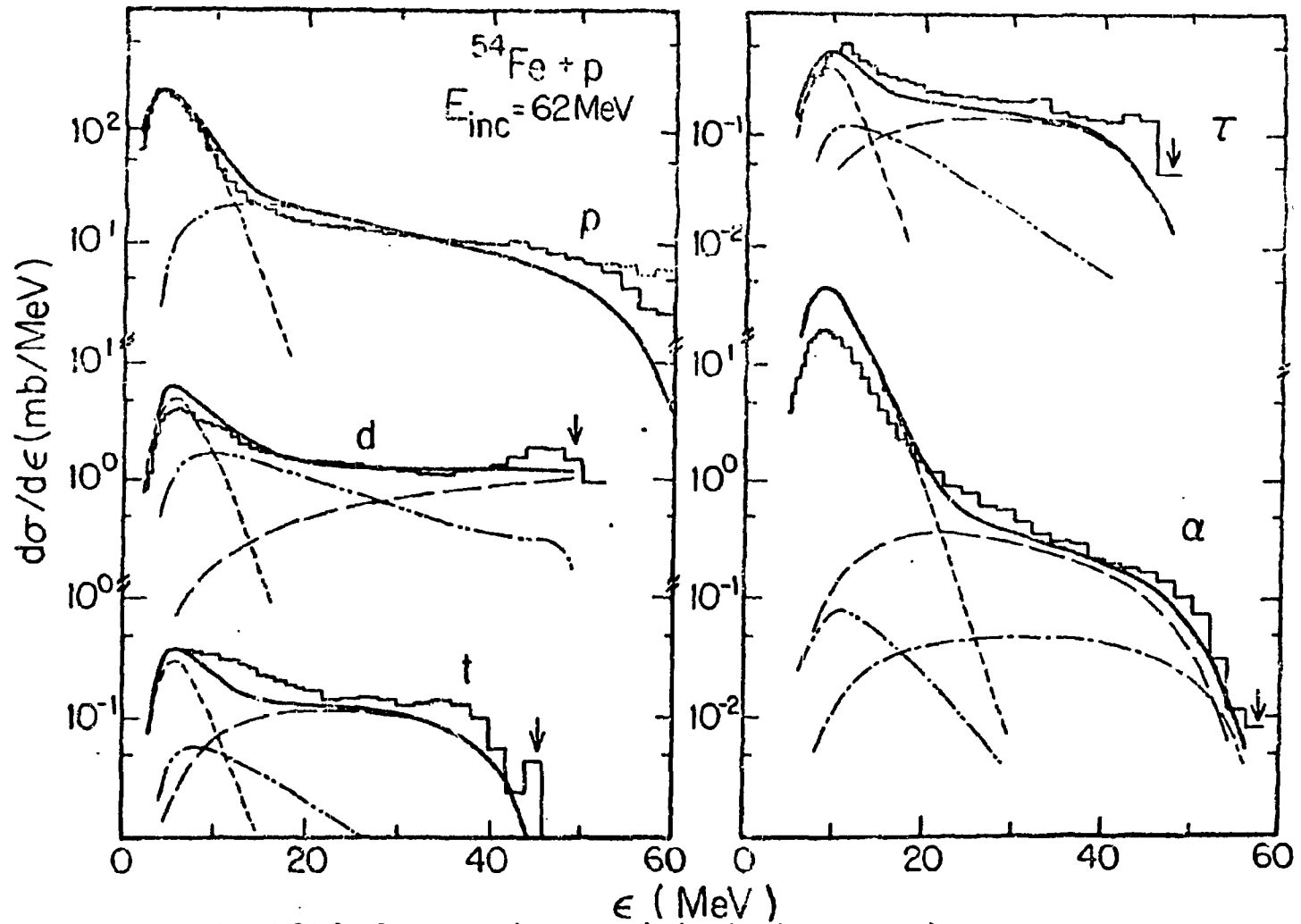


Fig. M26-1. Comparisons between calculated and experimental energy spectra. The bar graphs represent the data. (For p, p') the dashed bar graph shows the data before subtraction of known collective strength). The solid curves are the calculated spectra. The long dash and dot-dash curves show the pickup and alpha knock-out components, respectively; the dash-double dot curves give the preequilibrium components and the short dash curves are the equilibrium contributions.

APPENDIX I

TUNL JOURNAL ARTICLES AND ARTICLES BY TUNL PERSONNEL
January 1976-January 1977

1. Fine Structure of Analogue States, E. G. Bilpuch, A. M. Lane, G. E. Mitchell and J. D. Moses, *Phys. Reports* 28 (1976) 145.
2. A High-Resolution Study of the $^{30}\text{Si}(p,p)$ Reaction, D. A. Outlaw, G. E. Mitchell and E. G. Bilpuch, *Nucl. Phys.* A269 (1976) 99.
3. High Resolution Proton Scattering from ^{42}Ca , W. M. Wilson, E. G. Bilpuch and G. E. Mitchell, *Nucl. Phys.* A271 (1976) 49.
4. Energy Range Extension for an Electrostatic-Analyzer Homogenizer System, D. S. Flynn, E. G. Bilpuch, F. O. Purser, H. W. Newson, L. W. Seagondollar and G. E. Mitchell, *Nucl. Instr. and Meth.* 137 (1976) 125.
5. Electromagnetic Decay of Fragmented Analogue States in ^{45}Sc , J. F. Wimpey, G. E. Mitchell and E. G. Bilpuch, *Nucl. Phys.* A269 (1976) 46.
6. Polarization of Neutrons Elastically Scattered from ^3He , P. W. Lisowski, T. C. Rhea, R. L. Walter, C. E. Busch and T. B. Clegg, *Nucl. Phys.* A259 (1976) 61.
7. Polarization Transfer Effects in (\vec{p}, \vec{n}) Reactions on Light Nuclei at $\theta = 0^\circ$, P. W. Lisowski, R. C. Byrd, R. L. Walter and T. B. Clegg, *Nucl. Phys.* A264 (1976) 188.
8. Compound-Nucleus Effects in Nucleon Depolarization, W. J. Thompson, *Physics Letters* 62B (1976) 245.
9. Systematics of Isospin Mixing in Proton Elastic Scattering from Light Nuclei, P. G. Ikossi, W. J. Thompson, T. B. Clegg, W. W. Jacobs and E. J. Ludwig, *Phys. Rev. Letters* 36 (1976) 1357.
10. Runs Tests as Predictors of Intermediate Structure in the Continuum, R. F. Haglund, J. M. Bowen and W. J. Thompson, *Phys. Rev. Letters* 37 (1976) 553, 878.
11. Comment on "On the Negative-Energy Wave Functions for the Coulomb Field", E. Merzbacher, *Am. J. Phys.* 43 (1976) 101.
12. The Structure of K Hypersatellite Spectra of Cu, Ni and Fe as a Test of Intermediate Coupling, J. P. Briand, A. Touati, M. Frilley, P. Chevallier, A. Johnson, J. P. Rozet, M. Tavernier, S. M. Shafroth and M. O. Krause, *Journal of Physics B Atom. Mole. Phys.* 9 (1976) 1055.

APPENDIX I (Continued)

TUNL JOURNAL ARTICLES AND ARTICLES BY TUNL PERSONNEL

13. Self Consistent K-Matrix-Model Calculation for Finite and Super Heavy Nuclei, R. Y. Cusson, H. P. Trivedi, H. W. Meldner, M. S. Weiss, and R. E. Wright, *Phys. Rev.* C14 (1976) 1615.
14. Realistic Heavy Ion Adiabatic Potentials, R. Y. Cusson, R. A. Hilko, and D. Kolb, *Nucl. Phys.* A270 (1976) 437.
15. Dynamics of $^{12}\text{C} + ^{12}\text{C}$ in a Realistic Time Dependent H. F. Model, R. Y. Cusson and J. Maruhn, *Phys. Lett.* 62B (1976) 134.
16. Time Dependent H. F. Calculation of $^{12}\text{C} + ^{12}\text{C}$ with a Realistic Potential, J. Maruhn and R. Y. Cusson, *Nucl. Phys.* A270 (1976) 471.
17. Time Dependent H. F. Calculation of the Reaction $^{16}\text{O} + ^{16}\text{O}$ in Three Dimensions, R. Y. Cusson, J. Maruhn and R. K. Smith, *Phys. Rev. Lett.* 36 (1976) 1166.
18. Measurement of γ -Ray Angular Distributions and Linear Polarizations for ^{48}V , D. G. Rickel, N. R. Roberson, C. P. Cameron, R. D. Ledford, S. G. Buccino, and D. R. Tilley, *Nucl. Phys.* A256 (1976) 152.
19. Giant Resonance Region of ^{15}N Studied by Polarized and Unpolarized Proton Capture Measurements, H. R. Weller, R. A. Blue, N. R. Roberson, D. G. Rickel, S. Maripuu, C. P. Cameron, R. D. Ledford, and D. R. Tilley, *Phys. Rev.* C13 (1976) 922.
20. Comment on "E1 Excitations in $A = 15$ Nuclei, H. R. Weller, N. R. Roberson, D. G. Rickel, C. P. Cameron, and R. D. Ledford, *Phys. Rev.* C13 (1976) 2052.
21. Assignment of 0^- to the 2.99-MeV level in ^{38}K via the $^{40}\text{Ca}(d,\alpha)^{38}\text{K}$ Reaction, D. G. Rickel, N. R. Roberson, J. David Turner, H. R. Weller, and D. R. Tilley, *Phys. Rev.* C13 (1976) 2077.
22. Mean Lifetimes of Levels in ^{55}Co , R. O. Nelson, J. R. Williams, D. R. Tilley, D. G. Rickel, N. R. Roberson, S. Maripuu, C. P. Cameron, and R. D. Ledford, *Nucl. Phys.* A261 (1976) 427.
23. Giant Dipole Resonance in ^{56}Fe Observed Via (p,γ) and (α,γ) Reactions, D. G. Rickel, C. P. Cameron, R. D. Ledford, N. R. Roberson, H. R. Weller, D. R. Tilley, *Phys. Rev.* C14 (1976) 338.
24. Giant Dipole Resonances in $^{55,57,59}\text{Co}$ Using Polarized Proton Capture, C. P. Cameron, N. R. Roberson, D. G. Rickel, R. D. Ledford, H. R. Weller, R. A. Blue, and D. R. Tilley, *Phys. Rev.* C14 (1976) 553.

APPENDIX I (Continued)

TUNL JOURNAL ARTICLES AND ARTICLES BY TUNL PERSONNEL

25. g Factor of the 738 keV State in ^{43}K , S. A. Wender, C. R. Gould, D. R. Tilley, D. G. Rickel, J. D. Turner, and N. R. Roberson, *Phys. Rev.* C14 (1976) 1174.
26. s- and p-wave Neutron Spectroscopy. Xe. Intermediate Structure in ^{90}Y and The Generalized R-Matrix Theory, S. Ramavataram, J. Bergeron, M. Divandeenam, and H. W. Newson, *Annals of Phys.* 97, No. 2, (1976) 245.
27. Scattering of Polarized Neutrons from ^3He , P. W. Lisowski, T. C. Rhea, R. L. Walter, C. E. Busch, and T. B. Clegg, *Nucl. Phys.* A259 (1976) 61.
28. Depolarization Effects in Stripping a Polarized Negative Ion Beam, G. G. Ohlsen, P. A. Lovoi, R. A. Hardekopf, R. L. Walter and P. W. Lisowski, *Nucl. Instr. and Meth.* 131 (1975) 489.
29. Note Concerning the Misnomer "Proton X-Ray Fluorescence" and the Acronym PIXEA, R. L. Walter, *X-Ray Spectrometry* 5 (1976) 115.
30. Remeasurement of p_y for the $^2\text{H}(d, \bar{n})^3\text{He}$ Reaction and Its Bearing on The Reported f-wave Admixture of The Lowest 2^- State in ^4He , W. Tornow, S. E. Skubic, R. C. Byrd, P. W. Lisowski, and R. L. Walter, *Phys. Rev.* C13 (1976) 2080.
31. Reaction $^3\text{H}(d, n)^4\text{He}$ As A Calibrated Polarized Neutron Source And The Analyzing Power of $^4\text{He}(n, n)^4\text{He}$ from 20 to 30 MeV, P. W. Lisowski, R. L. Walter, G. G. Ohlsen, and R. A. Hardekopf, *Phys. Rev. Lett.* 13 (1976) 809.
32. Equality of Analyzing Power and Polarization in The Reaction $^3\text{H}(p, n)^3\text{He}$, T. R. Donoghue, Sr., M. A. Doyle, H. W. Clark, L. J. Dries, J. L. Regner, W. Tornow, R. C. Byrd, P. W. Lisowski, and R. L. Walter, *Phys. Rev. Letters* 15 (1976) 981.
33. Proton-Induced X-Ray Emission Analysis--A Promising Technique for Studying The Metal Content of Plants and Soils, J. M. Stanford, R. D. Willis, R. L. Walter, W. F. Gutknecht, and J. Antonovics, *Rad. and Environm. Biophys.* 12 (1975) 175.
34. Polarized Triton Experiments on The Five-Nucleon System, G. G. Ohlsen, R. A. Hardekopf, Nelson Jarmie, R. V. Poore, R. L. Walter, and P. W. Lisowski, *Phys. Rev.* C14 (1976) 1688.

APPENDIX I (Continued)

JOURNAL ARTICLES ACCEPTED FOR PUBLICATION

1. High Resolution Proton Inelastic Scattering from ^{50}Cr , T. R. Dittrich, C. R. Gould, G. E. Mitchell, E. G. Bilpuch and K. Stelzer, accepted for publication in Nuclear Physics A.
2. Dissipative Forces and Quantum Mechanics, J. S. Eck and W. J. Thompson, to be published in American Journal of Physics.
3. Compound-Nucleus Effects in Spin-Spin Cross Sections, W. J. Thompson, to be published in Physics Letters.
4. Isospin-forbidden $T = 3/2$ Resonances in ^{25}Al , ^{29}P , and ^{33}Cl , and The Systematics of Isospin Mixing, P. G. Ikossi, T. B. Clegg, W. W. Jacobs, E. J. Ludwig and W. J. Thompson, accepted for publication in Nucl. Phys.

APPENDIX I (Continued)

JOURNAL ARTICLES SUBMITTED FOR PUBLICATION

1. High Resolution Proton Scattering from ^{54}Fe , D. S. Flynn, E. G. Bilpuch and G. E. Mitchell, submitted to Nuclear Physics A.
2. Spectroscopy of the $^{50}\text{Cr}(\vec{d}, p)^{51}\text{Cr}$ Reaction and the Deuteron D-state Effects, A. K. Basak, J. A. R. Griffiths, M. Irshad, O. Karban, E. J. Ludwig, J. M. Nelson, S. Roman and G. Tungate, submitted to Nucl. Phys.
3. Comment on the Comparison of Observed Two Electron-One Photon Transition Energies with Calculated Values, J. A. Tanis, J. M. Feagin, W. W. Jacobs and S. M. Shafroth. Submitted to Phys. Rev. Letters, December 1976.
4. Superposition of the Radiation from N Independent Sources and the Problem of Random Flights, E. Merzbacher, J. Feagin and T. Wu. Submitted to American Journal of Physics.
5. The Application of Proton-Induced X-Ray Emission to Bioenvironmental Analysis, R. L. Walter, R. D. Willis, W. F. Gutknecht, R. W. Shaw. Submitted to Nucl. Instr. and Meth.
6. Computer Analysis of Proton-Induced X-Ray Emission Spectra, R. L. Walter and R. D. Willis. Submitted to Nucl. Instr. and Meth.
7. Proton Induced X-Ray Emission Analyses of Thick and Thin Targets, R. L. Walter, R. D. Willis, W. F. Gutknecht, and R. W. Shaw. Submitted to Nucl. Instr. and Meth.

APPENDIX II

TUNL CONFERENCE REPORTS AND REPORTS BY TUNL PERSONNEL

January 1976-January 1977

1. "Compound Nucleus Fluctuation Effects," W. J. Thompson in Proc. of the 4th Int. Symposium on Polarization Phenomena in Nuclear Reactions, ed. W. Grubler and V. König (Birkhäuser Verlag, Basel, 1976), p. 349.
2. "Depolarization Studies in $^{14}\text{N}(p,p)^{14}\text{N}$ ", T. B. Clegg, W. J. Thompson, R. A. Hardekopf, and G. G. Ohlsen, *ibid.*, p. 634.
3. "Vector Analyzing Powers for the (d,a) Reaction on ^{14}N , ^{16}O , and ^{28}Si ", E. J. Ludwig, T. B. Clegg, P. G. Ikossi, and W. W. Jacobs, *ibid.*, p. 687.
4. "Compound-Nuclear Polarization Effects in Deuteron Elastic Scattering", R. J. Eastgate, T. B. Clegg, R. F. Haglund, and W. J. Thompson, *ibid.*, p. 620.
5. "The $^{207}\text{Pb}(\vec{d},t)^{206}\text{Pb}$ Reaction Using 15 MeV Vector Polarized Deuterons", M. D. Kaitchuck, T. B. Clegg, W. W. Jacobs, and E. J. Ludwig, *ibid.*, p. 681.
6. "Vector Analyzing Powers for $(\vec{d},^6\text{Li})$ on ^{12}C and ^{16}O ", W. W. Jacobs, T. B. Clegg, P. G. Ikossi, and E. J. Ludwig, *ibid.*, p. 697.
7. "Comparison of P_y and A_y for $^9\text{Be}(p,n)^9\text{B}$ at 8.1 and 9.1 MeV", P. W. Lisowski, G. Mack, R. C. Byrd, W. Tornow, S. E. Skubic, R. L. Walter, and T. B. Clegg, *ibid.*, p. 499.
8. "Neutron Polarization and Analyzing Power in $^{15}\text{N}(p,n)^{15}\text{C}$ Reaction", R. C. Byrd, P. W. Lisowski, S. E. Skubic, W. Tornow, R. L. Walter, and T. B. Clegg, *ibid.*, p. 501.
9. "Polarization Transfer Effects in (\vec{p},\vec{n}) Reactions on Light Nuclei at 0° ", P. W. Lisowski, C. E. Busch, and T. B. Clegg, *ibid.*, p. 638.
10. "Polarization Transfer in the $D(\vec{p},\vec{n})p,p$ Reaction from 10 to 15 MeV", R. L. Walter, R. C. Byrd, P. W. Lisowski, and T. B. Clegg, *ibid.*, p. 489.
11. "Neutron-Proton Polarization Measurement at 14.2 MeV", W. Tornow, P. W. Lisowski, R. C. Byrd, S. E. Skubic, R. L. Walter, and T. B. Clegg, *ibid.*, p. 439.
12. "Elastic Scattering of Polarized Neutrons from ^4He ", P. W. Lisowski, T. C. Rhea, R. L. Walter, and T. B. Clegg, *ibid.*, p. 534.
13. "Measurement of Polarization Transfer Coefficients for (\vec{d},\vec{n}) Reactions on ^{14}N , ^{16}O , and ^{28}Si ", P. W. Lisowski, R. C. Byrd, W. Tornow, R. L. Walter, and T. B. Clegg, *ibid.*, p. 653.

APPENDIX II (Continued)

TUNL CONFERENCE REPORTS AND REPORTS BY TUNL PERSONNEL

14. "Measurement of $K_Y^1(0^\circ)$ Over Resonance Region in $^{12}\text{C}(d,n)^{13}\text{N}$ ", R. L. Walter, R. C. Byrd, P. W. Lisowski, G. Mack, and T. B. Clegg, *ibid.*, p. 649.
15. "Determination of Polarization Transfer Coefficient $K_Y^1(0^\circ)$ for the Breakup Reactions $^4\text{He}(\vec{d}, \vec{n})^4\text{He}, p$ and $\text{D}(\vec{d}, \vec{n})\text{D}, p$ ", P. W. Lisowski, R. C. Byrd, R. L. Walter, and T. B. Clegg, *ibid.*, p. 573.
16. "Application of Multi-Step Processes to Nuclear Reaction Studies: The $^{28}\text{Si}(\vec{d}, p\gamma)$ Reaction", H. Clement, R. N. Boyd, T. B. Clegg, and C. R. Gould, *ibid.*, p. 805.
17. "A Study of Fluctuations in the Cross-section and Analyzing Power of $^{28}\text{Si}(\vec{d}, d)$ and $^{28}\text{Si}(\vec{d}, p)$ Reactions", R. Henneck, T. B. Clegg, R. F. Haglund, E. J. Ludwig, and G. Graw, *ibid.*, p. 795.
18. "Progress in Polarized Ion Source Development", T. B. Clegg (Invited Paper), *ibid.*, p. 111.
19. "Polarized Beam Angular Correlation Measurements in ^{41}Ca ", C. R. Gould, D. R. Tilley, C. Cameron, R. D. Ledford, N. R. Roberson, and T. B. Clegg, *ibid.*, p. 807.
20. "Two-Nucleon Transfer Reactions Induced by Polarized Deuterons", J. M. Nelson, O. Karban, S. Roman and E. J. Ludwig, *ibid.*, p. 691.
21. "Analyzing Powers of the $^{19}\text{F}(d, t)^{18}\text{F}$ Reaction", J. M. Nelson, D. Karban, E. J. Ludwig, and S. Roman, *ibid.*; pp. 679.
22. "Probability Distributions for Compound Nuclear Fluctuations in Vector Analyzing Powers", R. F. Haglund, J. M. Bowen, and W. J. Thompson, *ibid.*, p. 785.
23. "Mass-Number Systematics of Deuteron Folding-Model Potentials", J. A. Ramirez and W. J. Thompson, *ibid.*, p. 613.
24. "Polarization in Heavy-Ion Scattering", W. J. Thompson, *ibid.*, p. 831.
25. "The New Polarized Ion Source for SATURNE II", T. B. Clegg, A. i. P. Conference Series 35, No. 11 (1976) In Press.
26. "Deformation Lengths from Scattering of Strongly Interacting Projectiles", W. J. Thompson and J. S. Eck, Radial Shape of Nuclei Conference, Krakow, Poland, 22-25 June 1976.
27. "Evidence for $2e-1\gamma$ Transitions in Cl^{n+} Bombardment of KCl", W. W. Jacobs, B. L. Doyle, S. M. Shafroth, J. A. Tanis, and A. W. Waltner, International Conference on the Physics of X-ray Spectra, National Bureau of Standards, Extended Abstracts, 1976, pp. 177.

APPENDIX II (Continued)

TUNL CONFERENCE REPORTS AND REPORTS BY TUNL PERSONNEL

28. "K X-rays and REC from Cl^{n+} Bombardment of Targets in the Region $19 \leq Z \leq 35$ ", J. A. Tanis, B. L. Doyle, W. W. Jacobs, and S. M. Shafroth, *ibid.*, p. 186.
29. "Trace Element Analysis with Characteristic X Rays Excited by Fast Cl^{n+} Ions", S. M. Shafroth, B. L. Doyle, W. W. Jacobs, and J. A. Tanis, Conference on Heavy Metals in the Environment, University of North Carolina School of Medicine, Chapel Hill, N. C. 24-25 May 1976. To be published in "Environmental Health Perspectives", 1976.
30. "Wavelength Dispersion Analysis of PIXE Spectra", R. D. Willis, R. L. Walter, B. L. Doyle and S. M. Shafroth, International Conference in Particle Induced X-ray Emission and its Analytical Applications, Lund, Sweden, 23-26 August 1976. To be published in "Nuclear Instruments and Methods", 1976.
31. "K X Rays and REC Arising from Fast Cl^{n+} Ion Bombardment of Cu", J. A. Tanis, B. L. Doyle, W. W. Jacobs and S. M. Shafroth, Second International Conference on Inner Shell Ionization Phenomena, Freiburg, Germany, 29 March-2 April 1976, Abstracts 115-117.
32. "Inner-shell Physics after Fifty Years of Quantum Mechanics", E. Merzbacher, Proceedings of the Second International Conference on Inner Shell Ionization Phenomena, Freiburg, 1976. W. Mehlhorn and R. Brenn, editors. p. 1-13.
33. "Differential Elastic and Inelastic Scattering of 9- to 15-MeV Neutrons from Carbon", D. W. Glasgow, F. O. Purser, H. H. Hogue, J. C. Clement, K. Stelzer, G. Mack, J. R. Boyce, D. H. Epperson, S. G. Buccino, P. W. Lisowski, S. G. Glendinning, E. G. Bilpuch, H. W. Newson, and C. R. Gould, *Nucl. Science and Engineering*: 61. (1976).
34. "7-15 MeV Neutron Scattering from 6Li , 7Li , 9Be and C", E. G. Bilpuch, D. H. Epperson, D. W. Glasgow, S. G. Glendinning, C. R. Gould, H. H. Hogue, P. W. Lisowski, C. E. Nelson, H. W. Newson, F. O. Purser, L. W. Seagondollar, W. Tornow and P. Von Behren, Proceedings of The International Conference on The Interactions of Neutrons with Nuclei, Lowell, Massachusetts, July 6-9, 1976, Vol II, p. 1309.
35. "Radiative Capture of Fast Neutrons", H. R. Weller and R. A. Blue, P. L. Von Behren, N. R. Roberson, D. G. Rickel, F. O. Purser, C. R. Gould and D. R. Tilley, *ibid.*, p. 1371.

APPENDIX ii (Continued)

TUNL CONFERENCE REPORTS AND REPORTS BY TUNL PERSONNEL

36. "Neutron Spectra and Yields from Charged Particle Bombardment of Thick Lithium Targets", C. E. Nelson, F. O. Purser, P. Von Behren and H. W. Newson, *ibid.*, p. 1476.
37. "Neutron Spectra and Yields from Charged Particle Bombardment of Thick Lithium Targets", C. E. Nelson, F. O. Purser, P. Von Behren, and H. W. Newson, *Proceedings of Fourth International Conference on Medical Physics, Ottawa, Canada, July 25-30. 1976.*

APPENDIX III

 ABSTRACTS OF TALKS AT AMERICAN PHYSICAL SOCIETY MEETINGS
 January 1976-January 1977

1. High Resolution Proton Inelastic Scattering on ^{56}Fe , W. K. Wells, D. A. Outlaw, E. G. Bilpuch and G. E. Mitchell, *Bull. Am. Phys. Soc.* 21 (1976) 662.
2. Channel Spin Mixing Ratios in High Resolution Proton Inelastic Scattering on ^{44}Ca , T. R. Dittrich, C. R. Gould, G. E. Mitchell, E. G. Bilpuch, M. E. Bleck and K. Stelzer, *Bull. Am. Phys. Soc.* 21 (1976) 662.
3. Energy Range Extension for an Electrostatic-Analyzer Homogenizer, D. S. Flynn, E. G. Bilpuch, F. O. Purser, H. W. Newson, L. W. Seagondollar and G. E. Mitchell, *Bull. Am. Phys. Soc.* 21 (1976) 611.
4. A Linear Beam Optics Code, S. Stevenson and T. B. Clegg, *Bull. Am. Phys. Soc.* 21 (1976) 610.
5. Comparison of the Polarization and Analyzing Power in (p, n) Mirror Reactions on ^{15}N and ^9Be , R. C. Byrd, P. W. Lisowski, G. Mack, S. E. Skubic, W. Tornow, R. L. Walter and T. B. Clegg, *Bull. Am. Phys. Soc.* 21 (1976) 637.
6. Vector Analyzing Powers for Several (d, α) Reactions, E. J. Ludwig, W. W. Jacobs, and S. A. Tonsfeldt, *Bull. Am. Phys. Soc.* 21 (1976) 990.
7. Compound-Nucleus Effects in Spin-Spin Cross Sections, W. J. Thompson, *Bull. Am. Phys. Soc.* 21 (1976) 964.
8. Vector Analyzing Power Measurements of Isobaric Analog Resonances in ^{209}Bi , S. A. Tonsfeldt, T. B. Clegg, W. W. Jacobs, E. J. Ludwig, and W. J. Thompson, *Bull. Am. Phys. Soc.* 21 (1976) 991.
9. Recoil Ranges and Range Straggling of Nuclei Resulting from $^{59}\text{Co}(^{16}\text{O}, X)Y$ Reactions, A. W. Waltner, T. W. Godfrey, D. M. Peterson, S. M. Shafroth, W. W. Jacobs, and J. A. Tanis, *Bull. Am. Phys. Soc.* 21 (1976) 983.
10. Calculation of $2e-1\gamma$ (K_{α}^h) and K_{α}^* X-Ray Energy Shifts by HFS and Desclaux Codes, J. A. Tanis, J. M. Feagin, W. W. Jacobs and S. M. Shafroth, *Bull. Am. Phys. Soc.* 21 (1976) 1247.
11. Intensity Ratio for $2e-1\gamma$ to K Shell Hypersatellite Transitions for Cl, K and Ca, W. W. Jacobs, S. M. Shafroth, J. A. Tanis and W. W. Waltner, *Bull. Am. Phys. Soc.* 21 (1976) 1247.
12. Efficiency Calibration from 2.7-8 keV Using 3 MeV Proton Excitation of Characteristic K X Rays, J. A. Tanis, W. W. Jacobs, and S. M. Shafroth, Southeastern Section of APS, 11-13 November 1976. p. 5 of program.

APPENDIX III (Continued)

ABSTRACTS OF TALKS AT AMERICAN PHYSICAL SOCIETY MEETINGS

13. Sum Rules for Atoms in Sudden Rearrangement Collisions, J. Feagin and E. Merzbacher, *ibid.*, p. 1 of program.
14. Superposition of N. Independent Monochromatic Waves, E. Merzbacher, J. Feagin, and T. Wu, *ibid.*, p. 9 of program.
15. Study of the Giant Dipole Resonance of ^{89}Y , N. R. Roberson, R. D. Ledford, C. P. Cameron, D. G. Rickel, J. D. Turner, D. R. Tilley, R. McBroom and H. R. Weller, *Bull. Am. Phys. Soc.* 21, 4 (1976) 516.
16. The $^3\text{H}(p, \gamma_0)^4\text{He}$ Reaction for $17 < E_p < 30$ MeV, R. McBroom, H. R. Weller, N. R. Roberson, D. G. Rickel, J. D. Turner, C. P. Cameron, R. D. Ledford and D. R. Tilley, *Bull. Am. Phys. Soc.* 21, 4 (1976) 534.
17. The Giant Dipole Resonance Region of ^{31}P , C. P. Cameron, R. D. Ledford, D. G. Rickel, J. D. Turner, N. R. Roberson, D. R. Tilley, R. C. McBroom, R. A. Blue, H. R. Weller, *Bull. Am. Phys. Soc.* 21, 4 (1976) 556.
18. Assignment of 0^- to the 2.99 MeV Level in ^{38}K via the $^{40}\text{Ca}(\bar{d}, \alpha)^{38}\text{K}$ Reaction, D. G. Rickel, N. R. Roberson, J. David Turner, H. R. Weller and D. R. Tilley, *Bull. Am. Phys. Soc.* 21, 4 (1976) 556.
19. Magnetic Moment of the $7/2^-$ State in ^{43}K , S. A. Wender, D. R. Tilley, C. R. Gould, D. G. Rickel, D. J. Turner and N. R. Roberson, *Bull. Am. Phys. Soc.* 21, 4 (1976) 556.
20. Investigation of the $3/2^+$ Analogue State in ^{89}Y at $E_{\text{ex}} = 14.62$ MeV Using the $^{88}\text{Sr}(\bar{p}, \gamma_0)^{89}\text{Y}$ Reaction, R. D. Ledford, C. P. Cameron, D. G. Rickel, J. D. Turner, N. R. Roberson, D. R. Tilley, R. McBroom and H. R. Weller, *Bull. Am. Phys. Soc.* 21, 4 (1976) 581.
21. Search for Collective E2 Resonances Above the Giant Dipole Resonance, C. P. Cameron, R. D. Ledford, J. D. Turner, N. R. Roberson, H. R. Weller, R. A. Blue, R. McBroom and D. R. Tilley, *Bull. Am. Phys. Soc.* 21, 8 (1976) 996.
22. Evidence for $J^\pi = 2^+$ States in ^4He , R. McBroom, H. R. Weller, N. R. Roberson, J. D. Turner, C. P. Cameron, R. D. Ledford and D. R. Tilley, *Bull. Am. Phys. Soc.* 21, 8 (1976) 997.
23. Realistic Adiabatic Heavy-Ion Potential and Polarization of ^{16}O , K. A. Sage, and R. Y. Cusson, *Bull. Am. Phys. Soc.* 21, 4 (1976) 512.
24. Optical Model Potential from a Realistic K-Matrix Model, K. A. Sage and R. Y. Cusson, *Bull. Am. Phys. Soc.* 21, 8 (1976) 973.
25. Nuclear Reactions Due to ^{16}O Bombardment of ^{59}Co , A. W. Waltner, T. W. Godfrey, S. M. Shafroth, B. Doyle, W. Jacobs and J. A. Tanis, *Bull. Am. Phys. Soc.* 21 (1976) 680.

APPENDIX IV

MISCELLANEOUS PUBLICATIONS

January 1976-January 1977

1. Report of the Ad Hoc Panel on Accelerator-Related Atomic Physics Research, E. Merzbacher with B. Crasemann and others. Committee on Atomic and Molecular Physics, National Academy of Sciences, National Research Council, Washington 1976.
2. Review of B. Cagnac and J. C. Pebay-Peyroula, Modern Atomic Physics, Fundamental Principles, Hasted Press (1975) American Scientist, E. Merzbacher, 64 (1976) 78.

APPENDIX V (Continued)

- Vol. 17, No. 2 The Probability of Positron Annihilation-in-Flight for Allowed Beta Decay
G. Azuelos and J.E. Kitching
- Cross-Sections for L-Shell X-Ray and Auger-Electron Production by Heavy Ions
T.L. Hardt and R.L. Watson
- Consistent Calculations of (n, x) and (n, xy) Cross Sections for ^{40}Ca . $E_n = 1-20$ MeV
C.Y. Fu
- Tables of Shore and Fano Parameters for the Helium Resonances $2s^2\ ^1S$, $2p^2\ ^1D$, and $2s\ 2p\ ^1P$
A. Bordenave-Montesquieu, P. Benoit-Cattin, A. Gleizes, and H. Merchez
- Vol. 17, No. 3 Transport Properties of Gaseous Ions over a Wide Energy Range
H.W. Ellis, R.Y. Pai, E.W. McDaniel, E.A. Mason, and L.A. Viehland
- Tables for Reaction Gamma-Ray Spectroscopy. Part III. $A = 33$ to $A = 44$
R.J. de Meijer and A.G. Drentje
- Vol. 17, No. 4 Positron-Annihilation Data Tables
R.M. Singru, K.B. Lal, and S.J. Tao
- Vol. 17, Nos. 5-6 1975 Mass Predictions
S. Maripuu, Special Editor; W.D. Myers; H.v. Groote, E.R. Hilf, and K. Takahashi; P.A. Seeger and W.M. Howard; S. Liran and N. Zeldes; M. Bauer; M. Beiner, R.J. Lombard, and D. Mas; J. Jänecke; E. Comay and I. Kelson; J. Jänecke and B.P. Eynon; and A.H. Wapstra and K. Bos
- Vol. 18, No. 1 Reaction List for Charged-Particle-Induced Nuclear Reactions, 1974-1976
F.K. McGowan and W.T. Milner

APPENDIX V (Continued)

Vol. 18, No. 2

E2, M1 Multipole Mixing Ratios in Odd-Mass
Nuclei, $A > 150$
K.S. Krane

Relativistic Matrix Elements of the Energy Operator
in the Case of Complex Electronic Configurations
Z.B. Rudzikas, V.I. Sivcev, and I.S. Kiřkin

Matrix Elements of the Relativistic Electron-Transition
Operators
Z.B. Rudzikas, A.A. Stepcov, and I.S. Kiřkin

Vol. 18, No. 3

Experimental Widths of K and L X-Ray Lines
S.I. Salem and P.L. Lee

Neutral-Atom Electron Binding Energies from Relaxed-
Orbital Relativistic Hartree-Fock-Slater
Calculations, $2 \leq Z \leq 106$
K.-N. Huang, M. Aoyagi, M.H. Chen, B.
Crasemann, and H. Mark

Accurate Wavefunction for Atomic Beryllium
C.F. Bunge

Vol. 18, No. 4

Tables of Thermonuclear-Reaction-Rate Data for
Neutron-Induced Reactions on Heavy Nuclei
J.A. Holmes, S.E. Woosley, W.A. Fowler,
and B.A. Zimmerman

APPENDIX VI
TUNL PERSONNEL

Newson, H. W. (director, professor)	Duke
Bilpuch, E. G. (deputy director, professor)	Duke
Blue, R. A. (associate professor)	Univ. of Florida
Clegg, T. B. (professor)	UNC
Gould, C. R. (associate professor)	NCSU
Lisowski, P. W. (assistant professor)	Duke
Ludwig, E. J. (professor)	UNC
Mitchell, G. E. (professor)	NCSU
Nelson, C. E. (assistant professor)	Duke
Purser, F. O. (assistant to the director)	Duke
Roberson, N. R. (professor)	Duke
Seagondollar, L. W. (professor)	NCSU
Shafroth, S. M. (professor)	UNC
Tilley, D. R. (professor)	NCSU
Walter, R. L. (professor)	Duke
Walmer, A. W. (professor)	NCSU
Weller, H. R. (associate professor)	Univ. of Florida

Research Associates and Instructors

Dittrich, T. R. (research associate)	NCSU
Jacobs, W. W. (research associate) Left 11/76	UNC
Outlaw, D. A. (instructor)	Duke
Rickel, D. G. (instructor) Left 4/76	Duke
Tanis, J. (research associate)	UNC
Tornow, W. (research associate)	Duke
Von Behren, P. L. (research associate)	Duke
Wender, S. (research associate)	NCSU

Associated Theorists

Bjordenharn, L. C. (professor)	Duke
Cotanch, S. (assistant professor)	NCSU
Cusson, R. Y. (associate professor)	Duke
Kalbach, C. (assistant professor)	Tenn. and NCSU
Maripuu, S. (senior research scientist)	Duke
Merzbacher, E. (professor)	UNC
Park, J. (professor)	NCSU
Thompson, W. J. (associate professor)	UNC
Way, K. (adjunct professor)	Duke

APPENDIX VI (Continued)

Technical Support Staff for TUNL

Bailey, D. M.
Edwards, S. E.

Gibson, P. M.
Harris, E. P.
Harward, J. T.
Hogen, R. G.
Larkins, A.
Lovette, A. G.
Lovette, A. W.

McCrary, P.
Rummel, R. L.

Skubic, S.

Draftswoman
Computer Maintenance
Supervisor
TUNL Secretary
Instrument Maker
Electronics Technician
Instrument Maker
Electronics Technician
Accelerator Technician
Shop Foreman, Instrument
Maker
TUNL Secretary
Accelerator Maintenance
Supervisor
Laboratory Assistant

APPENDIX VI (Continued)

Graduate Students

Beyerle, A.	NCSU
Bleck, M.	Duke
Byrd, R. C.	Duke
Cameron, C.	Duke
Chandler, J.	NCSU
Doyle, B. (Left 8/76)	UNC
El Kadi, S.	Duke
Epperson, D.	Duke
Feagin, J.	UNC
Flynn, D. (Left 10/76)	Duke
Glendinning, S. G.	Duke
Hogue, H.	Duke
Jensen, M.	NCSU
Ledford, R. D. (Left 11/76)	Duke
McBroom, R. (Left 10/76)	Univ. of Florida
Olsewski, E. (Left 6/76)	UNC
Ramirez, Jr. (Left 6/76)	UNC
Sage, K.	Duke
Sales, K.	NCSU
Stevenson, D. (Left 6/76)	UNC
Tonsfeldt, S.	UNC
Turner, D.	Duke
Watson, W. A.	Duke
Wells, W. K.	Duke
Westerfeldt, C.	NCSU
Willis, J.	UNC
Willis, R. D.	Duke
Wu, H. (Left 6/76)	UNC
Wu, T.	UNC